UV-Vis imaging for characterizing dissolution performance of ionizable drug substances and measuring microenvironmental pH

Johanna Åberg

DIVISION OF FOOD AND PHARMA/CHEMICAL ENGINEERING | DEPARTMENT OF PROCESS AND LIFE SCIENCE ENGINEERING FACULTY OF ENGINEERING LTH | LUND UNIVERSITY

2024

MASTER THESIS

A COLLABORATION BETWEEN LUND UNIVERSITY AND UNIVERSITY OF COPENHAGEN

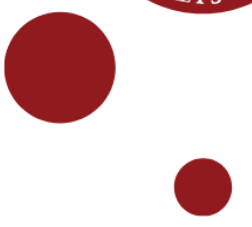

LUND UNIVERSITY

Johanna Åberg

KLGM16 Degree Project in Pharmaceutical Formulation 30 ECTS

Master of Science in Chemical Engineering

Division: Food and pharmaceutical engineering

Published by

Department of Process and Life Science Engineering

Faculty of Engineering LTH, Lund University

P.O. Box 118, SE-221 00 Lund, Sweden

Supervisor	Stephen Burleigh	jesper.ostergaard@sund.ku.dk
Co-supervisor	Jesper Østergaard	stephen.burleigh@ple.lth.se
Examiner	Marie Wahlgren	marie.wahlgren@ple.lth.se

Abstract

Studying dissolution of oral drug substances is crucial throughout the drug development process. Current methods are time consuming and require large quantities of both the drug and dissolution media. Thus, exploring new methods is highly desirable. UV imaging, an analytical technique based on real-time absorbance measurements, can be used in early drug discovery to study drug dissolution and has significant potential to overcome these obstacles. This work aimed to develop a UV imaging setup to study the dissolution of two drug compounds, salicylic acid and sodium salicylate, and to investigate the possibility of determining microenvironmental pH during dissolution. IDR (intrinsic dissolution rate) values were determined for both compounds in different dissolution mediums and images from the experiments were analyzed. The results demonstrated that UV imaging could distinguish between the dissolution profiles of the two compounds and that dissolution was highly dependent on the pH of the dissolution medium. By preparing solutions of salicylic acid and sodium salicylate of different pH and measuring absorbance, it was concluded that these compounds could serve as their own pH probes. The two-wavelength spectrophotometric method to determine pH was investigated using both the UV imaging system SDi2 and a spectrophotometer. This method was subsequently applied to calculate microenvironmental pH during the dissolution of the drug compounds. This novel approach requires further studies but holds significant potential for future applications.

Populärvetenskaplig sammanfattning

Att studera upplösning av orala läkemedel är avgörande för att förstå deras biotillgänglighet och terapeutiska effekt. Då dagens metoder för att studera upplösning är tidskrävande och kräver stora mängder av läkemedel och media så finns det ett stort behov av att fram nya metoder. En potentiell metod är UV-Vis imaging som kan användas för att studera upplösning av läkemedel i realtid. Detta projekt har utforskat denna teknik samt utvecklat en metod för att studera pH-förändringar i mikro-miljön under upplösning av utvalda läkemedel. Detta har genererat väldigt intressanta och unika resultat och metoden har stor potential inför framtiden

Upplösning av orala läkemedel påverkas av flera olika faktorer, men bestäms huvudsakligen av affiniteten mellan läkemedlet och upplösningsmediet. Intrinsic dissolution rate, (IDR), är en form av upplösningshastighet som ofta används för att karakterisera läkemedel. IDR definieras som mängden läkemedel som löser sig per tidsenhet och area. Ett vanligt problem inom läkemedelformulering är svårlöslighet, och ett tillvägagångsätt för att förbättra detta hos joniserbara läkemedel är saltbildning. Lösligheten hos dessa läkemedel är ofta starkt beroende av pH i det omgivna mediet, vilket gör det intressant att studera pH förändringar vid upplösning av läkemedel och deras salter.

UV-Vis imaging är en analytisk metod för att studera upplösning av små mängder läkemedel i realtid. Genom att föra in sitt prov in en cell där upplösningsmedium flödar och mäta UV absorbansen genom cellen så kan information om händelser vid ytan av läkemedlet och koncentrationen av läkemedlet i upplösningsmediet erhållas. IDR kan beräknas och bilder från experiment kan studeras. I detta projekt har dessutom en spektrofotometrisk metod använts, där absorbansen mäts vid två olika våglängder för att beräkna pH vid upplösningsexperiment. Denna metod för att beräkna pH är helt ny och har tidigare endast använts för pH-bestämning av havsvatten. Ett tillgängligt UV-imaging-instrument, Sirius SDi2, har använts i detta projekt.

Resultaten visade att UV-imaging kunde skilja mellan de två föreningarnas upplösningsprofiler och att upplösningen var starkt beroende av upplösningsmediets pH. Natriumsalicylat hade en signifikant högre upplösningshastighet i jämförelse med salicylsyra vilket var väntat. Genom att förbereda lösningar av salicylsyra och natriumsalicylat med

kända pH-värden och mäta absorbansen, drogs slutsatsen att dessa föreningar kunde fungera som sina egna pH-indikatorer. Den spektrofotometriska metoden för att bestämma pH undersöktes med både UV-Vis imaging instrumentet SDi2 och en spektrofotometer. Denna metod tillämpades sedan för att beräkna mikro-miljö pH under upplösning av salicylsyra at natriumsalicylat. Metoden fungerade bra för att bestämma intermediära pH-värden men stor osäkerhet observerades vid höga och låga pH-värden. Denna nya metod kräver ytterligare studier men har stor potential för framtida tillämpningar.

Acknowledgement

This project was performed at University of Copenhagen, department of pharmacy as a master thesis for the Department of Process and Life Science Engineering at the Faculty of Engineering, Lund University (LU). This project makes up 30 credits within pharmaceutical formulation and lasted from January to June 2024.

I would like to express a special thank you to my supervisor at UCPH, Jesper Østergaard, for giving me this opportunity and sharing your knowledge with me. You have helped, supported, and given me your time whenever I needed it. Thank you to Stephen Burleigh for being my supervisor guiding me through the entire process, and Marie Wahlgren for being my examiner.

Table of content

1. Background and Introduction

When developing orally administered drugs, the understanding of solubility and dissolution behavior is crucial to increase bioavailability of poorly soluble drug substances. In vitro drug dissolution testing of oral drugs is used throughout the development life-cycle and some of the most widely used methods for measuring dissolution include the pharmacopeia methods such as basket dissolution, paddle dissolution, and the rotating disc. However, these methods often require large amounts of active pharmaceutical ingredient (API) and dissolution medium, posing limitations in early drug discovery and development (Østergaard et al., 2014b). To address these challenges in predicting drug performance upon oral administration, it is essential to develop approaches that enhance our understanding of the dissolution processes.

UV imaging, sometimes called dissolution imaging, is a micro-dissolution technique which can overcome some of the challenges mentioned. This technique monitors drug dissolution in real-time and can be used to, for example, identify solid form transformations, and measure the intrinsic dissolution rate (IDR) (Østergaard et al., 2014b). UV imaging may be particularly suited for studying dissolution of ionizable drug substances and their salts. Salt formation is a common approach to increase the solubility, and thereby the bioavailability, of ionizable drug substances. However, incomplete or unpredictable dissolution behavior of salts is often observed in the GI tract, and it is important to better understand the interplay between dissolution, solubility and microenvironmental pH. Thanks to the UV-Vis absorbance spectra of many ionizable substances being dependent on pH, UV imaging can also be used to measure microenvironmental pH changes during dissolution (Østergaard et al., 2014a). For example, Figure 1 shows a real-time spatially resolved measurement of pH during dissolution of sodium naproxenate in 0.01 M HCl using UV imaging. This project aimed at addressing how microenvironmental pH changes during dissolution of weakly acidic and basic drugs affected their solubility and dissolution rate.

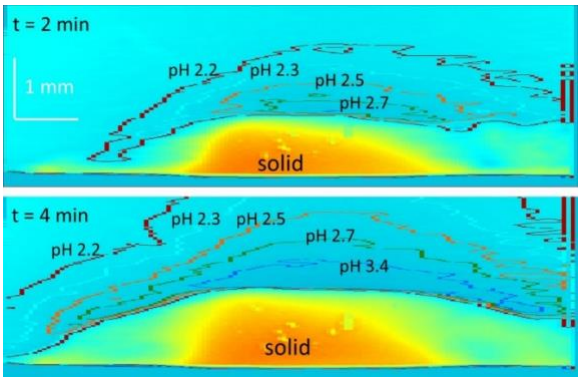

Figure 1: Proof of concept study to investigate pH effects during dissolution of sodium naproxenate in 0.01 M HCl by UV-Vis imaging. Sodium naproxenate can significantly alter the local pH of the dissolution medium, however the salt is eventually neutralized and precipitates as the acidic species naproxen (Østergaard et al., 2014a).

1.2 Aim

The overall aim was to develop UV/Vis imaging methods (utilizing SDi2 instrumentation) for measurement of the microenvironmental pH during drug dissolution and to apply the methodology for characterization of selected drugs. More specifically the following objectives were addressed.

1. Develop a UV-Vis imaging setup for measurement of the dissolution of salicylic acid and sodium salicylate in different media.
2. Investigate the possibility of a drug substance serving as its own pH probe/indicator and to define requirements for such an approach.
3. Calculate pH changes during dissolution of salicylic acid and sodium salicylate using UV imaging.

2. Theoretical background

This section covers the fundamental theory of drug substance dissolution. It describes the two analytical methods: UV-Vis spectrophotometry and UV-vis imaging, highlighting their utility in studying dissolution processes and measuring pH during dissolution. Lastly, physicochemical properties of the drug substances salicylic acid and sodium salicylate are discussed, explaining why salicylic acid is a suitable compound for this project.

2.1 Dissolution of drug substances

2.1.1 The dissolution process

Dissolution is the process by which a solid dissolve in a liquid, that is mass transfer from solid surface to liquid phase. This process is primarily governed by the relative affinity between the solid substance and the solvent. The solubility is dependent on various factors including the drugs chemical composition and structure. The dissolution of a solid in liquid is composed of two consecutive stages. Firstly, an interfacial reaction takes place which results in the liberation of solutes molecules from the solid phase to the liquid phase. This step is determined by the relative affinity of the various molecules involved. Secondly, there is diffusional transport of solute molecules through the boundary layer surrounding the crystal to the bulk solution (Taylor and Aulton, 2018).

2.1.2 Dissolution rate

Dissolution rate describes the amount of drug substance that goes into solution per time unit under standardized conditions of temperature and solvent composition. Dissolution rate can be either interface-controlled or diffusion controlled where diffusion-controlled is the most prevalent state for drug substances by far (Taylor and Aulton, 2018). In case of diffusion-controlled dissolution the dissolution rate is defined according to the Noyes – Whitney Equation.

$$\frac{dm}{dt} = \frac{D*A*(C_S - C)}{h} \quad (1)$$

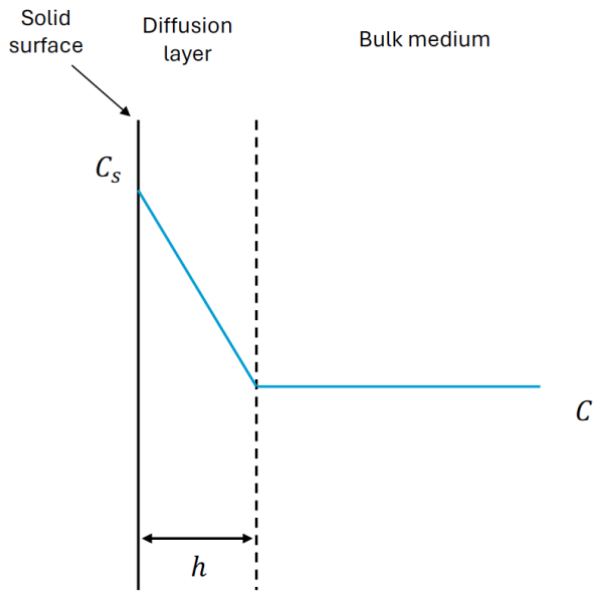

Figure 2: Concentration profile surrounding a dissolving particle. Figure made using Microsoft Powerpoint.

The rate of mass transfer of solute molecules or ions thorough a static diffusion layer (dm/dt) is directly proportional to the area available for migration (A) and the concentration difference (C_s-C) across the boundary layer and is inversely proportional to the thickness of the boundary layer (h). C is the concentration of solute in bulk and C_s is the concentration at the solid interface, assuming saturation at the solid interface (Taylor and Aulton, 2018). The constant D is a physical constant, known as the diffusion coefficient which is dependent on properties of the diffusing substance. At sink conditions, when the volume of solvent is large or if solute is removed from the bulk of the dissolution medium by some process faster than it passes into solution, C remains close to zero, and the term (C_s-C) can be approximated to C_s, the solubility.

$$\frac{dm}{dt} = \frac{D*A*C_S}{h} \quad (2)$$

Since the rate of dissolution is dependent on many factors it can be advantageous to have a measure of the rate of dissolution independent of some of these factors, in particular rate of agitation and solute available. Intrinsic dissolution rate (IDR) is a useful parameter which is defined as the amount of compound (API) dissolved per unit time per unit area. The IDR measures the intrinsic properties of the drug only as a function of the dissolution medium, assuming that sink conditions have been reached (Taylor and Aulton, 2018).

The Noyes – Whitney Equation is typically used for calculating IDR using methods such as the rotating disk system. It provides a convenient frame for studying dissolution processes occurring in vessels or vials. However, when calculating IDR in the flow-through UV imaging instrument Sirius SDi2 a convective diffusion drug dissolution model developed by Nelson and Shah is used as the quantitative basis. The dissolution rate, *R*, for a circular compact of radius *r* is defined by Equation 3 (Nelson and Shah, 1975) where *D* is the diffusion coefficient, C_o is the solubility and α is the rate of shear over the dissolving surface.

$$R = 2.157 * D^{\frac{2}{3}} * c_0 \alpha^{\frac{1}{3}} * r^{5/3} \quad (3)$$

Throughout an experiment, IDR surface area is kept constant, and a constant flow of dissolution medium is maintained to ensure sink conditions. IDR is calculated according to Equations 4 and 5 by the Sirius SDi2 Software (Brown et al., 2021).

$$IDR = \frac{\sum_{z=0}^{\frac{H}{2}} (v_z M c_z W \Delta z)}{S} \quad (4)$$

$$v_z = \frac{3Q}{2HW}\left(1 - \left(\frac{(2z - H^2)}{H^2}\right)\right) \quad (5)$$

where z is the height above z-origin, v_z is the velocity at z, M is the molecular weight, c_z is the concentration at z, W is the width of flow cell channel, Δz is the effective pixel height, S is the surface area of sample, H is the height of flow cell channel in observation region and Q is the volumetric flow rate (Nelson and Shah, 1975).

2.1.2 Effects of salt formation and "microenvironmental" pH changes on dissolution

Chemically, a salt is a product from a neutralization reaction between an acid and a base. Most drug substances are either a weak acid or base, and salt formation is possible using a counter ion (Pratap Chandra Acharya et al., 2018). Salts have in general, higher solubilities than the corresponding acid and base forms and is therefore widely used in drug development. According to Equation 2, dissolution rates are proportional to both the solubility (C_s) and the surface area of the drug substances, however increasing C_s is the more effective way of improving the dissolution rate. This is because of practical limits on how much the surface area can be decreased, as the smallest particles size that can be achieved from milling is 2 to 3 μm. Increasing solubility can increase the dissolution rate hundreds of times, which is not possible from decreasing surface area (Serajuddin, 2007). The aqueous solubility of an acidic or basic drug depends on pH and can be described by two equations, each of which describe an independent curve which is limited by the solubility of either the ionized or unionized species. These curves intersect at pH_{max}, which is the pH of maximum solubility, the only point where both the free base and salt form of a basic drug, or the free acid and salt form of acidic drug can coexist as solids. Of an acidic drug, the solid phase in equilibrium with a saturated solution at $pH < pH_{max}$ is the free acid and the solid phase at $pH > pH_{max}$ is the salt (Serajuddin, 2007), see Figure 3 which shows a schematic representation of the pH-solubility

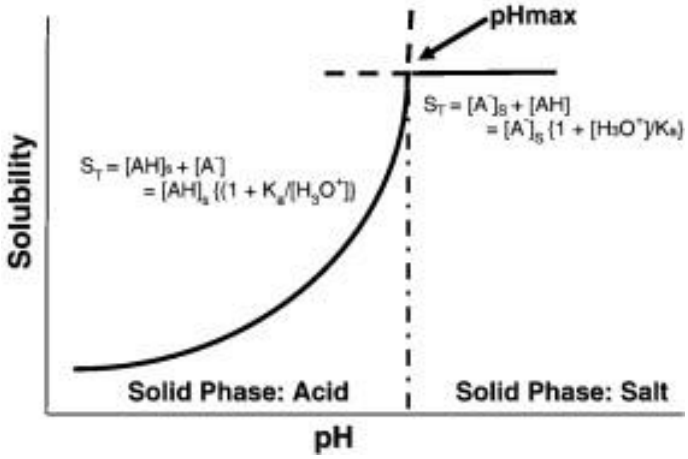

Figure 3: An example of a pH-solubility profile of an acidic group indicating the two equations which describes solubility and the point where they intersect, pH_{max}. Figure taken from (Serajuddin, 2007).

profile of an acidic drug. The pH is dependent on many factors, including the pK_a values of the drug and the potential counterions, their solubility as well as interactions with the constituents of the dissolution medium/simulated intestinal fluid (Serajuddin, 2007). Studying the local pH (also known as microenvironmental pH) is of great importance and one approach for doing so is described below.

2.2 UV-Vis Spectrophotometry

UV-Vis (ultraviolet-visible) spectroscopy is an analytical technique used to identify and quantity analytes. It measures the amount of UV or visible light that is absorbed by a sample. The extent of absorbed light depends on the structure of the molecule, with the part responsible for light absorption is known as the chromophore (Harris, 2007). When a substance absorbs light its electrons are promoted to higher energy states. The energy required for this promotion depends on the environment of the electrons, hence absorption occurs at different wavelengths for different substances. UV-Vis spectroscopy utilize light of wavelengths 190-800 nm, with the UV range falling between 190-400 nm, and visible light between 400-800 nm (Østergaard, 2016). The absorption of UV and visible light is quantitively described by Beer-Lamberts law.

$$log_{10}\left(\frac{I_0}{I}\right) = log_{10}\left(\frac{1}{T}\right) = A = \varepsilon lc \quad (6)$$

where I_0 is the intensity of incident light, I is the intensity of transmitted light, T is the transmittance, A is the absorbance, ε is the molar absorption coefficient, l is the light path and c is the concentration of the absorbing molecule. Beer-lamberts law is only valid for monochromatic light, which consist of a single wavelength.

Deviations from Beer-lamberts law is caused by chemical or instrumental artifacts. For instance, high analyte concentration causes the absorbing molecules to come close together, alters the charge distribution and can lead to changes in absorptivity. Furthermore, presence of particles in solution can induce light scattering. When it comes to the instrument, using a narrower wavelength minimizes deviations from Beer lamberts law. Additionally, light that reaches the detector without having passed the sample, known as stray light, which also cause deviations from Beer-Lamberts law (Østergaard, 2016).

2.2.1 Agilent Cary 60 UV-vis spectrophotometer

Different types of spectrophotometers are available, but the basic components include a light source, a wavelength detector, a sample compartment and a detector. The Agilent Cary 60 will be used in this project and is an advanced UV spectrophotometer used for absorbance measurements. It has a double-beam with a powerful xenon lamp that flashes 80 times per second, a wavelength range of 190-1100 nm and can be fitted with cuvettes of different path lengths (Agilent, 2024).

2.3 UV imaging

UV imaging is a technology relying on absorbance measurements for the generation of pictures that are resolved spectrally, spatially and temporally. It quantifies the intensity of UV light that passes through a volume element of a quartz cell as a function of time and position. This technique is used to create images of analyte components to characterize and analyze drugs, normally in relation to dissolution and release testing (Østergaard et al., 2014b). A cell for flow-through dissolution testing has been developed to provide real-time information about dissolution, swelling, disintegration, microenvironmental pH and precipitation of drug compacts at the solid-liquid interface. Using the flow-through cell, IDR values can be measured in minutes, using minimal amounts of sample, 3-10 mg (Østergaard, 2016).

2.3.1 The SDi2

One suitable instrument for dissolution imaging in a flow-through setup is the Sirius SDi2. The basic components of the instrument can be seen in Figure 4. The flow cell consists of PEEK sample holder inside a rectangular quartz tube which constitutes the walls to both contain the dissolution medium and to allow light to pass through the quartz cell. The SDi2 has a dual wavelength capability with for wavelengths in the UV range (255, 280, 300 and

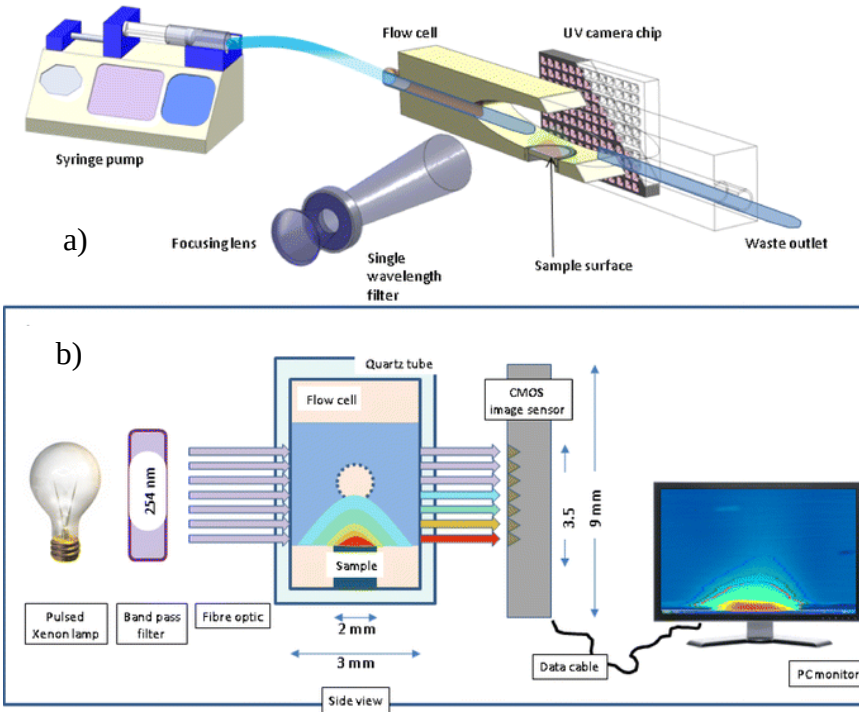

Figure 4: Schematic showing general set up for UV imaging instrumentation: a) key components, b) side view of flow cell, c) picture for flow cell with sample holder inserted and d) sample holder. Fig a and b taken from Østergaard et al., 2014b.

320 nm $\pm$ 5 nm) and one in the visible range (520 nm $\pm$ 5). The SDi2 has a detection area (CMOS chip) of 28 x 28 mm^2 (Bock et al., 2022), the compact cell can hold compacts of 3 mm in diameter and has a total volume of 1.54 ml. When performing a dissolution experiment in the SDi2, the sample holder which contains the compressed sample is placed into flew cell. Before entering the cell, the dissolution medium is preheated by passing through a heat chamber set at 37 ºC and the syringe pump then moves dissolution medium into the flow cell which carries the drug downstream. The instrument software is used to for analyzing, for example calculating the IDR (Østergaard et al., 2014b).

2.4 Spectrophotometric method to determine pK_a

To be able to calculate pH from spectrophotometric measurements, one requirement is that the dissociation constant (pK_a) of the drug substance is known. (pK_a) is normally determined

from potentiometric pH measurements and titrations but can also be determined from absorbance measurements.

2.4.1 Calculating pK_a of weak acids

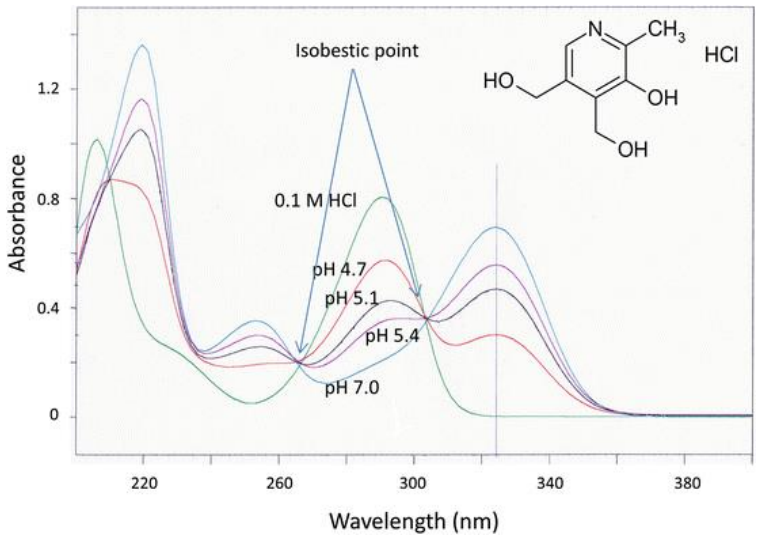

Figure 5: Absorbance spectra of pyridoxine solutions of varied pH. Taken from Østergaard, 2016.

The absorbance spectra of ionizable drugs substances, for example pyridoxine, are often affected by pH because of the acid-base equilibrium taking place. Figure 5 shows the absorbance spectra of pyridoxine in solutions with different pH (Østergaard, 2016), which allows for calculation of pK'_a from absorbance measurements.

When dissolving a weak acid in water, the following acid-base equilibrium takes place

$$HA\ (aq) \rightleftharpoons H^+(aq) + A^-(aq) \tag{7}$$

At a given wavelength, the absorbance of a solution containing absorbing species is the sum of absorbance of each species, according to Equation 8 where HA corresponds to the acidic form and A^- to the basic form and x to the partially transformed compound.

$$A_x = c_{HA}\varepsilon_{HA}l + c_{A^-}\varepsilon_{A^-}l \tag{8}$$

The thermodynamic dissociation constant K_a is defined by equation 9, while the mixed apparent dissociation constant K_a' is defined by Equation 10 (Sinko and Martin, 2011).

$$K_a = \frac{a_{H^+} * a_{A^-}}{a_{HA}} \tag{9}$$

$$K'_a = \frac{a_{H^+} * [A^-]}{[HA]} \tag{10}$$

The mixed apparent dissociation constant takes ionic strength into account and is obtained from concentration measurements of the acid or bases added, while for the H^+ ion the activity is measured from a pH electrode. Therefore, this this will be used for the following calculations. From Equation 10, the mixed apparent acidity constant $pK'_a\ is\ defined$ (Sinko and Martin, 2011).

$$pK'_a = pH - log\left(\frac{[A^-]}{[HA]}\right) \quad (11)$$

Combining Equation 8 and the definition of pK'_a, Equation 12 is derived, see Appendix 1. Plotting measured absorbance values against pH allows fitting Equation 12 using non-linear regression and pK'_a can be calculated. Absorbance measurements are obtained from solutions of the drug compound in the fully protonated form, the fully deprotonated form and in a few intermediate. All solutions need to have the same concentration of the absorbing compound and the same ionic strength in order for Equation 12 to be applicable (Østergaard, 2016).

$$A_x = \frac{A_{HA} + A_{A^-} * 10^{(pH - pK'a)}}{10^{(pH - pK'a)}} \quad (12)$$

2.4.2 Spectrophotometric pH determination according to Clayton & Byrne

The pH of a solution containing a light absorbing compound can also be determined from absorbance measurements at two different wavelengths Clayton & Byrne (1993) used spectrophotometry to measure absorbance of a sulfonphtalein indicator in ocean water, calculating the pH of the water using Equation 13, see Appendix 1 for full derivation.

$$pH = log\, K_1 + log\left(\frac{R - e_1}{e_2 - R e_3}\right) \quad (13)$$

K_1 is the dissociation constant and R is defined as the ratio of indicator absorbance at wavelength λ_2 and λ_1 ($R = A_2/A_1$) and $e_1 = \frac{\varepsilon_{HA^-,2}}{\varepsilon_{HA^-,1}}$, $e_2 = \frac{\varepsilon_{A^-,2}}{\varepsilon_{HA^-,1}}$ and $e_3 = \frac{\varepsilon_{A^-,1}}{\varepsilon_{HA,1}}$.

In this project, this approached to measure pH of ocean water using a pH indicator is transferred to pH measurements of a drug substance, by the drug itself. This two-wavelength method is independent of concentration of the absorbing compound and light path, and therefore brings great opportunity to calculate pH in the SDi2, as the concentration and effective light path are now known. This is an entirely new approach in drug dissolution testing and requires that the drug substance which is studied is UV absorbing.

Using the apparent mixed dissociation constant, Equation 13 can be written according to Equation 14.

$$pH = pK'_a + log\left(\frac{R - e_1}{e_2 - R e_3}\right) \quad (14)$$

The MEC's, $\varepsilon_{HA,2}$, $\varepsilon_{HA,1}$, $\varepsilon_{A,2}$ and $\varepsilon_{A,1}$ can be calculated by constructing calibration curves of absorbance versus concentration and dividing the slope with the path length according to Beer-Lamberts law, see Equation 4. The approach described above makes it possible to

determine microenvironmental pH during dissolution of ionizable drug substances by measuring absorbance.

2.5 Salicylic acid

Salicylic acid (SA) is a drug substance used in skin care products, topical medicines, cosmetics and in production of other pharmaceuticals. SA is here used as a model substance because of it being an ionizable UV-Vis absorbing compound with a carboxylic group and a hydroxyl group, whose absorbance changes with pH. In aqueous solution, the carboxylic acid group dissociates and loses a proton from the carboxylic acid, see Figure 6. When dissolved in solutions of high pH it can also dissociate and loose a second proton from the hydroxyl group. According to literature the dissociation constants for salicylic acid are $pK_{a,1}$= 2.853 (Farajtabar and Gharib, 2010) and $pK_{a,2}$=13.3 (Dhat and D Jahagirdar, 1982) in water at 25ºC, determined potentiometric. Since only physiological pH range is relevant for his project, only the first dissociation will be examined in this study.

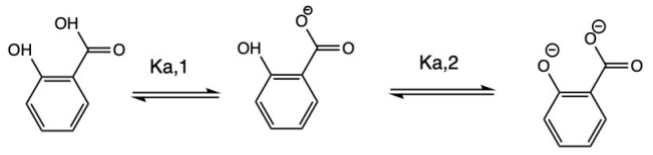

Figure 6: The dissociation of salicylic acid

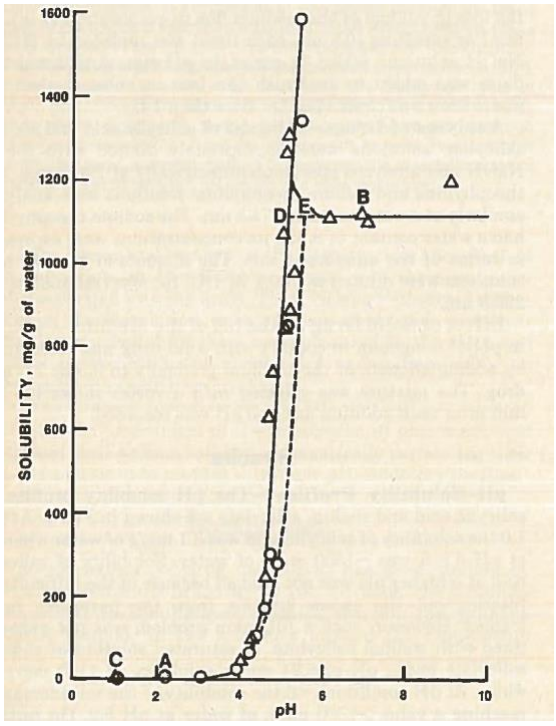

Figure 7: Graphical illustration of the pH-solubility profile of salicylic acid (white dots) and sodium salicylate (white triangles) at 37 ^{o}C. Points A and B represent pH values and concentrations of saturated solutions of SA and SS, respectively, in deionized water. Figure taken from Serajuddin and Jarowski, 1985.

Studies on the pH-solubility profile have been performed on salicylic acid and its sodium salt sodium salicylate which concluded that the pH-solubility profile were identical when controlling pH of the solutions, see Figure 7. This is because of the acid-base equilibrium existing between the neutral and charged forms. However, there was large difference in the intrinsic dissolution rates due to differences existing between the bulk pH and diffusion layer pH (Serajuddin and Jarowski,

1985). Salicylic acid and sodium salicylate exhibits self-buffering properties in the diffusion layer, leading to different pH in the diffusion layer, as compared to the bulk solution. These differences in pH lead to differences in drug solubilities of the two compounds, which can significantly influence the dissolution rate rates (Serajuddin and Jarowski, 1985). For example, studies that have been conducted on dissolution rates of mesylate salts and the free base form of haloperidol in solutions of varied pH. This showed that differences in Cs values under surface pH ($pH_{H=0}$, also known as microenvironmental pH) conditions are responsible for salts and bases dissolving in different rates, where the rates are, in general, higher for the salts (Li et al., 2005).

3. Materials and Methods

3.1 Materials

The following chemicals were used: Salicylic acid, sodium salicylate, sodium phosphate dibasic dihydrate, sodium chloride, sodium phosphate dibasic hydrate, sodium dihydrogen monohydrate, potassium phosphate monobasic, potassium chloride, sodium acetate anhydrous, sodium acetate trihydrate, 86% phosphoric acid, 5.0 M NaOH and 0.5 M HCl.

3.2 Solutions

For detailed solution preparation, see Appendix 2. The media used for dissolution experiments were a phosphate buffer pH 6.5, HCl acidic medium pH 1.2, 0.15 M NaCl solution, 0.165 M 1.0 M H_3PO_4/1.0 M NaH_2PO_4 pH 3 buffer and 0.041 M 1.0 M H_3PO_4/1.0 M NaH_2PO_4 pH 3 buffer.

Ten different buffer solutions with pH ranging from 1.4 to 6.54, see Appendix 2.

3.3 Instrumentation

The Agilent Cary 60 UV-vis spectrophotometer was used to record UV-vis spectra's of SS solutions, the Sirius SDi2 for dissolution experiments and the Methrom 744 pH meter was used for potentiometric pH measurements.

3.4 IDR experiment in SDI2

The general procedure for UV imaging to determine IDR using the SDi2 is described below. In addition, flow rate – and temperature control experiments were performed.

Compacts were prepared by weighing five to 10 mg of the drug and transferring to the sample holder. The sample was compressed at 80 kg for 1 min on grease proof paper. The accurate weight of the compact obtained was determined by weighing the sample holder before and after adding the sample to the sample holder and calculating the mass difference.

Before starting an experiment, the flow cell was flushed using deionized water and the method was created in the software "Sirius SDi2 Collection". All experiments were measured at two wavelengths, 280 nm and 320 nm and the instrument was set to 37 ^{o}C. Flow rate was varied depending on the experiment being conducted, see Appendix 3.

The recorded images were analyzed and IDR was calculated using the Sirius SDi2 Data Analysis application. The absorbance data can be viewed frame-by-frame and all calculations of IDR were made in the software are based on data captured in a zone with dimension of x = 25 mm, z = 0.6 mm, width = 0.5 mm and height = 3.0 mm.

3.4.1 Temperature control Experiments in SDi2

Experiments to measure the temperature in the SDi2 flow cell were conducted by inserting a FLUKE t3000 FC Digital thermometer (Fluke Corporation, United states, Everett) into the flow cell. Temperature was measured for flow rates 0.5, 1.0 and 3.0 ml/min for 30 minutes for each flow rate. All experiments were repeated three times and were conducted with deionized water.

3.4.2 Flow rate control experiments in SDi2

Flow rate control experiments were conducted for flow rates 0.5, 1.0, and 3.0 ml/min. For each flow rate, two samples were collected; flow rate was collected from t = 3 min to t = 10 min and from t = 20 min to t = 27 min by directing the outlet tube into a vial and weighing the vial before and after the measurement. This was repeated and in total, the pump program presented in Figure 8 was repeated 3 times.

	Duration (hh:mm:ss)	Rate (mL/min)	Linear Velocity (cm/min)
1	00:30:00	3.00	8.33
2	00:30:00	1.00	2.78
3	00:30:00	0.50	1.39

Figure 8: Pump program used for flow rate control experiments in the SDi2

3.5 Recording of UV-spectra in Agilent Cary 60 UV-Vis spectrophotometer

To scan a spectrum in the Agilent Cary 60 UV-vis spectrophotometer, blank solution was first pipetted into the quartz cuvette and used for baseline correction. The absorbance spectrum of the blank solution from 200 to 800 nm was recorded. Subsequently, the cuvette was emptied and filled with the first sample and the absorbance spectrum was scanned, this was repeated for all samples. If needed, a baseline adjustment was done in excel to make sure that the absorbance was zero in the visible range.

3.6 Simple absorbance measurement in Agilent Cary 60 UV-vis spectrophotometer

The instrument was set up by choosing the desired wavelengths (280 nm and 320 nm), placing the 10 mm quartz cuvette with blank solution in the cell compartment and zeroing the instrument. Absorbance was measured for each solution, including the blank.

3.7 Initial experiments to study the pH dependence of SA absorbance

Five different buffer solutions with pH ranging from 1.5 to 6.5 were prepared and SS was added in each to a final SS concentration of 20 μM. The absorbance spectrum was recorded for all solutions in a 10 mm cuvette according to the procedure described in 3.5.

3.8 Constructing Calibration curves.

To be able to determine $\varepsilon_{(HA^-)_2}$, $\varepsilon_{(HA^-)_1}$, $\varepsilon_{(H_2A)_2}$ and $\varepsilon_{(H_2A)_1}$ of SA, calibration curves were constructed using both the Sirius SDi2 and the Agilent Cary 60 UV-Vis spectrophotometer. SS was weighed out and dissolved in purified water to obtain the stock solution. Standards with concentrations of 3.0, 1.5, 0.8, 0.4, 0.2 and 0.1 mM were prepared by diluting down the stock solution using the mediums of interest, the phosphate buffer pH 6.5, and acidic medium pH 1.2.

3.8.1 Calibration curves using the Agilent Cary 60 UV-Vis

Simple absorbance measurements were conducted at 280 nm and 320 nm for each solution and absorbance vs concentration was plotted from which the slope could be used to calculate the molar extinction coefficients according to Beer Lamberts law, see Equation 6.

3.8.2 Calibration curve using Sirius SDi2

The following pump program was used to construct a calibration curve of absorbance versus concentration using the Sirius SDi2. For each calibration curve, a blank solution consisting of the media was used to prime the instrument. Subsequently each standard solution ran for 7 min at 2.5 ml/min flowrate with 1 min 0 ml/min flow rate in between to have time to change solutions and to prevent air bubbles from being introduced. Average absorbance values for each concentration were extracted from the software and plotted against concentration to obtain a calibration curve, see Appendix 3 for detailed method. The molar extinction coefficients were

	Duration (hh:mm:ss)	Rate (mL/min)	Linear Velocity (cm/min)
1	00:07:00	2.50	6.94
2	00:01:00	0.00	0.00
3	00:07:00	2.50	6.94
4	00:01:00	0.00	0.00
5	00:07:00	2.50	6.94
6	00:01:00	0.00	0.00
7	00:07:00	2.50	6.94
8	00:01:00	0.00	0.00
9	00:07:00	2.50	6.94
10	00:01:00	0.00	0.00
11	00:07:00	2.50	6.94
12	00:01:00	0.00	0.00
13	00:07:00	2.50	6.94
14	00:01:00	0.00	0.00

Figure 9: Pump program used to measure absorbance of standard solutions in the SDI2. Step 1 correspond to the blank solution, step 3 to 0.1 mM SS, step 5 to 0.2 mM SS, step 7 to 0.4 mM SS, step 9 to 0.8 mM SS, step 1 to 1.5 mM and step 13 to 3.0 mM SS.

calculated as the slope of the curve according to Beer-Lamberts law (Equation 6).

3.9 pH measurement using the Agilent Cary 60 UV-vis spectrophotometer

To study the pH-absorbance dependent properties of salicylic acid and to characterize the R value in Equation 14, solutions of different pH and SS concentrations were prepared and absorbance spectrum was scanned in the Cary using a 10 mm cuvette, see Table 1.

Table 1: Composition of all SS solutions prepared.

Solution name	SS Concentration (mM)	Buffer
1.5 A	0.3	1.0 M H_3PO_4/1.0 M NaH_2PO_4
1.5 B	0.5	1.0 M H_3PO_4/1.0 M NaH_2PO_4
2.0 A	0.3	1.0 M H_3PO_4/1.0 M NaH_2PO_4
2.0 B	0.5	1.0 M H_3PO_4/1.0 M NaH_2PO_4
2.5 A	0.3	1.0 M H_3PO_4/1.0 M NaH_2PO_4
2.5 B	0.5	1.0 M HAc/1.0 M NaAc
3.0 A	0.3	4.0 M H_3PO_4/1.0 M NaH_2PO_4
3.0 B	0.5	4.0 M H_3PO_4/1.0 M NaH_2PO_4
3.5 A	0.3	1.0 M HAc/1.0 M NaAc
3.5 B	0.5	1.0 M HAc/1.0 M NaAc
4.0 A	0.3	1.0 M HAc/1.0 M NaAc
4.0 B	0.5	1.0 M HAc/1.0 M NaAc
4.5 A	0.3	1.0 M HAc/1.0 M NaAc
4.5 B	0.5	1.0 M HAc/1.0 M NaAc
5.0 A	0.3	1.0 M HAc/1.0 M NaAc
5.0 B	0.5	1.0 M HAc/1.0 M NaAc
5.5 A	0.3	1.0 M HAc/1.0 M NaAc
5.5 B	0.5	1.0 M HAc/1.0 M NaAc
6.0 A	0.3	1.0 M HAc/1.0 M NaAc
6.0 B	0.5	1.0 M HAc/1.0 M NaAc
6.5 A	0.3	Blank FaSSIF phosphate buffer
6.5 B	0.5	Blank FaSSIF phosphate buffer

Solutions 1.5 A, 1.5 B, 3.0 A, 3.0 B, 4.0 A, 4.0 B, 6.0 A, 6.0 B, 6.5 A, 6.5 were also scanned in 1 mm and 2 mm quartz cuvettes.

Absorbance at 280 nm and 320 nm for all measurements were used to calculate pK'_a according to Equation 12 and pH according to Equation 14.

3.10 pH measurement of solutions in SDi2

	Duration (hh:mm:ss)	Rate (mL/min)
1	00:07:00	2.50
2	00:01:00	0.00
3	00:07:00	2.50
4	00:01:00	0.00
5	00:07:00	2.50
6	00:01:00	0.00
7	00:07:00	2.50
8	00:01:00	0.00
9	00:07:00	2.50
10	00:01:00	0.00
11	00:07:00	2.50
12	00:01:00	0.00
13	00:07:00	2.50
14	00:01:00	2.50

a)

	Duration (hh:mm:ss)	Rate (mL/min)
1	00:07:00	2.50
2	00:01:00	0.00
3	00:07:00	2.50
4	00:01:00	0.00
5	00:07:00	2.50
6	00:01:00	0.00
7	00:07:00	2.50
8	00:01:00	0.00
9	00:07:00	2.50
10	00:01:00	0.00
11	00:07:00	2.50
12	00:01:00	0.00

b)

10: Pump program used for absorbance measurements of SS in a) phosphate and b) acetate buffer solutions.

Four experiments were conducted to measure absorbance of all solutions listed in Table 2. Acetate and phosphate buffer solutions were measured separately, as well as solutions with different SS concentration. Blank solutions were measured in step 1 See figure 10 a) and b) for pump program.

A zone with dimensions of x = 13 mm, z = 2mm, width= 3mm and heigh = 1.5 mm was set up. Average absorbance values for each solution were extracted from the software and pH was calculated according to Equation 14, using Excel.

3.11 Dissolution experiments to calculate microenvironmental pH

To measure microenvironmental pH during dissolution of SS and SA, six dissolution experiments, see Table 2, were performed according to the method described in 3.4. For each experiment, two different flow rates were applied, see Figure 11 for pump program.

Table 2: Final dissolution experiments performed to calculate microenvironmental pH during dissolution experiments.

Experiment	Compound	Dissolution medium
1	SA	pH 3 buffer, C = 0.165 M
2	SS	pH 3 buffer, C = 0.165M
3	SA	pH 3 buffer, C = 0.041 M
4	SS	pH 3 buffer, C = 0.041 M
5	SA	0.15 M NaCl solution
6	SS	0.15 M NaCl solution

	Duration (hh:mm:ss)	Rate (mL/min)
1	00:02:00	3.00
2	00:15:00	0.50
3	00:15:00	1.00

Figure 11: Pump program used for dissolution experiments listed in Table 2.

pH was calculated by setting up two zones. A surface zone with dimensions of x = 14.2 mm, z = 0.74 mm, width = 3.0 mm and height = 0.2 mm and an IDR zone with dimensions of x = 25 mm, z = 0.64 mm, width = 0.5 mm and height = 3.0 mm was set up as shown in Figure 12. By extracting absorbance recorded at both wavelengths at selected time points, Equation 14 was used to calculate the microenvironmental pH in dissolution experiments. IDR was also calculated using the "Sirius SDi2 Collection" software.

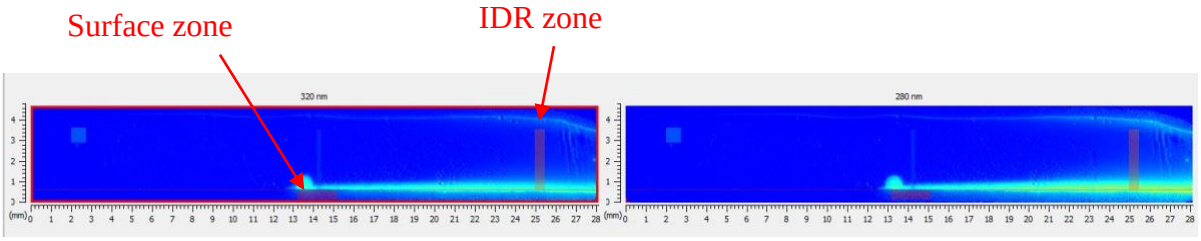

Figure 12: Dissolution experiments from which pH was calculated from absorbance values from the surface zone and IDR zone.

4. Results & Discussion

4.1 Initial dissolution experiments

In the following dissolution experiments, the dissolution medium flows from left to right, the drug compact is in the bottom of the cell and an IDR zone was set up to measure absorbance for IDR calculations. The color map "Jet" has been and applied and Figure 13 shows what absorbance the different colors correspond to. For the first experiment, images recorded at both 280 nm and 320 nm is presented and for the remaining experiments images recorded at 320 nm can be found in Appendix 4.

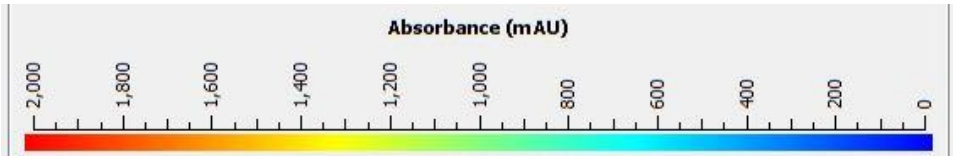

Figure 13: Absorbance scale applied for the following dissolution experiments.

4.1.1 Dissolution of salicylic acid

Figure 14 shows images from dissolution a 30 min experiments of SA in acidic medium pH 1.2. After a 1 min step with flow rate 3 ml/min to fill up the cell, the flow rate was changed to 0.5 ml/min for the rest of the experiment. The dark blue color corresponds to zero absorbance, meaning that there is no compound present. At the bottom of the flow cell, close to the compact, there is a lighter blue color which corresponds to an absorbance of between 0.4 to 0.8, this is compound that has dissolved from the compact. During the first 5 minutes, the compound is turbulently spread to left, probably due to decreasing the flow rate from 3.0 ml/min to 0.5 ml /min. After this, a "tai" is formed to the right of the compact, representing the compact being spread out in the direction of the flow. The absorbance of SA decreases over time, which could be explained by a decrease in sample left in the sample holder. After the experiment had finished, by looking at the sample holder it was observed that a significant amount of sample was left in the sample holder, although less than before, meaning that some had dissolved. Throughout the entire experiment, the absorbance at 280 nm and 320 nm appears very similar. At t = 5min, an air bubble was formed on the bottom of the flow cell, a problem which often occurred during dissolution experiments. An air bubble is also observed at the right upper corner.

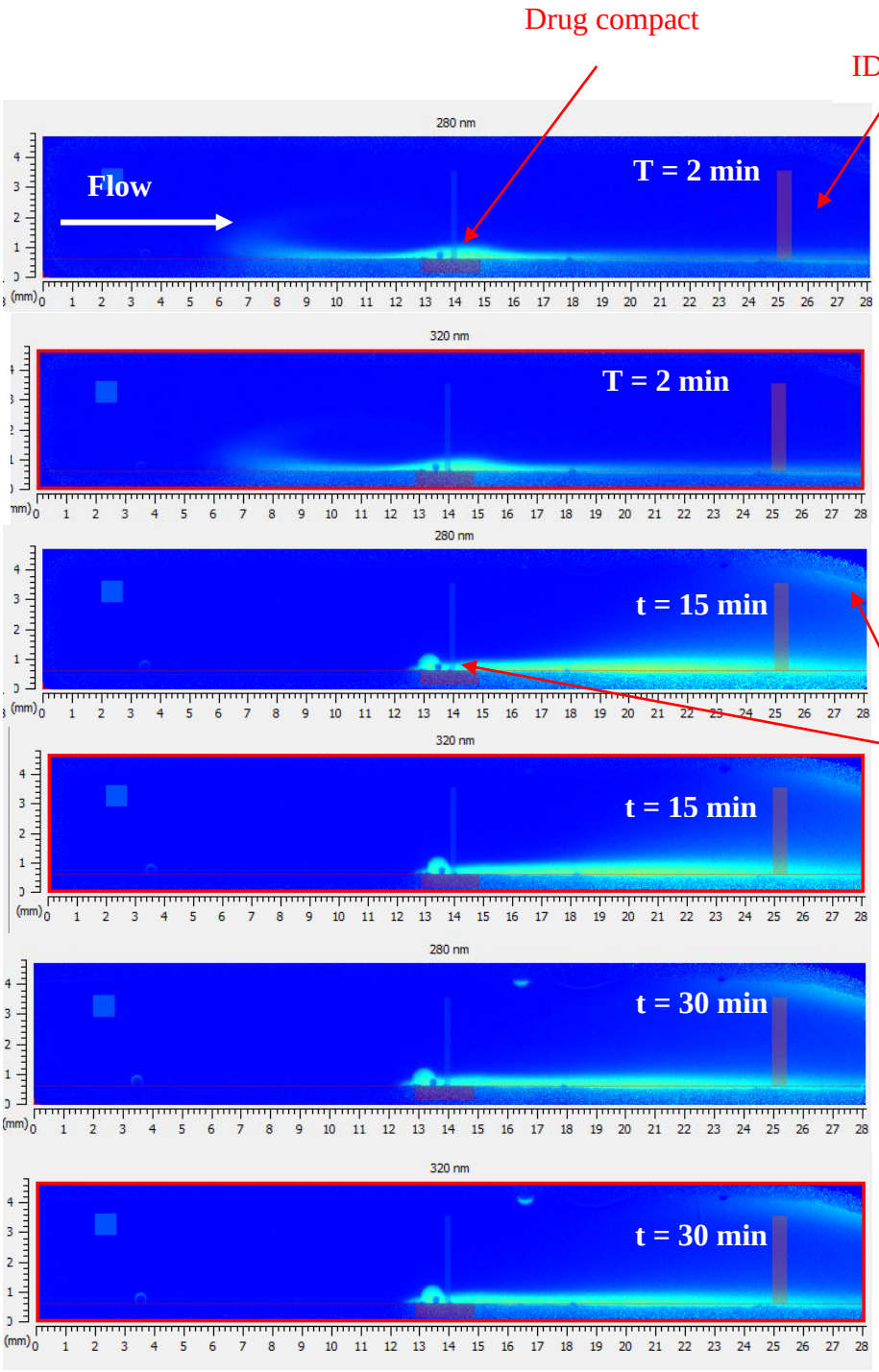

Figure 14: Selected absorbance maps from dissolution experiment on SA in acidic medium pH 1.2 with a flow rate of 0.5 ml/min. Images from t = 2 min, t = 15 min and t= 30 min, recorded at 280 nm and 320 nm.

When applying a higher flow rate, as seen in Figure 15, the spreading of compound to the left decreases. The absorbance profile stabilizes more rapidly, meaning that the tail to the right is formed, and the overall absorbance is lower, indicating a reduced concentration of SA. This is due to the higher flow rate moving SA out of the flow cell faster, as compared to having a lower flow rate. By looking at the sample holder after the experiment had finished it was observed that only a small amount of SA had dissolved, probably due to the low solubility of SA, see Figure 7 for the solubility profile.

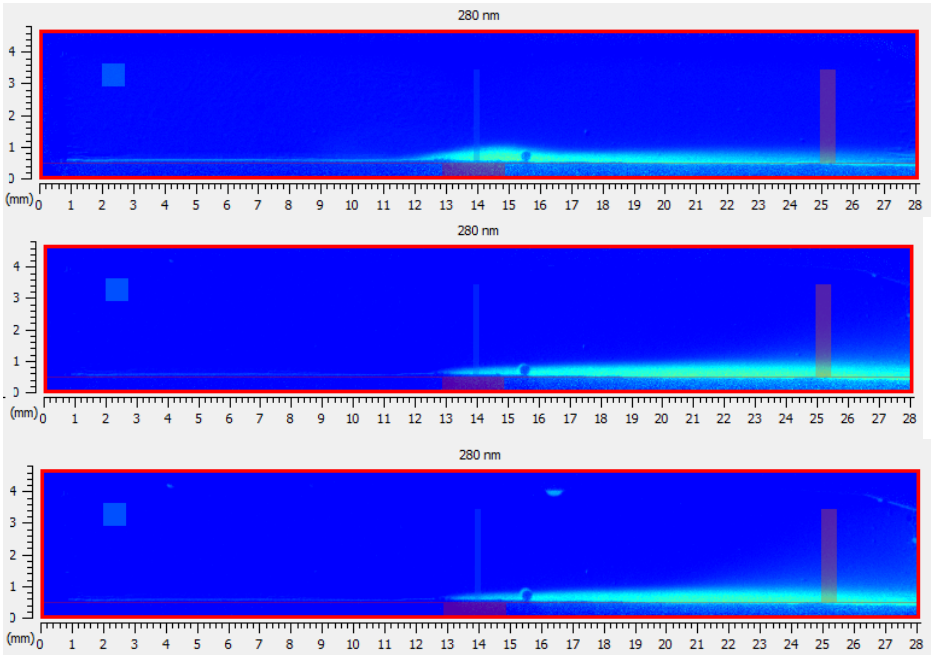

Figure 15: Selected absorbance maps from dissolution experiment on SA in acidic medium pH 1.2 with a flow rate of 1.0 ml/min. Images from t = 2 min, t = 15 min and t= 30 min

As Figure 16 shows, the absorbance of SA in pH 6.5 buffer is higher compared to that in pH 1.2 buffer. This suggests a higher solubility and dissolution rate, likely due to SA predominantly existing in the ionized form at pH 6.5. The same "tail forming" behavior is observed for the reasons described above. It is also important to note that absorbance at 280 nm is higher compared to the absorbance at 320 nm, as compared to the experiments in the acidic media where there was hard to tell a difference the two wavelengths.

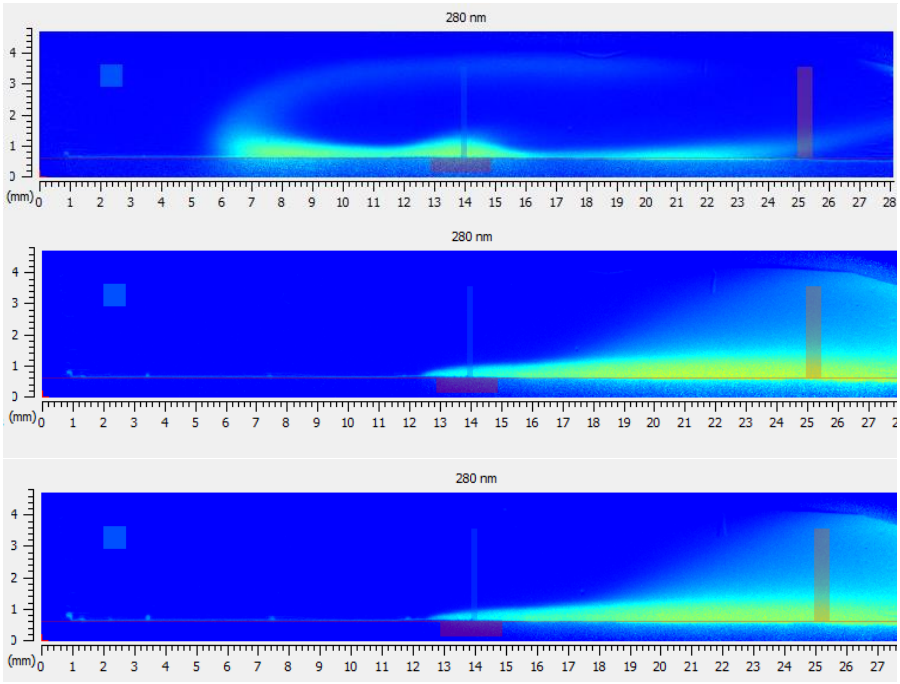

Figure 16: Selected absorbance maps from dissolution experiment on SA in phosphate buffer pH 6.5 with a flow rate of 0.5 ml/mi, recorded at 280 nm. Images from t = 2 min, t = 15 min and t= 30 min

4.1.2 Dissolution of sodium salicylate

The absorbance during dissolution of SS in pH 1.2 buffer, Figure 17, is significantly higher as compared of the absorbance of SA dissolving in the same medium. This was expected since salt formation increases the solubility, at controlled pH conditions. At t = 5 min, an "explosion" occurs in the middle of the flow cell, seen as the red areas. This is likely due to a very rapid dissolution of the salt. After the experiment, a very small, precipitated amount of SS was left in the sample holder which indicates that some compound had precipitated. After the "explosion", two air bubbles were formed at the top of the flow cell.

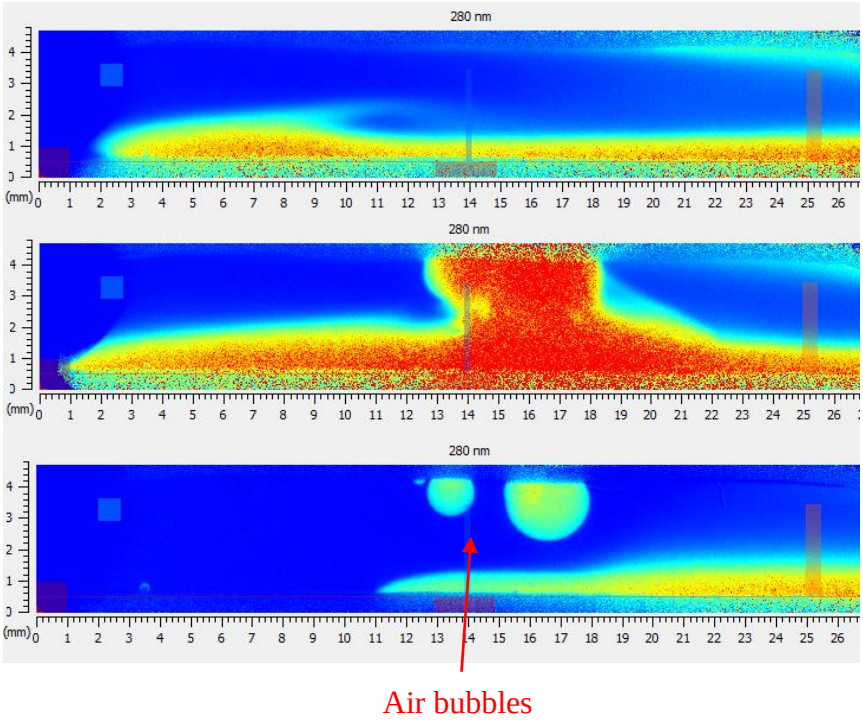

Figure 17: Selected absorbance maps from dissolution experiment on SS in acidic medium pH 1.2 with a flow rate of 0.5 ml/min. Images from t = 2 min, t = 5 min and t= 30 min.

In the experiment seen in Figure 18, a higher flow rate was applied. The images from this experiment are very similar to those from the experiment above, but overall the absorbance was lower. As mentioned, when discussing salicylic acid, this is reasonable as the higher flow rate "moves" the compound out of the cell at a faster rate.

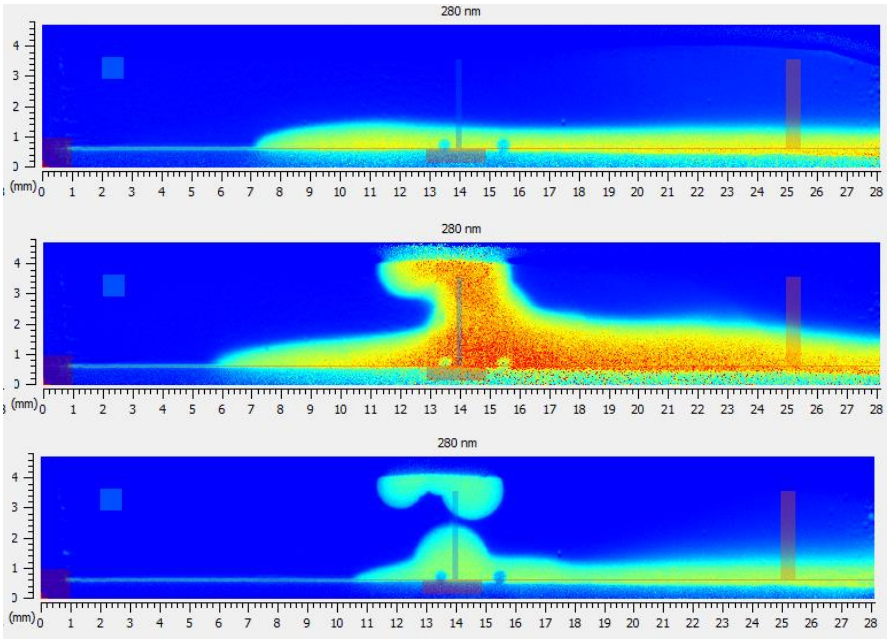

Figure 18: Selected absorbance maps from dissolution experiment on SS in phosphate buffer pH 1.2 with a flow rate of 1 ml/min. Images from t = 2 min, t = 5 min and t= 30 min.

As seen in Figure 19, the absorbance of SS in buffer pH 6.5 is initially slightly lower as compared to SS in pH 1.2 buffer. No "explosion is observed and instead the "tail" is formed at the beginning. In the beginning, there is a significant amount of SS dissolving to the left, against the flow of medium. At the end of the experiment the absorbance approaches zero, indicating complete dissolution of all SS, as no SS residue was detected in the sample holder.

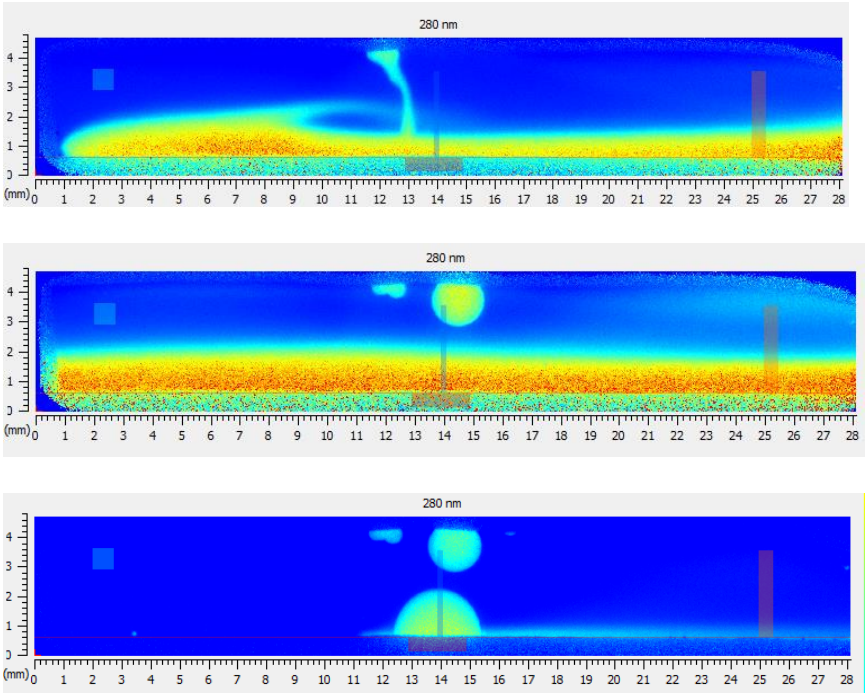

Figure 19: Selected absorbance maps from dissolution experiment on SS in phosphate buffer pH 6.5 with a flow rate of 0.5 ml/min Images from t = 2 min, t = 5 min and t= 30 min.

4.1.3 Summary of dissolution experiments

From the experiments presented above it is clear that SS has a higher dissolution rate in both mediums, as compared to SA. Both compounds dissolve more in the pH 6.5 buffer, which is consistent with the theory. It is also noted that for experiments with pH 6.5 buffer the absorbance is higher at 280 nm whereas for experiments performed with pH 1.2 buffer the absorbance is slightly higher at 320 nm. As will be shown in the following, this has applications for the base and acidic form absorbing light at different wavelengths.

4.1.4 Temperature – and Flow rate control experiments

Flow rate and temperature experiments are important in order to ensure that the data obtained from the SDi2, including IDR and pH calculations, are correct.

Table 3: Average temperature for each flow rate, between t = 20 min and t = 30, n = 3

Flow rate (ml/min)	Average temperature (°C)
0.5	36.6 ± 0.85
1.0	37.1 ± 0.29
3.0	37.1 ± 0.25

Table 4: Average temperature for each day, between t = 20 min and t = 30 min, n = 3

Day	Average temperature (°C)
1	37.4 ± 0.03
2	37.0 ± 0.10
3	36.3 ± 0.66

Overall, when performing 30 min long experiments with temperature set at 37 °C the SDi2 maintains a stable temperature. However, the temperature of the flow cell is probably affected by the temperature in the room, as the measured each day was different according to Table 4.

Table 5: Results from flow rate control experiments, n = 3

Flow rate (ml/min)	Average flow rate t= 3 min to t= 10 min (ml/min)	Average flow rate t = 20 min to t = 27 min (ml/min)	Average of all measurements (ml/min)	Average percentual difference of all experiments (%)
0.5	0.48 ± 0.001	0.47 ± 0.005	0.48 ± 0.004	3.26
1.0	0.97 ± 0.003	0.97 ± 0.02	0.97 ± 0.01	3.00
3.0	2.87 ± 0.03	2.85 ± 0.01	2.86 ± 0.02	4.71

The measured flow rate was 3.00 % to 4.71 % lower than the expected flow rate. No significant difference in measured flow rate was observed between the two different

measuring points. This suggests that the flow rate stays consistent throughout out a 30 min experiment. Considering that the pump program ran for 90 min, it can also be concluded that the instrument maintains a stable flow rate throughout a 90 min experiment.

4.2 Results from measurements in the Cary

Results from experiments conducted in the Agilent Cary 60 UV-Vis spectrophotometer are presented below. For additional details, see Appendix 5.

4.2.1 Initial experiments to study the pH dependence of SA absorbance

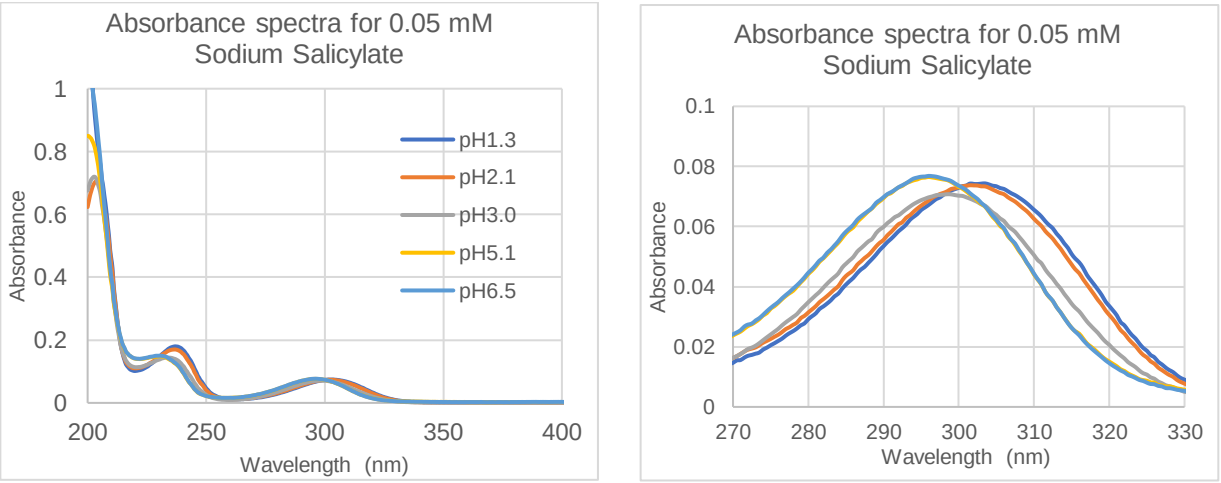

Figure 20: Absorbance spectrum of five SS solutions.

When performing dissolution experiments in the SDi2, there are 4 available wavelengths in the UV range; 255, 280, 300 and 320 nm. Among these, the most significant changes in absorbance with pH were observed at 280 nm and 320 nm as shown in Figure 20. At high pH (pH > pK_a) the charged form of SA is predominant whereas at low pH (pH< pK_a) the neutral is predominant. This suggests that the charged form has higher absorbance at 280 nm whereas the neutral form has a higher absorbance at 320 nm. It was noted that for further experiments a SS concentration higher than 0.05 M should be used, because of the low absorbance observed.

4.2.2 Calibration curves to calculate MEC of salicylic acid

See Appendix 5 for calibration curves. Assuming full protonation at pH 1.2 and full deprotonation at pH 6.5, the molar absorptivity constants were calculated. $\varepsilon_{H_2A,280nm} = 1.24$ $(mM)^{-1}cm^{-1}$, $\varepsilon_{H_2A,\ 320nm}$=1.56 $(mM)^{-1}cm^{-1}$, $\varepsilon_{HA^-,280nm}$=1.74 $(mM)^{-1}cm^{-1}$ and $\varepsilon_{HA^-,230nm} = 0.58$ $(mM)^{-1}$ cm^{-1}. e_1 was calculated to 0.80, e_2 to 1.12 and e_3 = 0.37

4.2.3 pH measurements

See Appendix 5 for full raw data set of absorbance measurements, calculated pH values and pH values measured using the pH-meter for all solutions listed in Table 1.

Calculating $pK'a$

In Figure 21 absorbance at 280 nm and 320 nm is plotted versus pH for the solutions listed in Table 1. This shows that for the acidic (low pH) solutions, absorbance is higher at 320 nm compared to 280 nm, for solutions of higher pH the opposite trend is observed. Additionally, the change in absorbance with pH is more pronounced at 320 nm. Equation 12 was used to

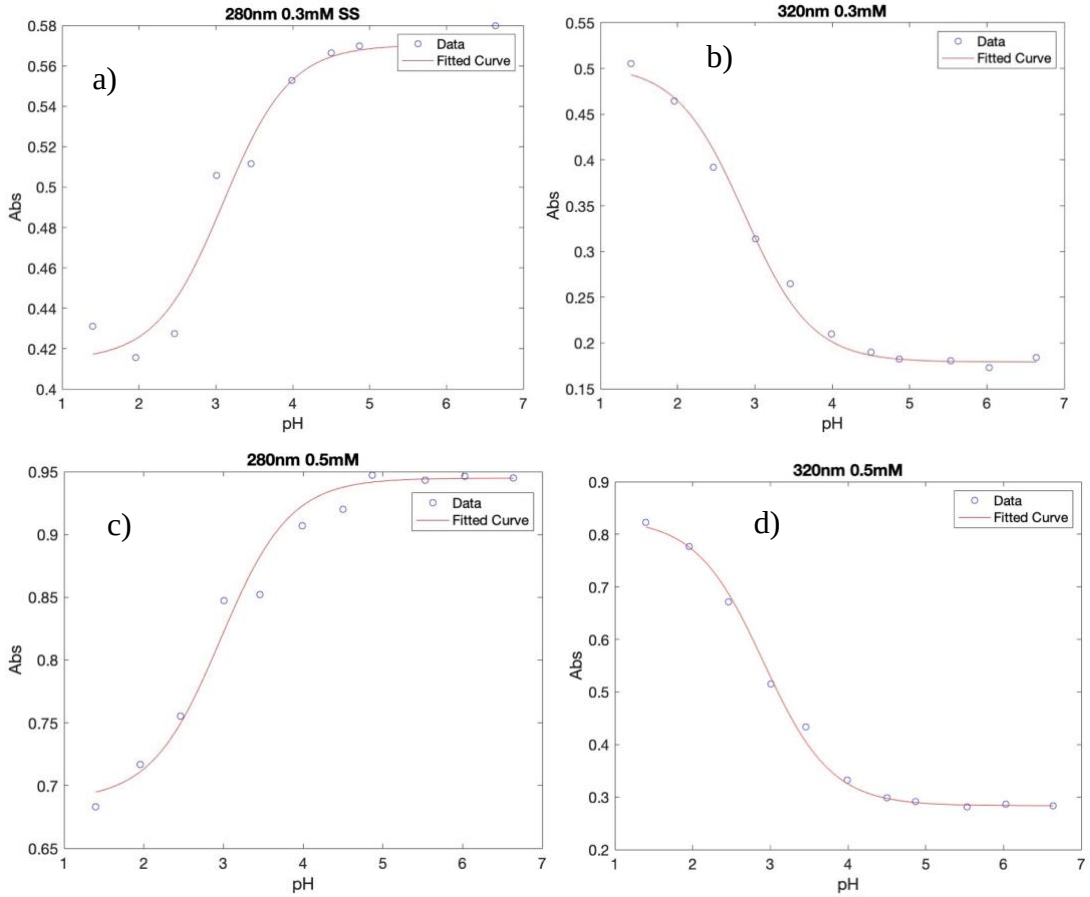

Figure 21: Plots of absorbance versus pH measured potentiometric for a) 0.3 mM SS at 280 nm, b) 0.3 mM SS at 320 nm, c) 0.5 mM SS at 280 nm and d) 0.5 mM at 320 nm.

determine $pK'a$ using MATLAB's curve fitting tool. A_{HA^-}, the absorbance of deprotonated salicylic acid was estimated to 0.570, 0.179, 0.945 and 0.284 for the four different plots in Figure 21. A_{H_2A}, the absorbance of fully protonated salicylic acid was left as an unknown as the graphs does not reach a plateau at low pH. Four $pK'a$ were calculated from Equation 14 with an average of 2.942.

pH calculations

Equation 14 was used to calculate the pH of solutions listed in Table 1. Figure 22 shows the calculated pH values, plotted against the potentiometric pH values, measured using the pH-meter. If the method of calculating pH from absorbance measurements were ideal, pH_{calc} = $pH_{potentiometric}$, this is represented by the black line in the graph.

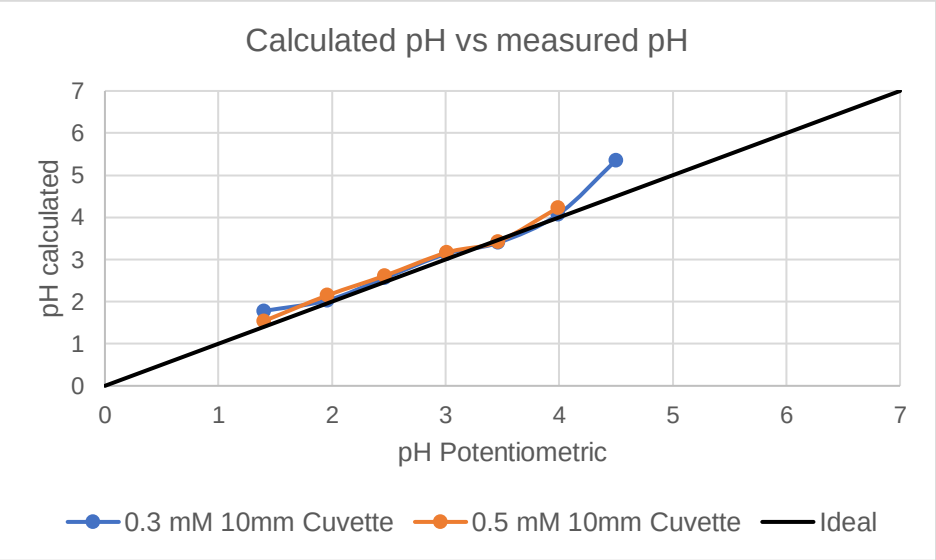

Figure 22: Calculated pH plotted against potentiometric pH measured in the pH meter. The graph only includes measurements conducted in a 10 mm cuvette.

As Figure 22 shows, calculated pH deviates from linearity at both high and low pH values. When calculating pH for solutions with pH 4.5 and above, invalid answers were obtained. This issue arises because Equation 14 is valid for Cary measurements only when the ratio R falls within the range of 0.80 to 3.00. According to the MEC's, the ratio of absorbance at the two different wavelengths should always fall within this range. If R falls outside of this range, the value within the log function becomes negative, rendering the logarithm undefined. In the case of these samples, R was higher than 3.00, resulting in invalid pH values. At high pH values, when pH >> $pK'a$ the substance SA is predominantly in its ionized form. By rearranging Equation 11, the fraction of ionized SA, denoted x_{HA^-}, is given by $\frac{10^{pH-pK'a}}{1+10^{pH-pK'a}}$. At pH 4.5, x_{HA^-} = 0.98 and increases to ≈ 1 at pH 6.5. As seen in Figure 21 absorbance reaches at plateau at high pH, and so will R. Consequently, at high pH, small changes in absorbance at either 280 nm or 320 nm result in minor changes in R, leading to significant changes in pH. The same reasoning applies at low pH, where x_{HA^-} approaches zero, causing the absorbance versus pH profile to reach an plateau. This indicates that calculating pH from absorbance at two wavelength is more sensitive at both high and low pH, i.e pH >> $pK'a$ or pH << $pK'a$ resulting in deviations from linearity. This sensitivity also leads to invalid answers, as a small change in absorbance can cause the R value to fall out of the valid range.

Doing these measurements in different light paths was of importance to ensure that the method is independent of light path. Results from measurements of pH 1.5, 3.0, 4.0, 6.0 and 6.5 in 1 mm and 2 mm cuvettes are presented in Figure 23. Invalid results were obtained from pH 6 and 6.5 solutions, and seen in the figure, the deviation from linearity is larger high and low pH values which can be explained by the same reason as above. The deviations larger is than observed in the 10 mm cuvette, this is reasonable since short path lengths give lower sensitivity in UV-Vis spectroscopy.

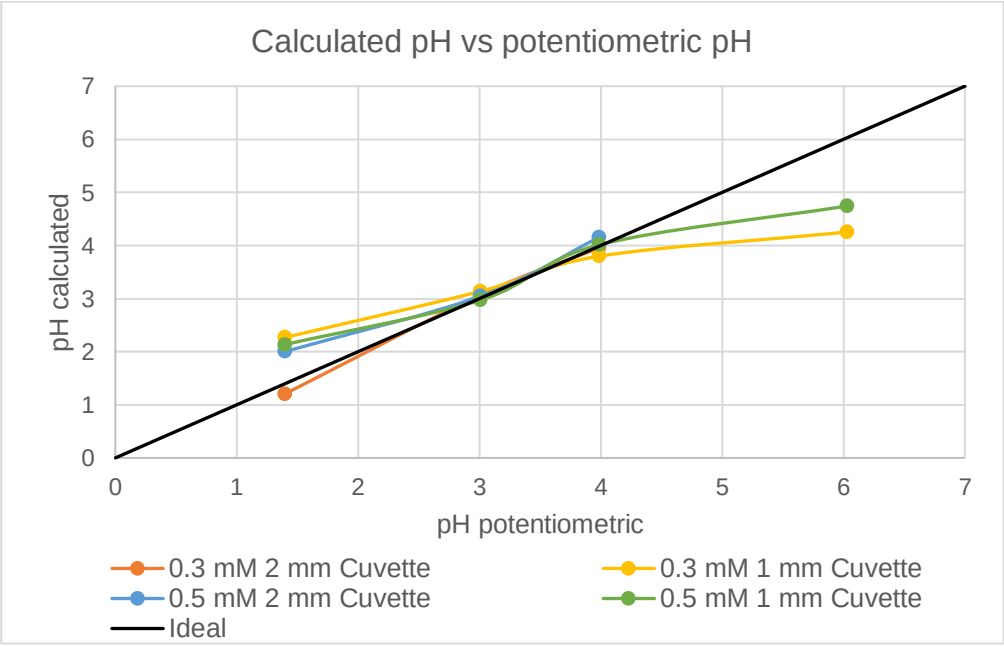

Figure 23: Calculated pH plotted against potentiometric pH measured in the pH meter. The graph only includes measurements conducted 1 mm and 2 mm cuvettes.

4.3 SDi2

Results from experiments conducted in the SDi2 are presented below. For additional details, see Appendix 6.

4.3.1 Calibration curves to calculate MEC of salicylic acid

The absorbance of the solutions with highest SS concentrations, 1.5 mM and 3.0 mM, showed a negative deviation from linearity and are therefore excluded from the calculations of MEC. The MEC's. were calculated too $\varepsilon_{H_2A,280nm}$ =1.26 $(mM)^{-1}$ cm^{-1}, $\varepsilon_{H_2A,\ 320nm}$= 1.17 $(mM)^{-1}$ cm^{-1}, $\varepsilon_{HA^-,280nm}$= 1.38 $(mM)^{-1}cm^{-1}$ and $\varepsilon_{HA^-,230nm}$ = 0.67 $(mM)^{-1}$ cm^{-1} using a path length of 9 mm. These MEC's are lower than the ones calculated from the Cary, indicating lower absorbance in the SDi2. e_1 was calculated to 1.08, e_2 to 1.17 and e_3 to 0.57. Negative deviation from linearity is observed at absorbance higher than 0.6, see Figure 24.

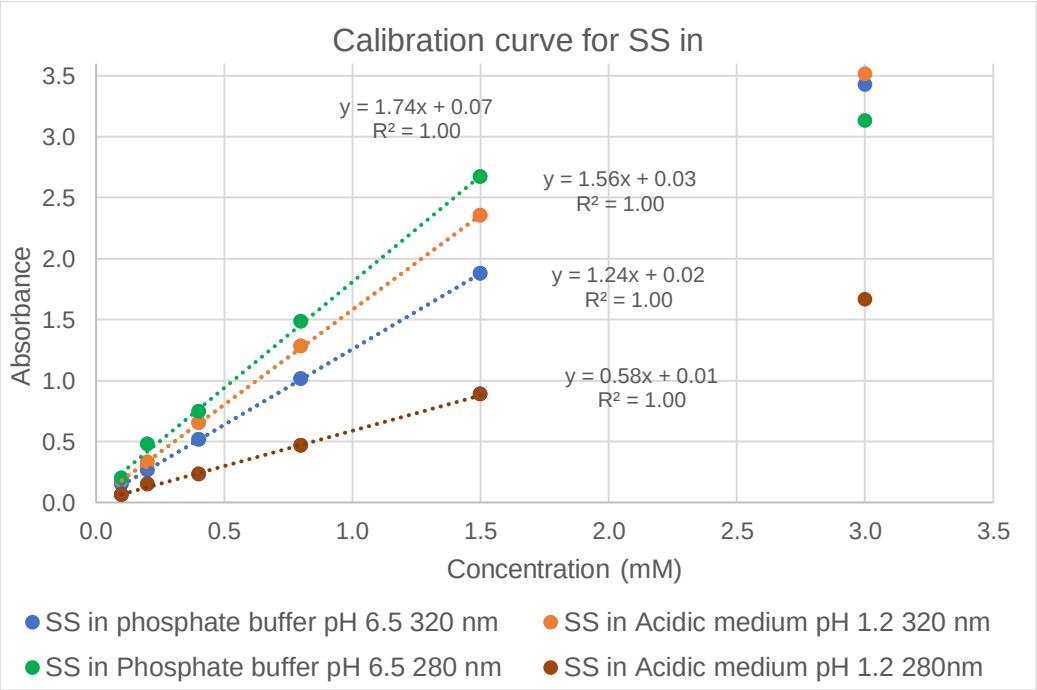

Figure 24: Calibration curves of sodium salicylate in phosphate buffer pH 6.5 and acidic medium pH 1.2 measured in the SDi2 at 280 nm and 320 nm.

4.3.2 Spectrophotometric pH measurements

Calculating $pK'a$

Matlab was used for plotting absorbance versus pH of the solutions and calculating $pK'a$ according to Equation 12, see Figure 25. However, the data points for the 280 nm

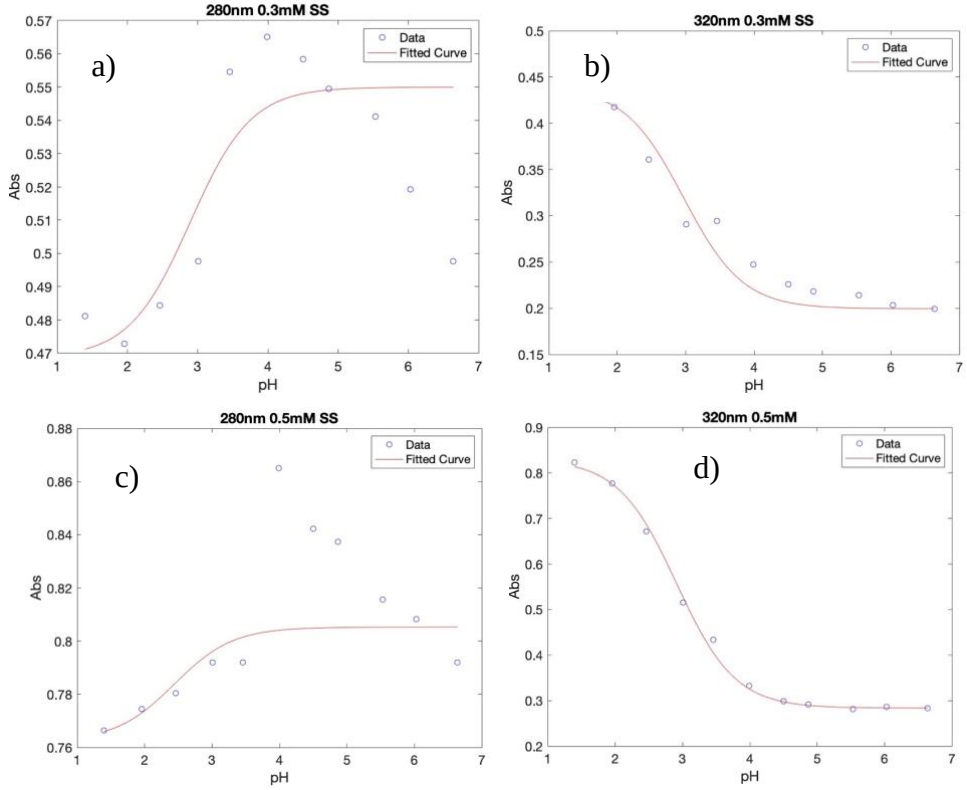

Figure 25: Plots of absorbance versus pH for a) 0.3 mM SS at 280 nm, b) 0.3 mM SS at 320 nm, c) 0.5 mM SS at 280nnmn and d) 0.5 mM at 320 nm.

measurements were very scattered leading to a low goodness of fit, $R^2 = 0.56$ for 0.3 mM SS and $R^2 = 0.32$ for 0.5 mM SS. Because of this, the $pK'a$ calculated using Cary was used for

pH calculations **(**$pK'a = 2.94$). The measurements at 280 nm does not reach a plateau at high pH, as would be expected. This will probably affect the pH calculations as will be explained below.

pH calculations

Equation 14 was used to calculate the pH of solutions listed in Table 1. Figure 26 shows the calculated pH values, plotted against the potentiometric pH values. For samples with pH values of 1.5, 4.0, 4.5, 5.0, 5.5, 6.0 and 6.5 invalid answers were obtained. For SDi2 measurements, Equation 14 is valid only when 1.08 < R < 2.05 and for the samples mentioned, R exceeds 2.05. Figure 26 shows that the calculated pH values from the SDi2 are generally higher than the potentiometric values, caused by the absorbance ratio R, being slightly higher than the ideal case. It is hard to be sure why this occurs, but it might be due to the scattering of measurements at 280 nm or the curvature of the calibration curve affecting the values of e_1, e_2 and e_3.

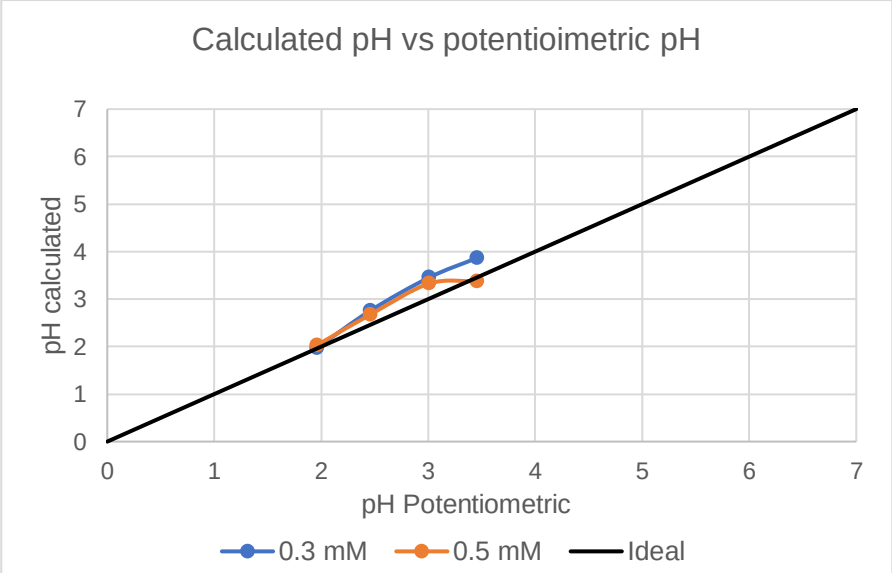

Figure 26: Calculated pH plotted against potentiometric pH measured in the pH meter.

4.3.3 IDR from dissolution experiments

The dissolution rate (IDR) was significantly higher for SS compared to SA, See Figure 27 and Table 6. For SA, dissolution rate was higher in the pH 6.5 buffers as expected, since at high pH, SA is mostly ionized, which increases its solubility. Increasing the flow for the acidic medium led to a lower IDR. This was unexpected, as a higher flow rate should increase IDR according to Equation 4. One possible explanation for this is the deviation from linearity at absorbance higher than 0.6 as seen in the calibration curves, Figure 24. This deviation causes

measured absorbance values to correspond to lower concentrations than actually present. Figures 13 and 14 show that absorbance at low flow rate is higher compared to at a high flow rates, causing the deviation from linearity to have a larger effect on the 0.5 ml/min experiment as compared to the 1.0 ml/min experiment. For the 0.5 ml/min experiment, there is also an air bubble at the top right corner contributing which increases the absorbance.

For sodium salicylate, absorbance for all SS experiments is far outside of the linear range, making IDR calculations unreliable. In order to determine reasonable IDR values, it is required that there is laminar flow and constant compact area, and it is possible that this was

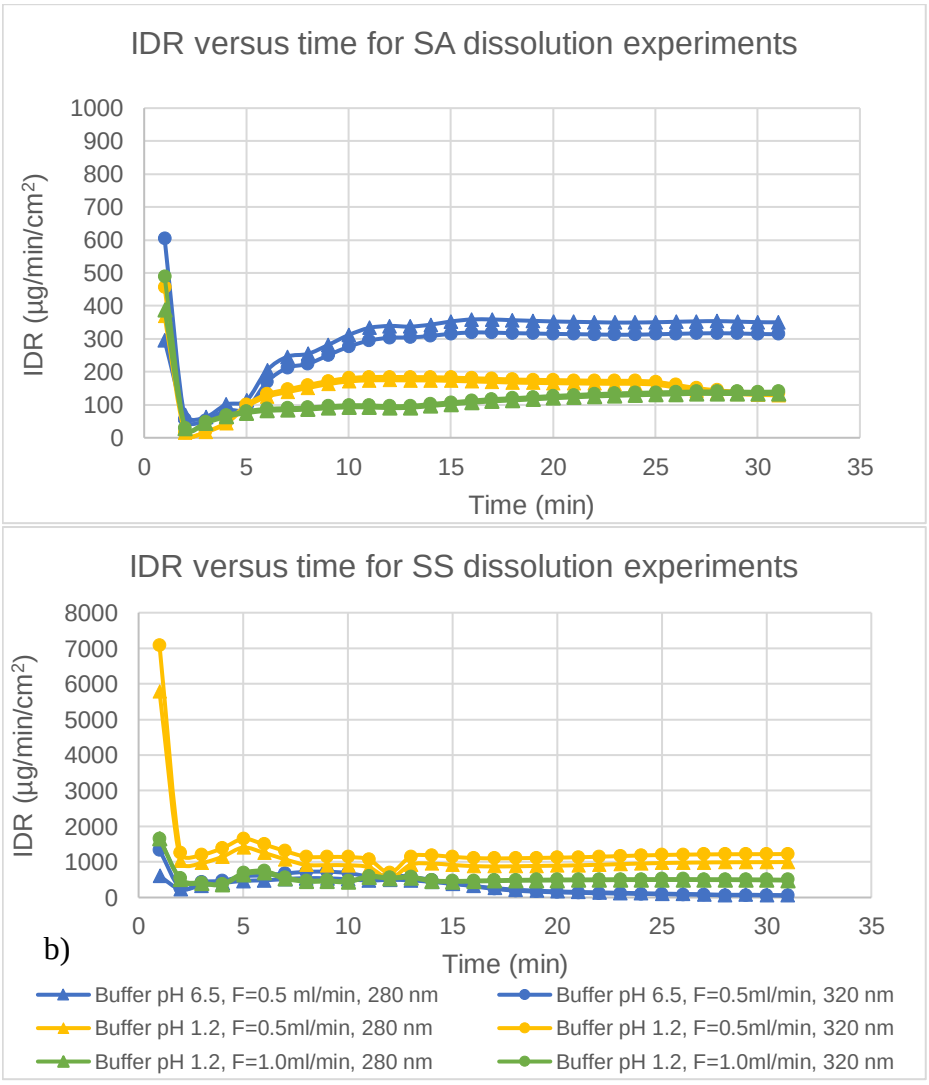

Figure 27: IDR for a) salicylic acid and b) sodium salicylate calculated in the SDi2 software according to Equations 4 and 5

not achieved for the SS experiments. The decrease in IDR with increased flow rate could be explained by most of the compound being dissolved before t = 17 min, and the little

compound left contributing to low absorbance and therefore low IDR, this applies especially to the SS in pH 6.5 buffer, where the absorbance in the end was close to zero, see Figure 19.

Table 6: Average IDR values for experiments in pH 6.5 and pH 1.2 buffers, calculated from t = 21 min to t=31 min and averaged over both wavelengths.

Experiment	**pH 1.2, F = 0.5 ml/min**	**pH 1.2, F = 1.0 ml/min**	**pH 6.5, F = 0.5 ml/min**
IDR SA (average) [µg/min/cm^2]	153	133	333
IDR SS (average) [µg/min/cm^2]	1072	498	100

Experiments were also conducted in pH 3 buffers and NaCl solutions, see Table 2. To be able to calculate the IDR of the pH 3 and NaCl solutions, the mean extinction coefficients were of SS in pH 3 solutions were calculated to $\varepsilon_{pH\ 3,280nm} = 1.33$ (mM)$^{-1}$cm^{-1}, $\varepsilon_{pH\ 2,320nm}$=0.88 (mM)$^{-1}$cm^{-1}, see Appendix 4 for calculations.

Calculated IDR for these experiments is found in Figure 28. Some of the same trends are described previously are observed, for example, IDR is higher for SS as compared to SA. A different pump program was applied to these experiments, where flow rate was increased from 0.5 ml/min to 1.0 ml/min after 17 minutes. Figure 28 shows that this causes the IDR to decrease which is as mentioned before unexpected. Why this occurs for the experiments with SA is hard to explain, but it could be caused by the deviation from linearity, as explained before. For the experiments with SS, absorbance is far from the linear range during the first 15 min, giving rise to unreliable results. SA has the lowest IDR in the NaCl solution which is explained by SA decreasing the pH of the NaCl solution, causing low solubility. SS has the highest IDR in the NaCl solution, probably due to the fact that SS does not decrease the pH and stays in the ionized form.

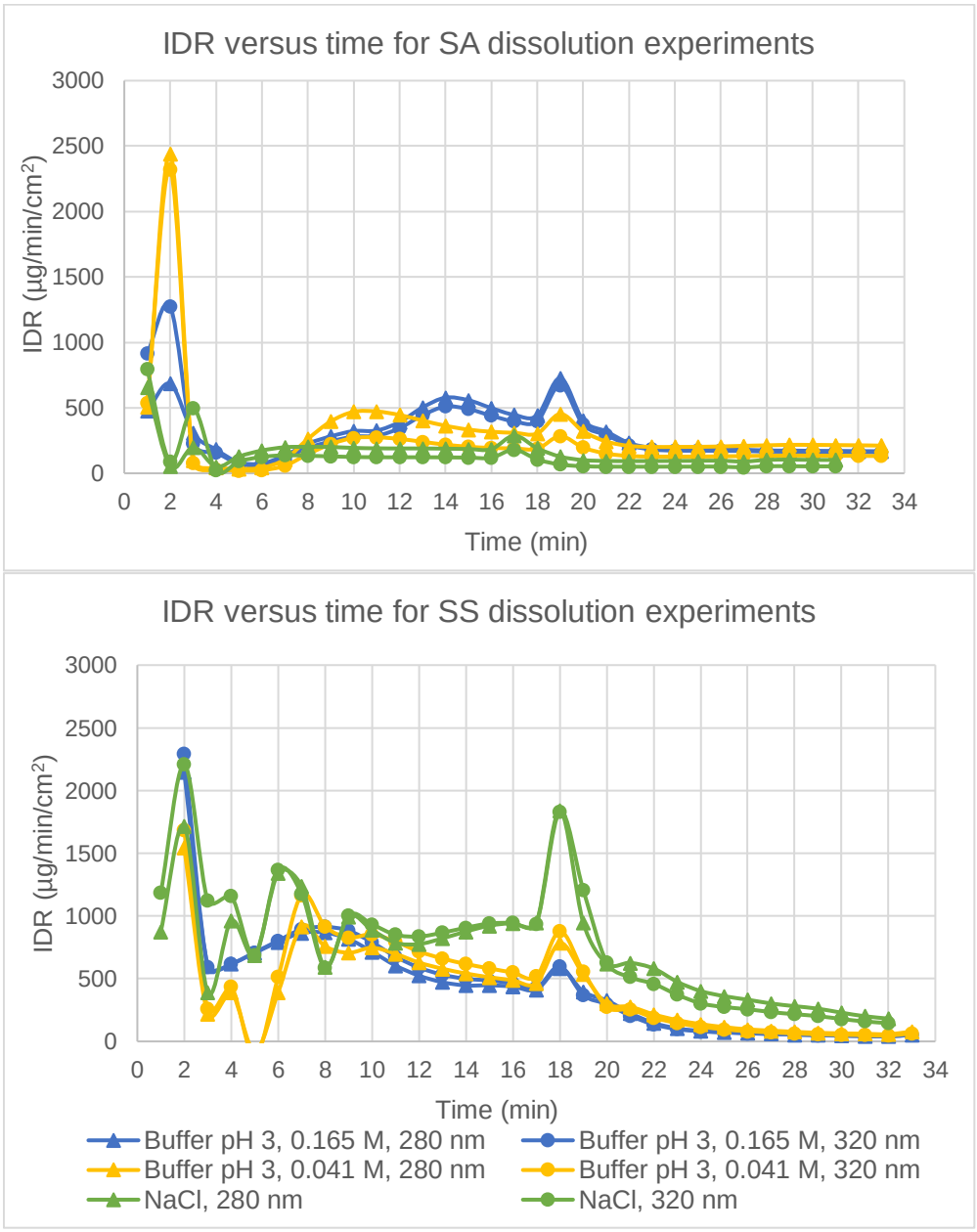

Figure 28: IDR for a) salicylic acid and b) sodium salicylate calculated in the SDi2 software according to Equations 4 and 5

4.3.4 Calculating microenvironmental pH during dissolution experiments

In order to compare pH measurements in the SDi2, solutions of SS and SA dissolved in the dissolution media was prepared and pH was measured in the pH meter.

Table 7: pH measured in pH meter and for SS and SA solutions of C = 0.3 mM

Solution	**pH potentiometric**
SS in NaCl	6.21
SA in NaCl	3.67
SS in pH 3, C = 0.041M	3.07
SA pH 3, C= 0.041M	2.95
SA in pH 3, C= 0.165 M	3.04
SS in pH 3, C=0.165 M	3.01

pH measurements in SDi2

Figures 30, 31, 33 and 34 shows calculated pH values from an experiment conducted in pH 3 buffer with a buffer capacity of 0.041 M. Absorbance was collected at two different zones and measurements at four time points were selected, two where a flow rate of 0.5 ml/min was applied and two where 1.0 ml/min was applied. Absorbance and calculated pH is plotted versus z, which is the height of the flow cell. As the Figures shows, many points are placed on the x-axis, this does not mean pH = 0, but rather these are the points where invalid answers were obtained, because of R being outside of the valid range. Far from the surface, (high z values), the calculated pH should be the same as pH of the buffer, pH 3.03. When looking at the results from the surface zone, this seems to be the case for all time points, although more scattering is observed at t = 20-21 min and t = 30-31 min. Close to the surface, (low z values), the pH is slightly lower which is in line with the measurement in the pH meter, see Table 7. For the IDR zone, a similar behavior is observed. pH is lower closer to the surface and approaches the pH of the buffer further from the surface. For the surface zone, more scattering occurs at the later time points, this is probably due to the fact that the absorbance is close to zero causing a larger sensitivity to errors in absorbance measurements.

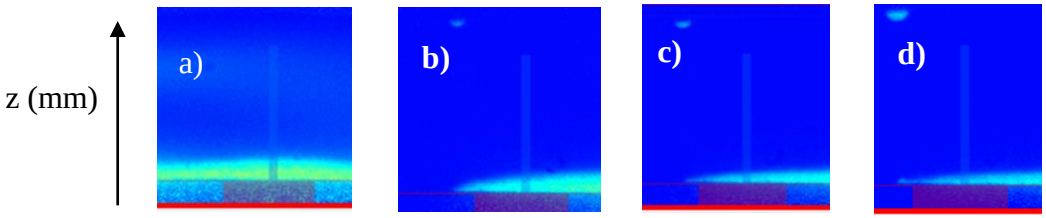

Figure 29: Images from the surface zone at a) t = 5 min, b) t = 15 min, c) t= 20 min and d) t= 30 min when SA dissolves in pH 3 buffer.

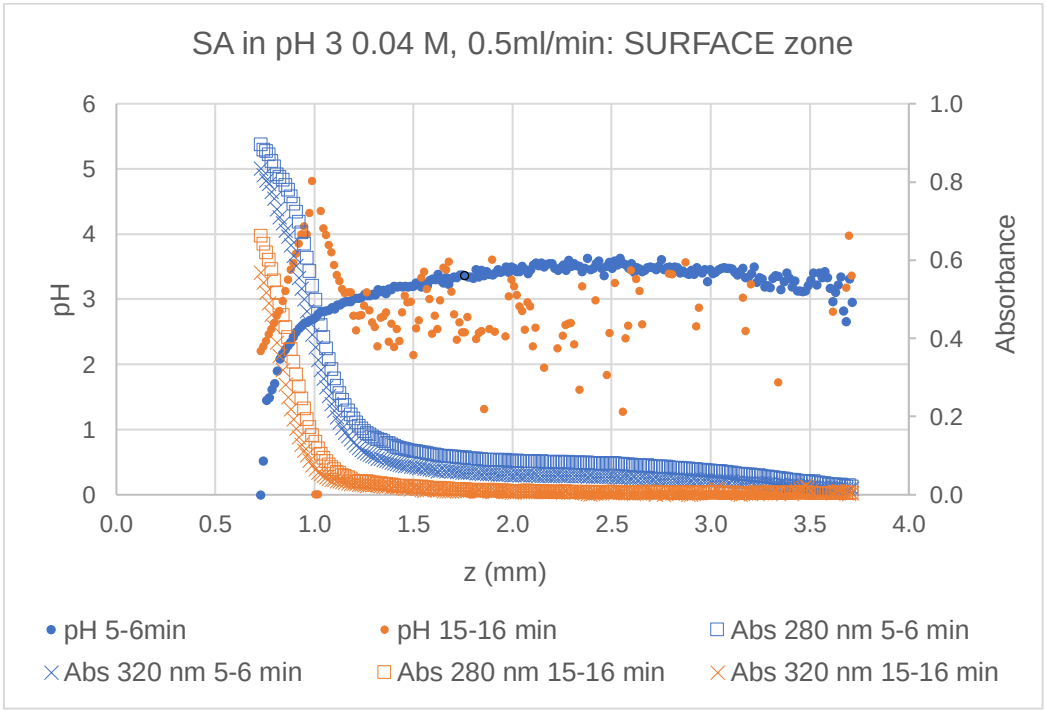

Figure 30: Average measured absorbance and calculated pH for two time intervals of SA dissolving in pH 3 buffer, C = 0.041M, plotted against z. Data was collected from the surface zone.

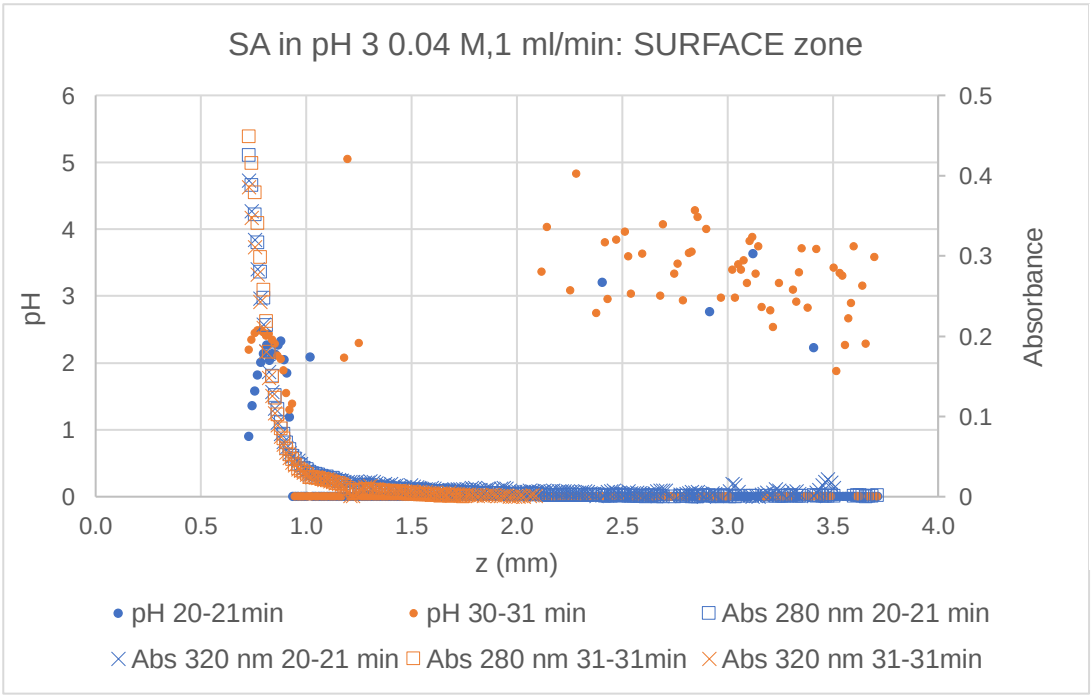

Figure 31: Average measured absorbance and calculated pH for two time intervals of SA dissolving in pH 3 buffer, C = 0.041M, plotted against z. Data was collected from the surface zone.

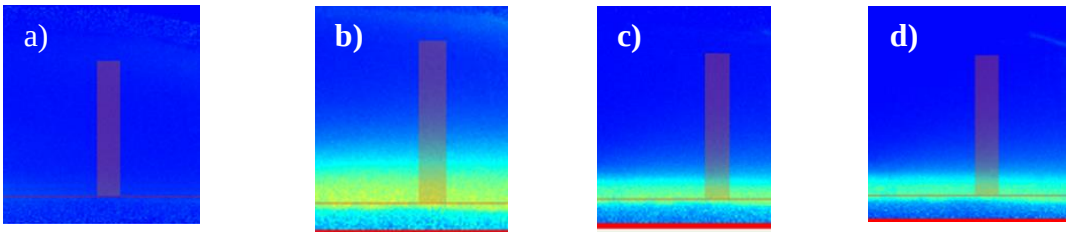

Figure 32: Images from the IDR zone at a) t = 5 min, b) t = 15 min, c) t = 20 min and d) t = 30 min when SA dissolves in pH 3 buffer.

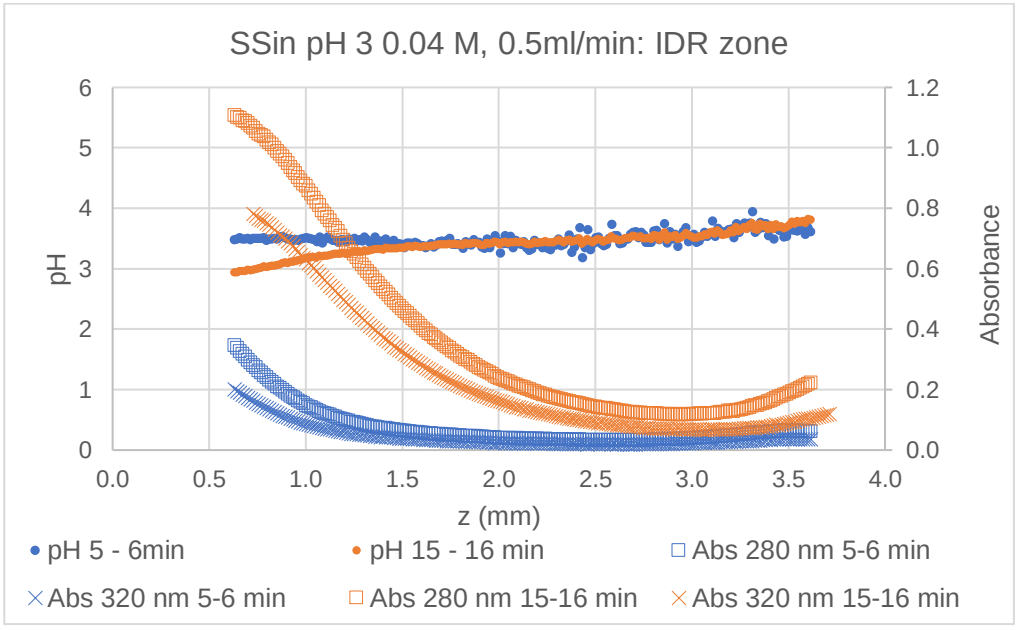

Figure 33: Average measured absorbance and calculated pH for two time intervals of SA dissolving in pH 3 buffer, C = 0.041M, plotted against z. Data was collected from the IDR zone.

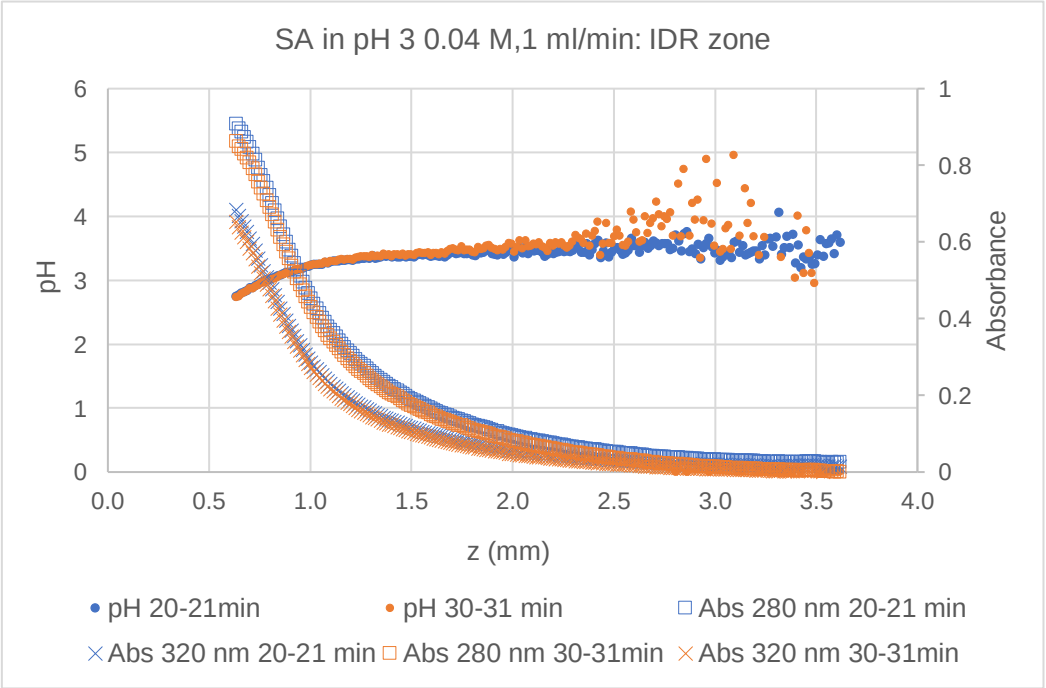

Figure 34: Average measured absorbance and calculated pH for two time intervals of SA dissolving in pH 3 buffer, C = 0.041M, plotted against z. Data was collected from the IDR zone.

Figure 35 shows a part of the result from dissolving SA in NaCl. The NaCl solution had a pH of 6.03, and as the figure shows pH approaches 6 at high z values, further from the surface. Close to the surface, where absorbance is higher, pH approaches 3 which is in line with the pH measured of SA in NaCl, 3.67. The fact that there are a lot of invalid results at high z values agree with that the method is more sensitive at high and low pH values. Absorbance is also very low at high Z values because of the small amount of compound being present, this may increase the sensitivity even more.

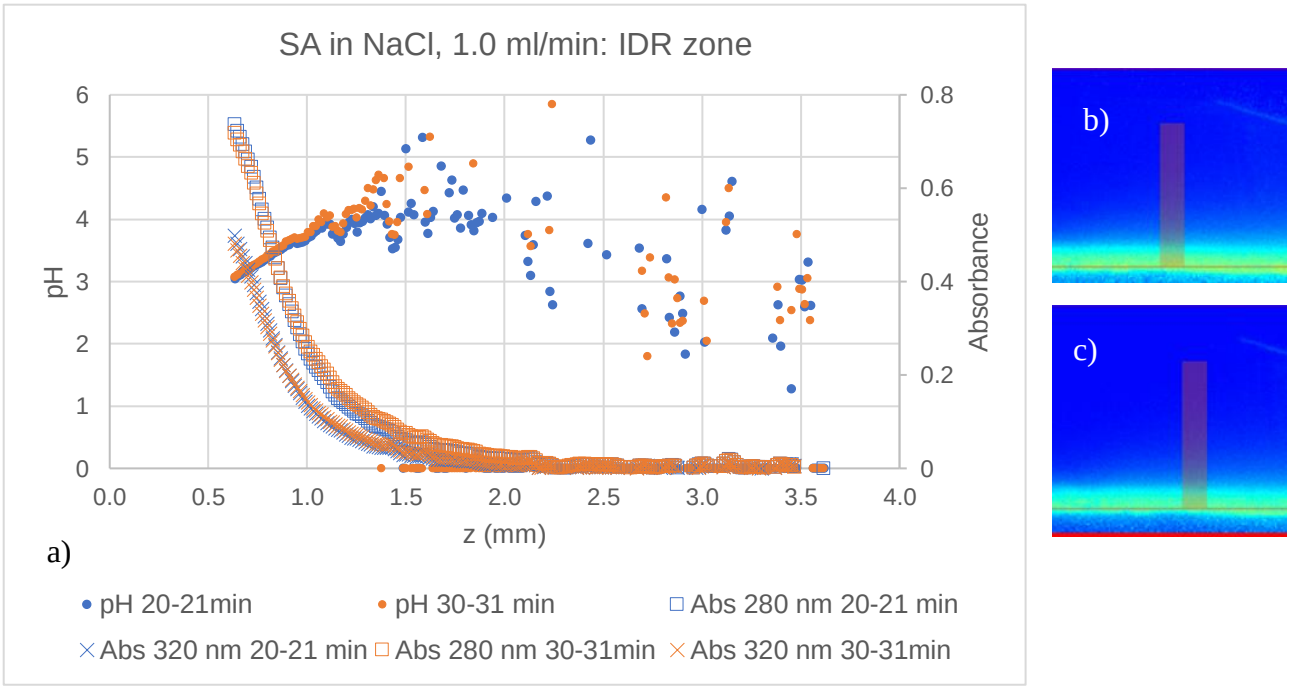

Figure 35: a) plot of absorbance and calculated pH versus z from, b) images from the IDR zone at t = 20 min and c) t = 30 min when SA dissolves in NaCl solution. Data was collected from the IDR zone.

More experiments to calculate microenvironmental pH during dissolution experiments in the SDi2 were performed and can be found in Appendix 6. The experiments using SA showed similar trends as described above. When it comes to SS, as mentioned before, the absorbance was far outside of the linear range causing many invalid results. Figure 36 shows a plot from an experiment dissolving SS in pH 3 buffer. Close to the surface, invalid answers were obtained since the R value was below 1.08, likely due to the high absorbance at both wavelengths, causing R to be close to 1. Far away from the surface, pH approaches 3, the pH of the bulk solution. As Figure 36 b) shows, an air bubble arose at t = 5 min, causing an increase in absorbance and consequently incorrect pH values where the air bubble is placed. Air bubbles occurred for all experiments with SS, making the results misleading. Low pH,

close to 1, was calculated in the middle of the flow cell. This may be due to the sensitivity of the method and absorbance being outside of the linear range, as it is unreasonable that SS decreases the pH of the dissolution medium to such an extent.

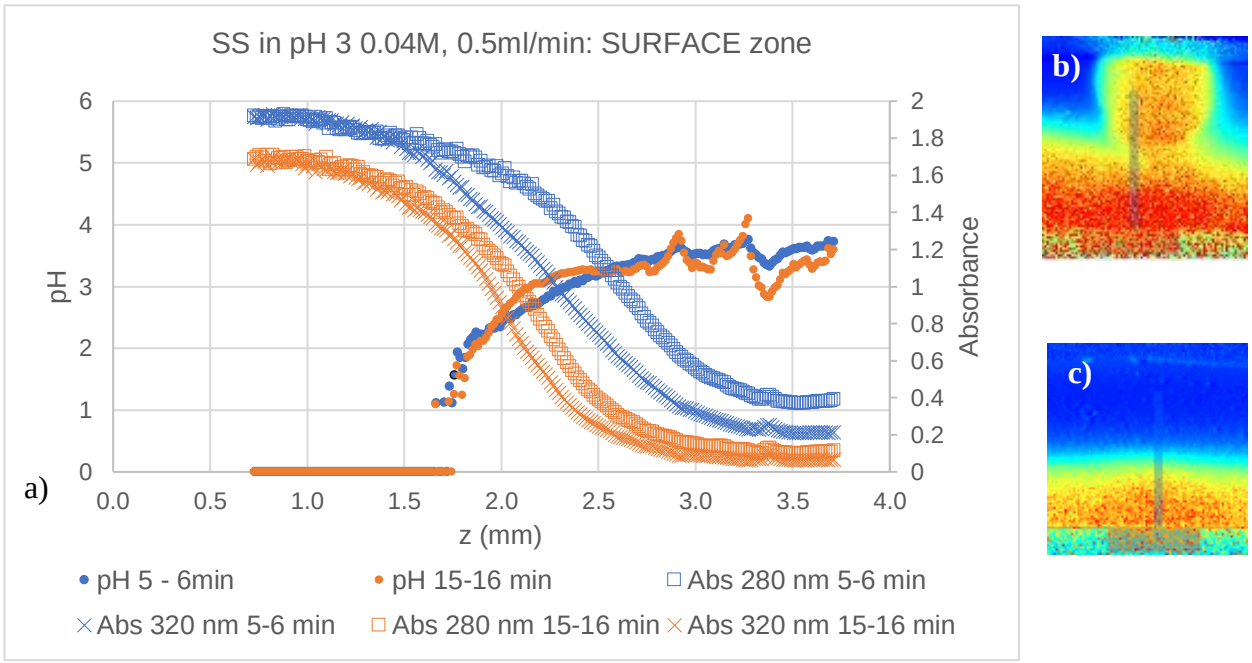

Figure 36: a) plot of absorbance and calculated pH versus z from, b) images from the surface zone at t = 5 min and c) t = 15 min when SS dissolves in pH 3 buffer.

.

5. Conclusion and future work

Experiments demonstrate that the SDi2 maintains a stable temperature and flow rate, which is crucial for analyzing dissolution experiments accurately. A recurring issue in these experiments is the presence of air bubbles, which can distort results and complicate analysis. The dissolution experiments indicate that sodium salicylate acid has significantly higher solubility and dissolution rates compared to salicylic acid, consistent with theoretical predictions. Experiments on salicylic acid suggest that its intrinsic dissolution rate (IDR) is higher in media with higher pH, as expected theoretically. However, due to the very high solubility and dissolution rate of sodium salicylate, drawing firm conclusions on how IDR is affected by the dissolution medium and flow rate is challenging, necessitating further experiments.

For a drug substance to serve as its own pH probe, meaning that the pH can be measured by the drug itself, it must be UV absorbing and a weak base or acid whose absorbance is affected by pH. Measurements in the Cary spectrophotometer show that the absorbance of salicylic acid solutions depends on pH, allowing salicylic acid to serve as its own UV probe. Using the SDi2, pH could be calculated using a two-wavelength approach. This is the first time this method has been applied to calculate the pH of a drug substance acting as its own pH probe, presenting significant future potential.

During salicylic acid dissolution experiments in the SDi2, it was shown that the pH close to the surface differed from the bulk pH, indicating that salicylic acid alters the pH of the dissolution medium. However, results obtained from pH measurements using the two-wavelength approached contained a significant high proportion of invalid or incorrect results, especially in solutions of pH far from the pK_a of the drug substance. This was likely due to deviations from linearity at high absorbance and measurement uncertainty. Therefore, this method requires further development.

One significant limitation to method is the UV imaging instrument the SDi2. Problem with air bubbles frequently occurred, and the narrow linear absorbance range allowed for accurate pH determination at low absorbance levels which limits the range of drug substances that can be studied. For instance, many salts of acidic or basic drugs have solubilities that are too high for pH to be measured accurately during dissolution. Furthermore, there are only five available

wavelengths in the SDi2 which precludes the possibility of examining the absorbance maxima of both the neutral and charged forms of the compound, something that might would be beneficial for pH determination.

Despite these limitations, the future of conducting dissolution experiments and measuring pH using this method appears promising. Further studies could include examining pH measurements of other drug substances that meet the criteria for serving as their own pH probes. Different dissolution media could be studied, measurements should be conducted at various wavelengths, and more replicates should be investigated to fully understand and validate the method.

Reference list

Agilent (n.d.). UV-Vis Spectrophotometer, Routine UV-Vis, Cary 60 | Agilent. [online] www.agilent.com. Available at: https://www.agilent.com/en/product/molecular-spectroscopy/uv-vis-uv-vis-nir-spectroscopy/uv-vis-uv-vis-nir-systems/cary-60-uv-vis-spectrophotometer?gad_source=1&gclid=CjwKCAjw5v2wBhBrEiwAXDDoJd5X6yFaQ64qXFQI_7YY1xmJ2dQm00zxx5S9KD_Vn8g_lPkuavwZDBoCpoEQAvD_BwE&gclsrc=aw.ds#productdetailsv [Accessed 17 Apr. 2024].

Bates, R.G. (1973). Determination of pH. 2nd ed. New York: Wiley, pp.135–162.

Bock, F., Johan Peter Bøtker, Susan Weng Larsen, Lu, X. and Jesper Østergaard (2022). Methodological Considerations in Development of UV Imaging for Characterization of Intra-Tumoral Injectables Using cAMP as a Model Substance. International journal of molecular sciences, [online] 23(7), pp.3599–3599. doi:https://doi.org/10.3390/ijms23073599.

Brown, B., Ward, A., Fazili, Z., Østergaard, J. and Asare-Addo, K. (2021). Application of UV dissolution imaging to pharmaceutical systems. Advanced Drug Delivery Reviews, 177, p.113949. doi:https://doi.org/10.1016/j.addr.2021.113949.

Clayton, T.D. and Byrne, R.H. (1993). Spectrophotometric seawater pH measurements: total hydrogen ion concentration scale calibration of m-cresol purple and at-sea results. Deep Sea Research Part I: Oceanographic Research Papers, 40(10), pp.2115–2129. doi:https://doi.org/10.1016/0967-0637(93)90048-8.

Dhat, C.R. and D Jahagirdar (1982). Copper(II) Chelates of Substituted Salicylic Acids-A Thermodynamic Study. Indian Journal of Chemistry, 21(8).

Farajtabar, A. and Gharib, F. (2010). Solvent effect on protonation constants of salicylic acid in mixed aqueous organic solutions of DMSO. Monatshefte für Chemie - Chemical Monthly, 141(4), pp.381–386. doi:https://doi.org/10.1007/s00706-010-0277-5.

French, C.R., Carr, J.J., Dougherty, E.M., Eidson, L.A.K., Reynolds, J.C. and DeGrandpre, M.D. (2002). Spectrophotometric pH measurements of freshwater. Analytica Chimica Acta, 453(1), pp.13–20. doi:https://doi.org/10.1016/s0003-2670(01)01509-4.

Harris, D.C. (2007). Quantitative Chemical Analysis. 7th ed. New York: W H Freeman And Company.

Li, S., Wong, S., Sethia, S., Almoazen, H., Joshi, Y.M. and Serajuddin, A.T.M. (2005). Investigation of Solubility and Dissolution of a Free Base and Two Different Salt Forms as a Function of pH. Pharmaceutical Research, 22(4), pp.628–635. doi:https://doi.org/10.1007/s11095-005-2504-z.

Nelson, K.G. and Shah, A.C. (1975). Evaluation of a Convective Diffusion Drug Dissolution Rate Model. Journal of Pharmaceutical Sciences, 64(9), pp.1518–1520. doi:https://doi.org/10.1002/jps.2600640920.

Østergaard, J. (2016). UV/Vis Spectrophotometry and UV Imaging. Advances in Delivery Science and Technology, pp.3–27. doi:https://doi.org/10.1007/978-1-4939-4029-5_1.

Østergaard, J., Jensen, H., Larsen, S.W., Larsen, C. and Lenke, J. (2014a). Microenvironmental pH measurement during sodium naproxenate dissolution in acidic medium by UV/vis imaging. Journal of Pharmaceutical and Biomedical Analysis, 100, pp.290–293. doi:https://doi.org/10.1016/j.jpba.2014.08.014.

Østergaard, J., Lenke, J., Sun, Y. and Ye, F. (2014b). UV Imaging for In Vitro Dissolution and Release Studies: Intial Experiences. Dissolution Technologies, 21(4), pp.27–38. doi:https://doi.org/10.14227/dt210414p27.

Pratap Chandra Acharya, Sarapynbiang Marwein, Mishra, B., Ghosh, R.S., Vora, A. and Tekade, R.K. (2018). Role of Salt Selection in Drug Discovery and Development. Elsevier eBooks, i, pp.435–472. doi:https://doi.org/10.1016/b978-0-12-814423-7.00013-7.

Serajuddin, A.T.M. (2007). Salt formation to improve drug solubility. Advanced drug delivery reviews, [online] 59(7), pp.603–16. doi:https://doi.org/10.1016/j.addr.2007.05.010.

Serajuddin, A.T.M. and Jarowski, C.I. (1985). Effect of Diffusion Layer pH and Solubility on the Dissolution Rate of Pharmaceutical Acids and Their Sodium Salts II: Salicylic Acid, Theophylline, and Benzoic Acid. Journal of Pharmaceutical Sciences, 74(2), pp.148–154. doi:https://doi.org/10.1002/jps.2600740209.

Shaolong, H., Jacobsen, J., Uhd Nielsen, C., Genina, N., Østergaard, J. and Mu, H. (2021). Exploration of in vitro drug release testing methods for saquinavir microenvironmental pH modifying buccal films. European Journal of Pharmaceutical Sciences, [online] 163(1 August 2021). doi:https://doi.org/10.1016/j.ejps.2021.105867.

Sinko, P.J. and Martin, A.N. (2011). Martin's physical pharmacy and pharmaceutical sciences : physical chemical and biopharmaceutical principles in the pharmaceutical sciences. 6th ed. Philadelphia, Pa. ; London: Lippincott Williams & Wilkins, pp.154–161.

Taylor, K.M.G. and Aulton, M.E. (2018). Aulton's Pharmaceutics E-Book : The Design and Manufacture of Medicines. 5th ed. Elsevier Ltd, pp.21–26.

Appendix 1

This section contains derivations of Equations 12 and 14.

Derivation of Equation 12

Definitions of the thermodynamic dissociation constant K_a and the mixed apparent dissociation constant $K_a{}'$

$$K_a = \frac{a_{H^+} * a_{A^-}}{a_{HA}} = \frac{[H^+]*[A^-]}{[HA]} * \frac{\gamma_{H^+} * \gamma_{A^-}}{\gamma_{HA}} \quad (1)$$

$$K'_a = \frac{a_{H^+} * [A^-]}{[HA]} = \frac{[H^+]*[A^-]}{[HA]} * \gamma_{H^+} \quad (2)$$

From Equations 1 and 2 the acidity constant pK_a and apparent acidity constant pK'_a are defined according to Equation 3 and 4 (Sinko and Martin, 2011).

$$pK_a = pH - log\left(\frac{[A^-]}{[HA]}\right) - log\left(\frac{\gamma_{A^-}}{\gamma_{HA}}\right) \quad (3)$$

$$pK'_a = pH - log\left(\frac{[A^-]}{[HA]}\right) \quad (4)$$

The mixed apparent dissociation constant takes ionic strength and temperature into account and is obtained from concentration measurements, therefore this will be used for the following calculations.

When dissolving a weak acid in water, the following acid-base equilibrium takes place:

$$HA\ (aq) \rightleftharpoons H^+(aq) + A^-(aq)$$

The concentration c, of a light absorbing species in solution can be determined by Beer Lamberts law. The absorbance of a solution at a given wavelength containing absorbing species being present is the sum of absorbance of each species, according to Equation 5 where HA corresponds to the acidic form and A^- to the basic form and x to the partially transformed compound.

$$A_x = c_{HA}\varepsilon_{HA}l + c_{A^-}\varepsilon_{A^-}l \quad (5)$$

If c is the total substance concentration, the concentration of the acidic and basic form becomes $(1-\alpha) * c$ and $\alpha * c$, respectively, where α is the degree of dissociation. Equation 5 therefore becomes

$$A_x = (1-\alpha)A_{HA} + \alpha A_{A^-} \quad (6)$$

Rearranging Equation 6 gives the ratio of the concentration of the acidic and basic form, $\alpha/(1-\alpha)$ (Bates, 1973)

$$\frac{\alpha}{1-\alpha} = \frac{A_x - A_{HA}}{A_A - - A_x} \tag{7}$$

By substituting Equation 7 in Equation 4,

$$pK'_a = pH - log\left(\frac{\alpha}{1-\alpha}\right) = pH - log\left(\frac{A_x - A_{HA}}{A^- - A_x}\right) \tag{8}$$

Rearranging Equation 8 and plotting measured absorbance values against pH gives Equation 9 (Østergaard, 2016).

$$A_x = \frac{A_{HA} + A_{A^-} * 10^{(pH - pK'a)}}{10^{(pH - pK'a)}} \tag{9}$$

Derivation of Equation 14

Salicylic acid exist in three different forms, H_2A HA^- and A^{2-}. The chemical equilibria between these forms can be described by the dissociation constants $K_{a,1}$ and $K_{a,2}$

$A^{2-} + H^+ \Leftrightarrow HA^-$ $\qquad K_{a,1} = \frac{[A^{2-}]\,[H^+]}{[HA^-]}$ (10a)

$HA^- + H^+ \Leftrightarrow H_2A$ $\qquad K_{a,2} = \frac{[HA^-]\,[H^+]}{[H_2A]}$ (10b)

The total concentration of salicylic acid, $C_{tot} = [A_2^-]^- + [HA^-] + [H_2A]$ can be written as

$$A_T = [A^{2-}]\left(1 + \frac{[H^+]}{K_{a,1}} + \frac{[H^+]^2}{K_{a,1}K_{a,2}}\right) \tag{11}$$

using Equations 10a and 10b. The total absorbance of salicylic acid is the sum of the absorbance of each species.

$$A_\lambda = \left({}_\lambda\varepsilon_{A^{2-}}[A^{2-}] + {}_\lambda\varepsilon_{HA^-}[HA^-] + {}_\lambda\varepsilon_{H_2A}[H_2A]\right) * l \tag{12}$$

Where A_λ is the absorbance at wavelength λ, ${}_\lambda\varepsilon_x$ is the molar absorptivity of species x at wavelength λ and l is the path length. Equation 12 can be written as

$$A_\lambda = [A^{2-}]\left({}_\lambda\varepsilon_{A^{2-}} + {}_\lambda\varepsilon_{HA^-}\frac{[H^+]}{K_{a,1}} + + {}_\lambda\varepsilon_{H_2A}\frac{[H^+]^2}{K_{a,1}K_{a,2}}\right) * l \tag{13}$$

Dividing Equation 13 by Equation 11 and introducing the variable ${}_\lambda a$

$${}_\lambda a = \frac{A_\lambda}{A_T * l} = \frac{\left({}_\lambda\varepsilon_{A^{2-}} + {}_\lambda\varepsilon_{HA^-} * \frac{[H^+]}{Ka,_1} + + {}_\lambda\varepsilon_{H_2A} * \frac{[H^+]^2}{K_{a,1}K_{a,2}}\right)}{\left(1 + \frac{[H^+]}{K_{a,1}} + \frac{[H^+]^2}{K_{a,1}K_{a,2}}\right)} \tag{14}$$

At low pH, where $[A^{2-}] \approx 0$ Equation 14 can be simplified to Equation 15

$$\varepsilon_{\lambda}a = \frac{\varepsilon_{\lambda}\varepsilon_{HA^-} + \varepsilon_{\lambda}\varepsilon_{H_2A} * \frac{[H^+]}{K_{a,1}}}{1 + \frac{[H^+]}{K_{a,1}}} \quad (15)$$

Since we are interested in salicylic acid at physiological pH, Equation 15 best describes the absorbance of salicylic acid. R = A_2/A_1 is the ratio of absorbance at wavelengths λ_2 and λ_1 is calculated according to Equation 16 (Clayton and Byrne, 1993).

$$R = \frac{\varepsilon_{2}\varepsilon_{HA^-} + \varepsilon_{2}\varepsilon_{H_2A} \frac{[H^+]}{K_{a,1}}}{\varepsilon_{1}\varepsilon_{HA^-} + \varepsilon_{1}\varepsilon_{H_2A} \frac{[H^+]}{K_{a,1}}} \quad (16)$$

Dividing Equation 16 with $\varepsilon_{1}\varepsilon_{H_2A}$ and introducing variables $e_1 = \frac{\varepsilon_{2}\varepsilon_{H_2A}}{\varepsilon_{1}\varepsilon_{H_2A}}$, $e_2 = \frac{\varepsilon_{2}\varepsilon_{HA^-}}{\varepsilon_{1}\varepsilon_{H_2A}}$ and $e_3 = \frac{\varepsilon_{1}\varepsilon_{HA^-}}{\varepsilon_{1}\varepsilon_{H_2A}}$ gives the following Equation

$$R = \frac{e_2 + e_1 * \frac{[H^+]}{K_{a,1}}}{e_3 + \frac{[H^+]}{K_{a,1}}} \quad (17)$$

Which can be rewritten to

$$R * e_3 + R * \frac{[H^+]}{K_{a,1}} = e_2 + e_1 * \frac{[H^+]}{K_{a,1}}$$

From this $\frac{[H^+]}{K_{a,1}}$ can be calculated according to Equation 18

$$\frac{[H^+]}{K_{a,1}} = \frac{e_2 - Re_3}{R - e_1} \quad (18)$$

Applying logarithms on both sides gives Equation 19

$$log \frac{[H^+]}{K_{a,1}} = log \left(\frac{R - e_1}{e_2 - Re_3}\right) \quad (19)$$

pH = $- log\ ([H^+])$ (French et al., 2002) this gives Equation 20

$$pH = -log\, K_{a,1} + log \left(\frac{R - e_1}{e_2 - Re_3}\right) \quad (20)$$

$$pH = pK_{a,1} + log \left(\frac{R - e_1}{e_2 - Re_3}\right) \quad (21)$$

In this case the apparent pK'_a will be used

$$pH = pK'_a + log \left(\frac{R - e_1}{e_2 - Re_3}\right) \quad (22)$$

(Eq 14 in report)

Appendix 2

This Appendix describes how all solutions were prepared

Stock solutions

25 ml 0.5 M Na_2HPO_4

2.22 g Na_2HPO_4 dihydrate was weighed up and dissolved in 25 ml Di water.

100 ml 1.0 M NaH_2PO_4

13.799 g NaH_2PO_4 monohydrate was weighed up and dissolved in 100 ml Di water.

10 0ml 1.0 M H_3PO_4

6.74 ml 85% H_3PO_4 was added to a measuring flask already containing 5 ml of DI water. The final volume was adjusted to 100 ml.

50 ml 4.0 M HAc

11.4381 ml HAc Glacius was added to a measuring flask already containing 5 ml of DI water. The final volume was adjusted to 50 ml.

200 ml 1.0 M HAc

11.4381 ml HAc Glacius was added to a measuring flask already containing 5 ml of DI water. The final volume was adjusted to 200 ml.

100 ml 1.0 M NaAc

13.608 g NaAc trihydrate was weighed up and dissolved in 100 ml DI water.

500 ml 0.2 M NaCl

5.85 g NaCl was weighed up and dissolved in 500 ml deionized water.

100 ml 0.2 M HCl

200 ml 0.5 M HCl was measured and added to a measuring cylinder, the final volume was adjusted to 100 ml using purified water.

100 ml 0.05 M HCl

10 ml 0.5 M HCL was added to a 100 ml measuring flask and the final volume was adjusted to 100ml using deionized water to achieve a final concentration of 0.05 M.

Buffer solutions

100 ml of each of the buffer solutions listed in Table 1 were prepared by adding the correct volume of acid and base to a measuring flask and diluting using deionized water to a final volume of 100 ml.

Table 1: Buffer solutions used to study the absorbance – pH dependent properties of SS

Buffer	**pH**	**Volume acid (ml)**	**Volume base (ml)**
1.0 M H3PO4/1.0 M NaH2PO4	1.40	48.09844	15
1.0 M H3PO4/1.0 M NaH2PO4	1.96	16.1254	15
1.0 M H3PO4/1.0 M NaH2PO4	2.46	4.949434	15
1.0 M H3PO4/1.0 M NaH2PO4	3.01	1.537744	15
4.0 M H3PO4/1.0 M NaH2PO4	3.46	48.76082	15
1.0 M HAc/1.0 M NaAc	3.99	61.16781	15
1.0 M HAc/1.0 M NaAc	4.50	19.50433	15
1.0 M HAc/1.0 M NaAc	4.87	6.16781	15
1.0 M HAc/1.0 M NaAc	5.53	1.950433	15
1.0 M HAc/1.0 M NaAc	6.03	0.616781	15
1.0 M NaH_2PO_4/0.5 M Na_2HPO_4 pH 6.5	6.54	2.359411	1.7603

Dissolution media

Phosphate buffer pH 6.5

8.166 g KH_2PO_2 and 14.91g KCl was weighed up and dissolved in 1.4 L deionized water. The pH was adjusted to 6.5 by titrating 5 M NaOH. The final volume was made up to 2 L with deionized water and the final pH was measured.

Hydrochloric acid medium pH 1.2

250 ml 0.2 M NaCl and 425 ml 0.2 M HCl was added to a measuring flask. The final volume was adjusted to 1 L using deionized water.

0.15 M NaCl solution

4.13446 g NaCl was weighed up and dissolved in deionized water. The final volume was made up to 500 ml.

1.0 M H_3PO_4/1.0 M NaH_2PO_4 pH 3 buffer, C=0.165 M

See Table 1

1.0 M H_3PO_4/1.0 M NaH_2PO_4 pH 3, C= 0.041 M

50 mL of the 1.0 M H_3PO_4/1.0 M NaH_2PO_4 pH 3, C=16.5 M buffer and 150 ml 0.15M NaCl was added to a measuring flask and mixed using a magnetic stirrer.

Appendix 3

This Appendix describes experiments in detail.

1. Dissolution experiments on SS and SA in SDi2

Initial experiments

Table 1: Compilation of initial dissolution experiments performed in the SDi2.

Experiment	Compound	Mass of compound (mg)	Dissolution medium	Flow rate step 2 (ml/min)
1	SA	7.91	Phosphate buffer pH 6.5	0.5
2	SS	8.02	Phosphate buffer pH 6.5	0.5
3	SA	6.96	Hydrochloric acid medium pH 1.2	0.5
4	SS	6.65	Hydrochloric acid medium pH 1.2	0.5
5	SA	6.86	Hydrochloric acid medium pH 1.2	1.0
6	SS	6.17	Hydrochloric acid medium pH 1.2	1.0
7	SS	6.14	Hydrochloric acid medium pH 1.2	1.0

	Duration (hh:mm:ss)	Rate (mL/min)	Linear Velocity (cm/min)
1	00:01:00	3.00	8.33
2	00:30:00	0.50	1.39

Figure 1: Pump program used for initial dissolution experiments in the SDi2.

Final dissolution experiments

Table 2: Final dissolution experiments performed to calculate the IDR and pH of SS and SA

Experiment	Compound	Mass of compound (mg)	Dissolution medium
1	SA	5.66	pH 3 buffer, C = 0.165 M
2	SS	5.89	pH 3 buffer, C = 0.165 M
3	SA	5.80	pH 3 buffer, C= 0.041 M
4	SS	5.81	pH 3 buffer, C = 0.041 M
5	SA	5.91	0.15 M NaCl solution
6	SS	5.77	0.15 M NaCl solution

	Duration (hh:mm:ss)	Rate (mL/min)
1	00:02:00	3.00
2	00:15:00	0.50
3	00:15:00	1.00

Figure 2: Pump program used for dissolution experiments listed in Table 2.

2. Initial experiments to study pH dependence of SA absorbance

The solutions listed in table 3 were used.

Table 3: Solutions used to study the pH dependent properties of Salicylic acid

Solution	pH
0.05 M HCl	1.3
1.0 M H_3PO_4/1.0 M NaH_2PO_4 +HCl	2.1
1.0 M H_3PO_4/1.0 M NaH_2PO_4	3.0
1.0 M H_3PO_4/1.0 M NaH_2PO_4. + NaOH	5.1
1.0 M NaH_2PO_4/0.5 M Na_2HPO_4	6.5

A 0.05 M SS stock solution in water was prepared. 4µl of the 0.05 M SS stock solution was added into a measuring flask. Buffer solution was added up to 10ml to achieve a final SS concentration of 20 µM.

Absorbance measurements were executed using the Agilent Cary 60 UV-vis spectrophotometer. 3 ml of blank pH 1.3 solution was pipetted into a 10 ml quartz cuvette and

used for baseline correction. After this, the cuvette were emptied and 3 ml of the 20 µM SS pH 1.3 was pipetted into the cuvette and the absorbance spectrum was measured.

3. Calibration curves of absorbance versus concentration for SS

Standard solutions

A stock solution of 100 mM SS in water was prepared. This stock solution was diluted to standard concentrations of 3.0 mM, 1.5 mM, 0.8 mM, 0.4 mM, 0.2 mM and 0.1 mM using the media of interest, phosphate buffer pH 6.5 and HCl medium pH 1.2.

Calibration Curve using Agilent Cary 60 UV-vis

In total, 4 calibration curves of absorbance versus concentration were constructed, SS in blank phosphate buffer pH 6.5 and hydrochloric acid medium pH 1.2 were both measured at 280 nm and 320 nm in the Agilent Cary 60 UV-vis by performing simple scan measurements. Absorbance vs concentration was plotted to determine the slope which was used to calculate the MEC according to beer lamberts law.

Calibration curve in the SDi2

Four calibration curves of absorbance versus concentration were constructed: SS in blank phosphate buffer pH 6.5 and hydrochloric acid medium pH 1.2 were both measured at 280nm and 320 nm. The following pump system was used to construct a calibration curve using the Sirius SDi2.

	Duration (hh:mm:ss)	Rate (mL/min)	Linear Velocity (cm/min)
1	00:07:00	2.50	6.94
2	00:01:00	0.00	0.00
3	00:07:00	2.50	6.94
4	00:01:00	0.00	0.00
5	00:07:00	2.50	6.94
6	00:01:00	0.00	0.00
7	00:07:00	2.50	6.94
8	00:01:00	0.00	0.00
9	00:07:00	2.50	6.94
10	00:01:00	0.00	0.00
11	00:07:00	2.50	6.94
12	00:01:00	0.00	0.00
13	00:07:00	2.50	6.94
14	00:01:00	0.00	0.00

Figure 3: Pump program used to measure absorbance of standard solutions in the SDI2. Step 1 correspond to the blank solution, step 3 to 0.1 mM SS, step 5 to 0.2 mM SS, step 7 to 0.4 mM SS, step 9 to 0.8 mM SS, step 1 to 1.5 mM and step 13 to 3.0 mM SS

Two separate experiments were performed, one using hydrochloric acid media solutions and one using the phosphate buffer solutions. An experiment was started by recording dark images and reference images with the flow cell filled with the blank solution according to the instruments default calibration sequence. Subsequently, the pump program seen in Figure 3 was executed. Each standard solution ran for 7 min at 2.5 ml/min flowrate with 1 min 0 ml/min flow rate in between to prevent air bubbles from being introduced.

The standard solutions were measured in the following order: blank solution (same as used for instrument calibration), 0.1 mM, 0.2 mM, 0.4 mM, 0.8 mM, 1.5 mM and 3.0 mM.

Analyzing absorbance measurements in SDi2

The data was opened in the Sirius SDi2 Data Analysis application software. A custom zone under the zone tab was created, according to Figure 4.

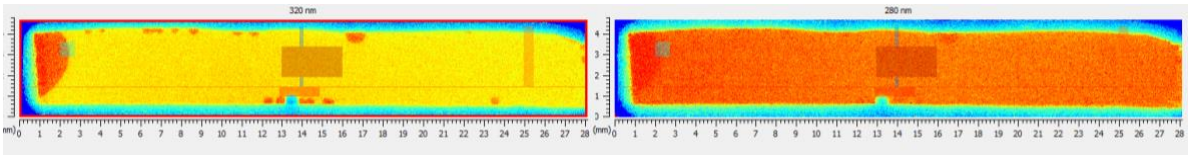

Active	Name	Colour	Type	Ref	Orientation	x (mm)	z (mm)	Width (mm)	Height (mm)
☑	Zone 1	Red	Signal		Vertical	13.00	2	3.00	1.5

Figure 4: The zone used to collect absorbance values.

Under the profile tab, zone 1 and Region-all was selected. The data was copied to an excel sheet, and average absorbance for each time interval (60s) was calculated. The average absorbance was then plotted against time and concentration values were selected from the flat parts of the curves, see the box in Figure 5. The absorbance values shouldn't deviate too much.

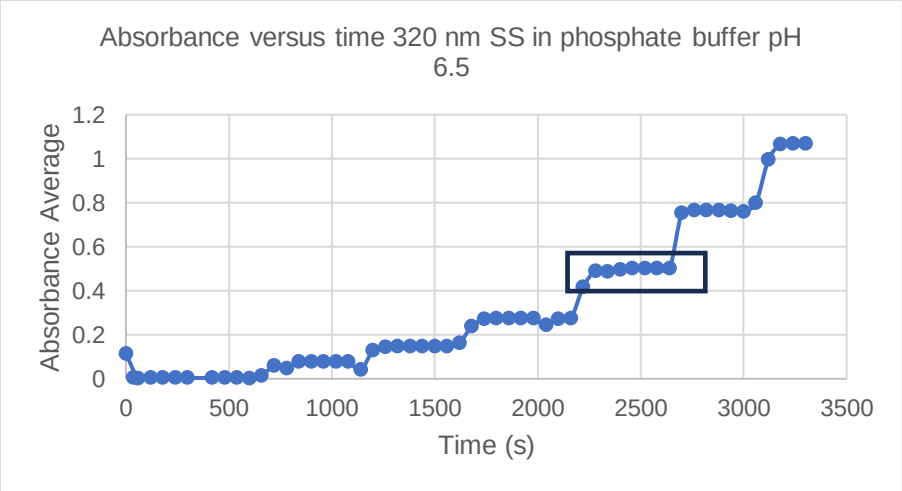

Figure 5: Example of plot of calculated average values of absorbance plotted against time. The box surrounds a flat part of the curve which corresponds to a concentration of 0.8 mM.

The average absorbance values for each concentration were extracted from the software and plotted against concentration to obtain a calibration curve. The MEC (Mean extinction coefficient) was calculated as the slope of the curve according to Beer-Lamberts law.

4. Temperature control experiments in SDi2

Experimental run

The following experimental procedure was conducted and repeated on three consecutive days. The flow cell was flushed, a temperature control experiment of 0.5 ml/min was conducted (see pump program), the flow cell was flushed, a temperature control experiment of 3 ml/min was conducted (see pump program), the flow cell was flushed and a temperature control experiment of 1 ml/min was conducted (see pump program). The flow cell was flushed using the default flush program of the SDi2 lasting 9 min using deionized water while the lid of the SDi2 was open. Temperature control experiments were started when a temp of 37 ºC was reached, according to the SDi2 instrument which measures the temperature of the dissolution medium. All experiments were conducted using deionized water.

	Duration (hh:mm:ss)	Rate (mL/min)	Linear Velocity (cm/min)	Solution	Loop	Total Time (hh:mm:ss)
1	00:01:00	3.00	8.33	Primary	Open	00:01:00
2	00:30:00	0.50	1.39	Primary	Open	00:31:00

Figure 6: The pump program used for temperature control in the SDi2.

Each experiment ran for 31 min at 37 ºC. Each experiment included two steps, a 1 min at 3 ml/min step to fill up the flow cell and step 2 where the flow rate was set to either 0.5 ml/min, 1 ml/min or 3 ml/min depending on the specific experiment being conducted. All experiments were conducted with deionized water.

The temperature was measured using a FLUKE t3000 FC Digital thermometer (Fluke Corporation, United states, Everett). The temperature probe was inserted into the sample holder and secured using adhesive putty, see Figure 7.

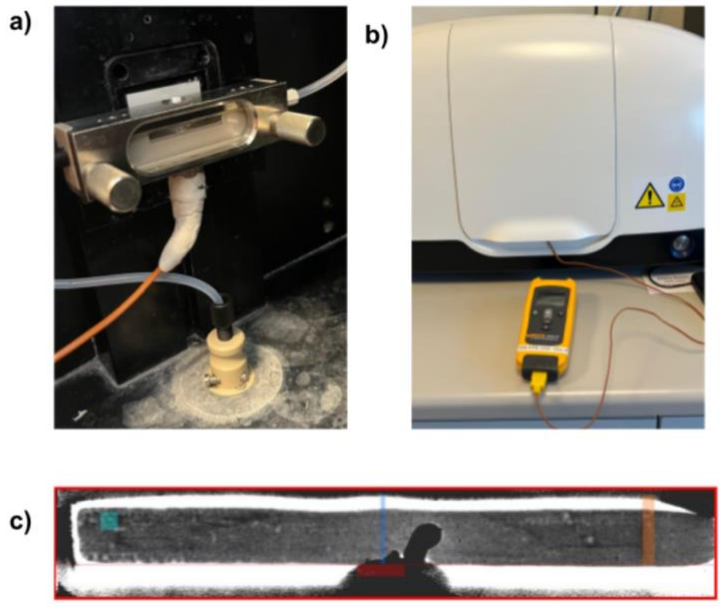

Figure 7: The experimental setup for temperature control experiments in the SDi2: a) The temperature probe inserted in the flow cell and secured using adhesive putty, b) The SDi2 with the FLUKE t3000 FC Digital thermometer connected to the flow cell, c) Image of the flow cell. The temperature probe is seen sticking up from the sample holder.

5. Flowrate control experiments in SDi2

Experimental procedure

Flow rate control experiments in the SDi2 were conducted for flow rats 3 ml/min, 1 ml/min and 0.5 ml/min according to the pump program presented in Figure 8. Before the experiment started, 18 glass vials (25ml) with lids were weighed and the weights was noted.

For each flow rate, two samples were collected; flow rate was collected from t = 3 min to t = 10 min by directing the outlet tube into a vial and allowing it to remain there for 7 minutes before taking the tube out and sealing the lid. Flow rate was also collected from t = 20 min to t = 27 min according to the same procedure. This was repeated for each flow rate and in total, the pump program presented in figure 8 was repeated 3 times, resulting in 18 samples (6 samples for each flowrate).

	Duration (hh:mm:ss)	Rate (mL/min)	Linear Velocity (cm/min)	Solution	Loop	Total Time (hh:mm:ss)	Total Volume (mL)
1	00:30:00	3.00	8.33	Primary	Open	00:30:00	90.00
2	00:30:00	1.00	2.78	Primary	Open	01:00:00	120.00
3	00:30:00	0.50	1.39	Primary	Open	01:30:00	135.00

Figure 8: Pump program used for flow rate control experiments.

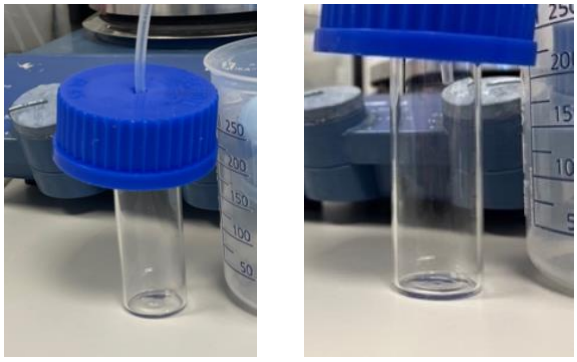

Figure 9: Outlet tube directed into vial

After the experiments, the vials were left in room temperature for 1 h before being weighed again. The weighed difference was calculated. The flow rate of the water was calculated using Equation 1, where φ_{water} is the density of water at 25 °C.

$$Flow\ rate_{measured} = \frac{m_{vial,after} - m_{vial,before}}{\varphi_{water} * 7} \quad (1)$$

The percentual difference between measured flow rate and expected flow rate was calculated according to equation 2.

$$Percentual\ difference = \frac{Flow\ rate_{expected} - Flow\ rate_{measured}}{Flow\ rate\ _{expected}} * 100 \quad (2)$$

6. pH measurement of SS solutions in Agilent Cary 60 UV-vis spectrophotometer and SDi2

Preparing Solutions

10 ml of a 50 mM stock solution of SS was prepared. For each buffer solution, sodium salicylate as added in two different concentrations, 0.3 mM and 0.5 mM by pipetting 0.150 ml 0.250 ml SS stock solution respectively.

Absorbance measurements

The following solutions were measured in three different cuvette sizes: pH 1.5, pH 3.0, pH 4.0, pH 6.0 and pH 6.5 of both SS concentrations. For the acetate buffers (pH 3.5, pH 4.0, pH 4.5, pH 5.0, pH 5.5 and pH 6.0) the pH 4.0 buffer were used as a blank. For the phosphate buffers (pH 1.5, pH 2.0, pH 2.5, pH 3.0 and pH 6.5) the pH 2.0 buffer were used as a blank. Absorbance spectrums were measured from 200 nm to 800 nm and the blank solutions were always measured to ensure zero absorbance in the visible range.

Table 4: All samples measured in the Aglient Cary 60 UV-vis spectrophotometer.

pH	Conc SA (mM)	Path length (mm)	pH	Conc SA (mM)	Path length (mm)
1.5	0.3	10	4.0	0.5	10
		2			2
		1			1
	0.5	10	4.5	0.3	10
		2		0.5	10
		1	5.0	0.3	10
2.0	0.3	10		0.5	10
	0.5	10	5.5	0.3	10
2.5	0.3	10		0.5	10
	0.5	10	6.0	0.3	10

3	0.3	10			2
		2			1
		1		0.5	10
	0.5	10			2
		2			1
		1	6.5	0.3	10
3.5	0.3	10			2
	0.5	10			1
4.0	0.3	10		0.5	10
		2			2
		1			1

This resulted in data sets of absorbance at 280 nm and 320 nm for all samples from which pK'_a and pH was calculated.

Absorbance measurements in the SDi2

The absorbance of acetate buffer solutions (pH 3.5, 4.0, 4.5, 5.0, 5.5 and 6.0) were measured using the pump program in figure 10 a) and the absorbance of the phosphate buffers (pH 1.5, 2.0, 2.5, 3.0 and 6.5) were measured using the pump program presented in Figure 10 b). 0.3 mM solutions and 0.5 mM solutions were measured separately.

	Duration (hh:mm:ss)	Rate (mL/min)
1	00:07:00	2.50
2	00:01:00	0.00
3	00:07:00	2.50
4	00:01:00	0.00
5	00:07:00	2.50
6	00:01:00	0.00
7	00:07:00	2.50
8	00:01:00	0.00
9	00:07:00	2.50
10	00:01:00	0.00
11	00:07:00	2.50
12	00:01:00	0.00

	Duration (hh:mm:ss)	Rate (mL/min)
1	00:07:00	2.50
2	00:01:00	0.00
3	00:07:00	2.50
4	00:01:00	0.00
5	00:07:00	2.50
6	00:01:00	0.00
7	00:07:00	2.50
8	00:01:00	0.00
9	00:07:00	2.50
10	00:01:00	0.00
11	00:07:00	2.50
12	00:01:00	0.00
13	00:07:00	2.50
14	00:01:00	2.50

Figure 10: The pump program used when measuring absorbance of calibration curves. Step 1 corresponds to the blank solution, step three too 0.1 mM, step five to 0. 2mM, step seven to 0.4 mM, step 9

Analyzing absorbance measurements in SDi2

The experiments were analyzed according to the procedure described under " 3 Calibration curves of absorbance versus concentration for Sodium Salicylate". This resulted in data sets of absorbance at 280 nm and 320 nm for all samples from which pK'_a and pH was calculated.

Appendix 4

Results from dissolution experiments in the SDi2.

1. Salicylic acid

F = 0.5 ml/min, acidic medium pH 1.2

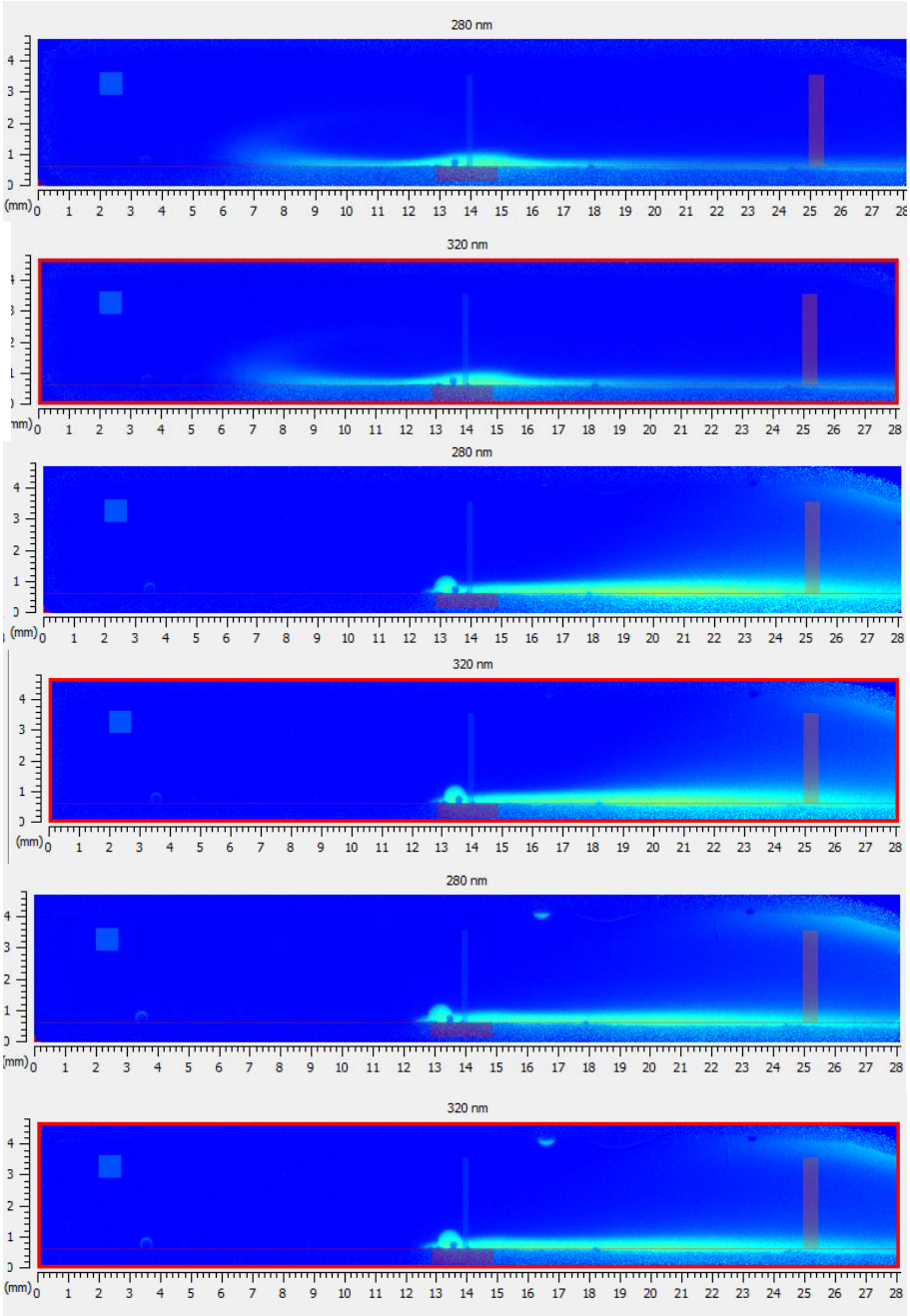

Figure 1: Selected absorbance maps from dissolution experiment on SA in acidic medium pH 1.2 with a flow rate of 0.5 ml/min. Images from t = 2 min, t = 15 min and t= 30 min

F = 1.0 ml/min, acidic medium pH 1.2

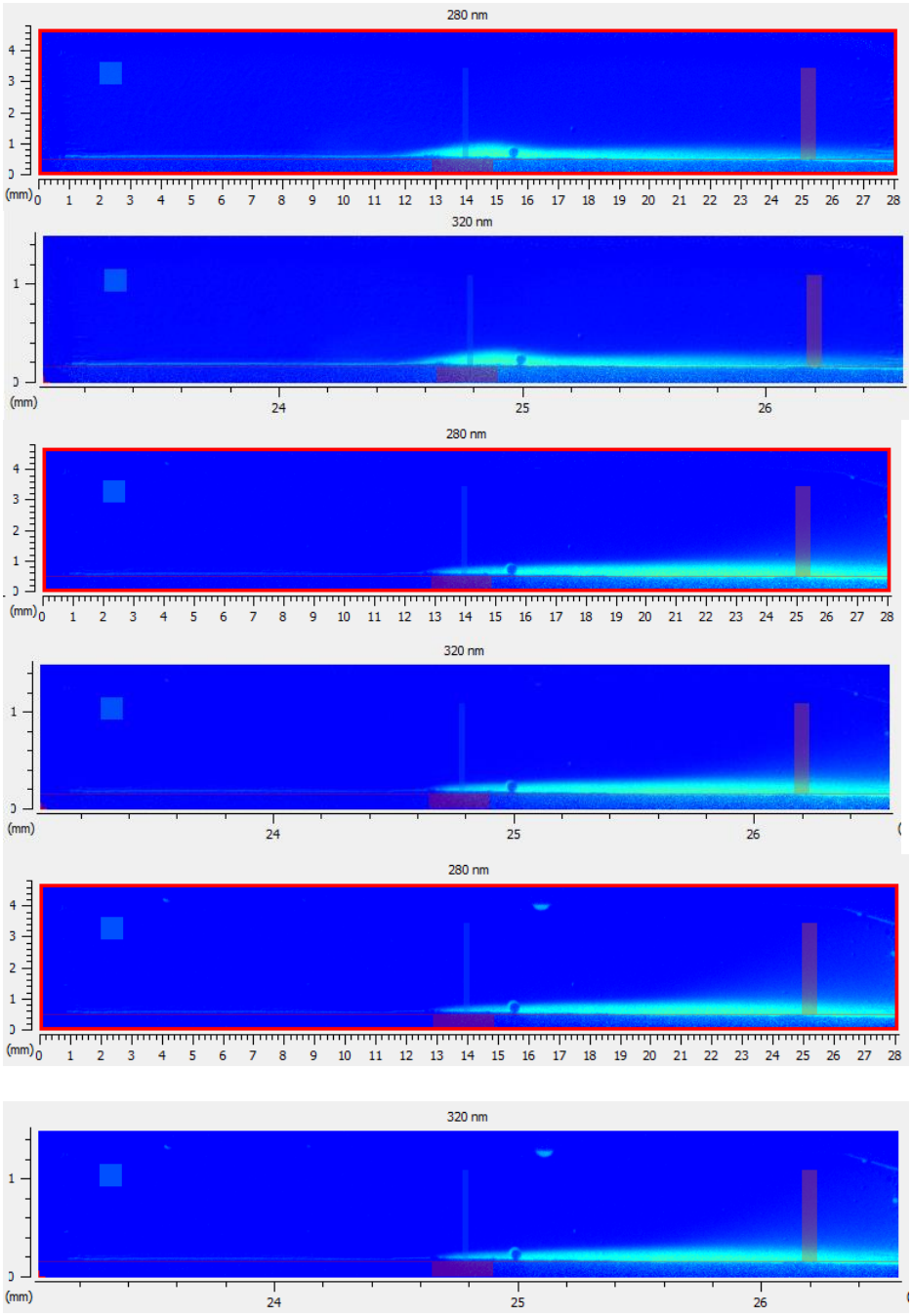

Figure 2: Selected absorbance maps from dissolution experiment on SA in acidic medium pH 1.2 with a flow rate of 1.0 ml/min. Images from t = 2 min, t = 15 min and t= 30 min

F = 0.5 ml/min, phosphate buffer pH 6.5

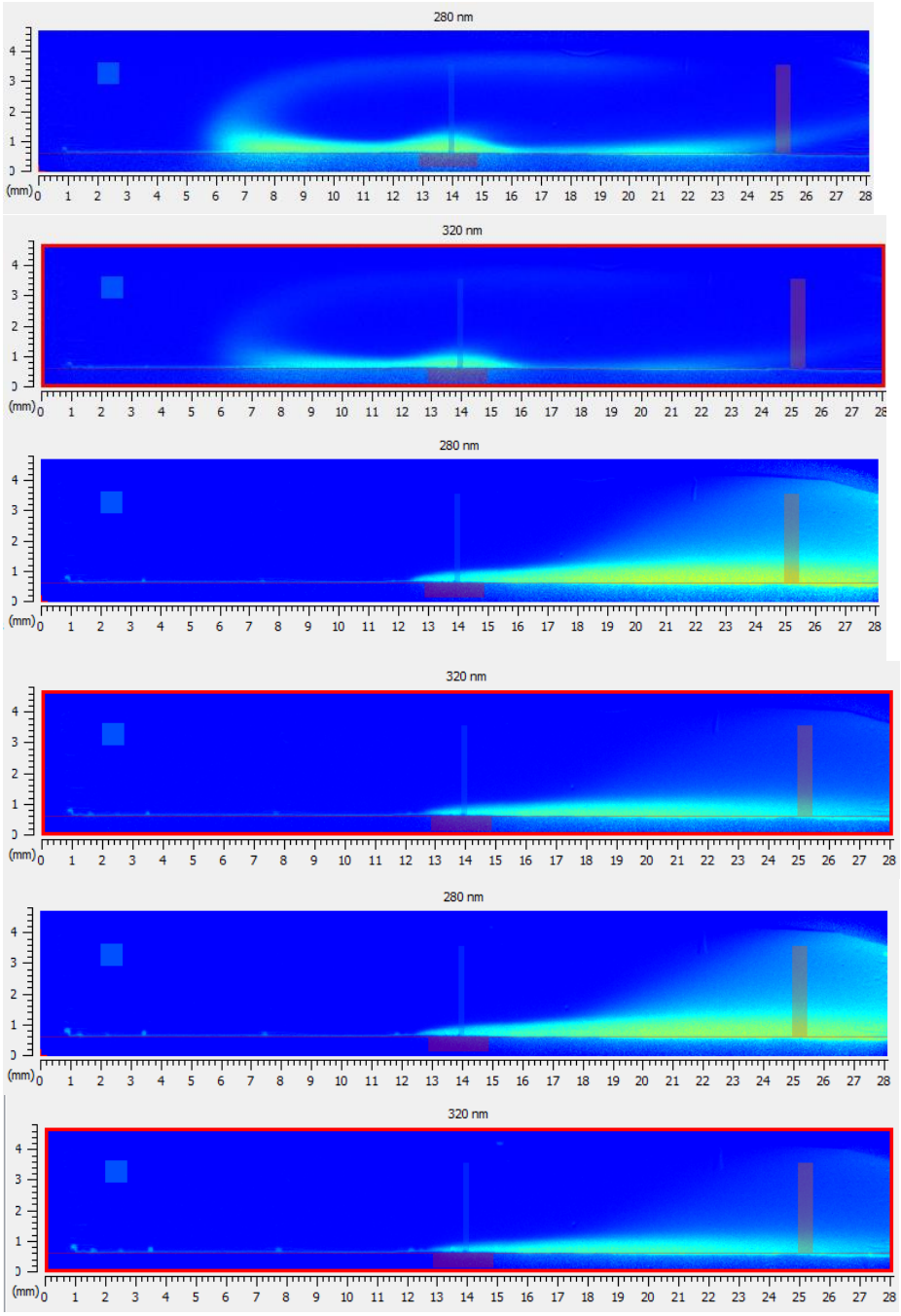

Figure 3: Selected absorbance maps from dissolution experiment on SA in phosphate buffer pH 6.5 with a flow rate of 0.5 ml/min. Images from t = 2 min, t = 15 min and t= 30 min

For the following experiments, F= 3 ml/min from t = 0 min to t = 2 min, F= 0.5 ml/min from t = 2 min to t = 17 min and F = 1 ml/min from t = 17 min to t= 32 min

pH 3 buffer, buffer strength = 0.165 M

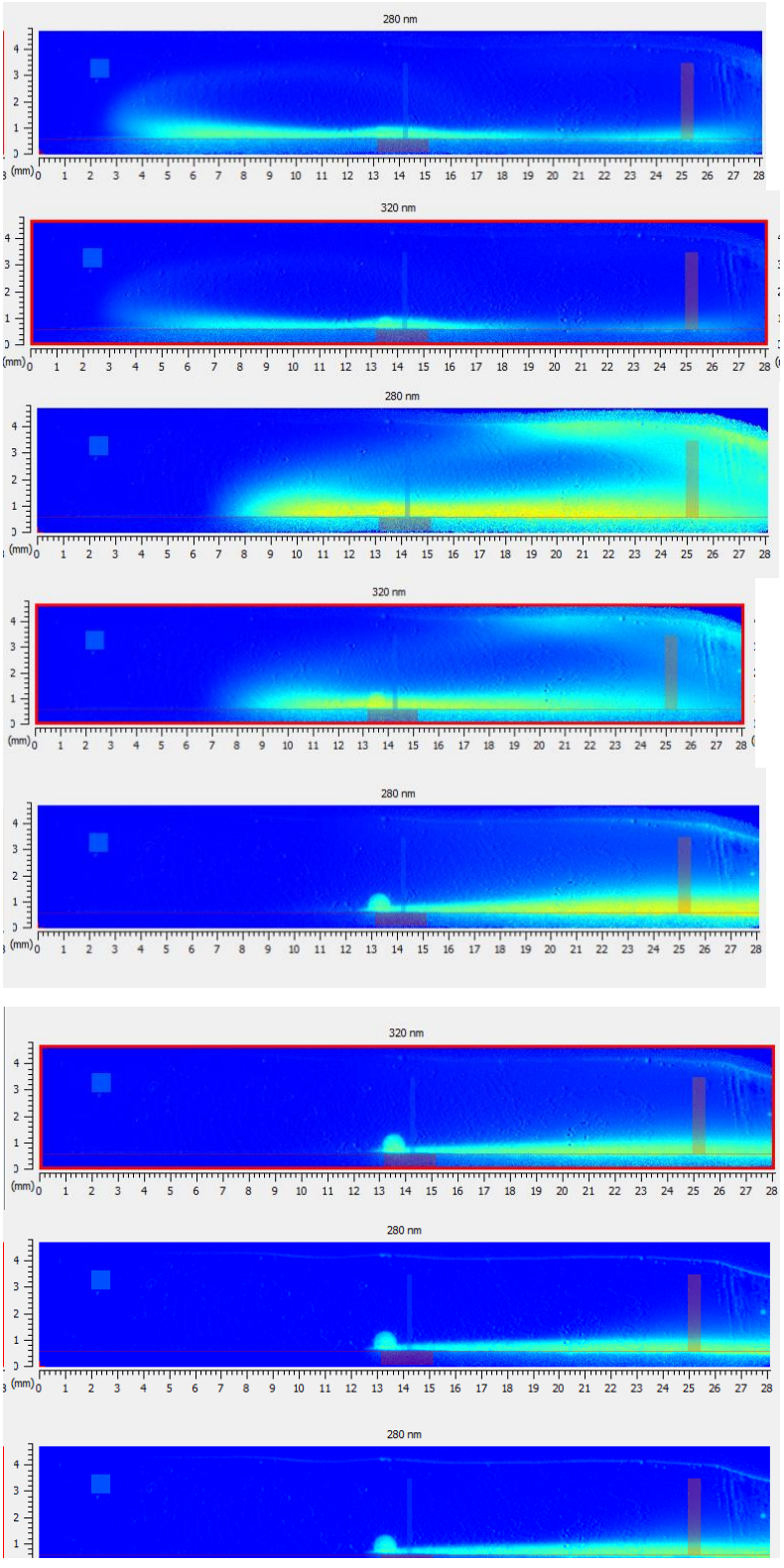

Figure 4: Selected absorbance maps from dissolution experiment on SA in pH 3 buffer. Images from t = 2 min, t = 16 min, t = 19 min and t = 30 min

pH 3, buffer strength = 0.041 M

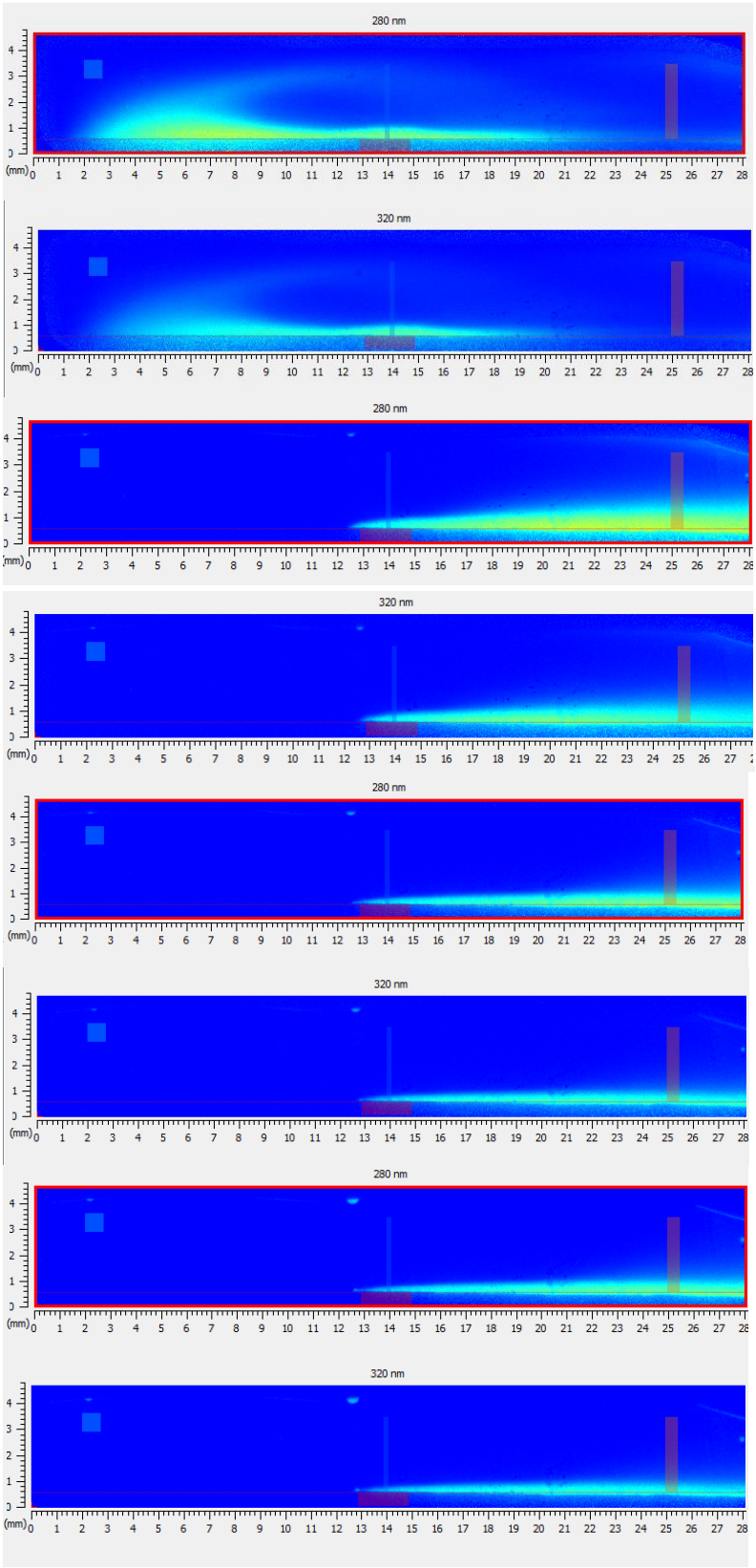

Figure 5: Selected absorbance maps from dissolution experiment on SA in pH 3 buffer. Images from t = 2 min, t = 16 min, t = 19 min and t = 30 min

NaCl solution

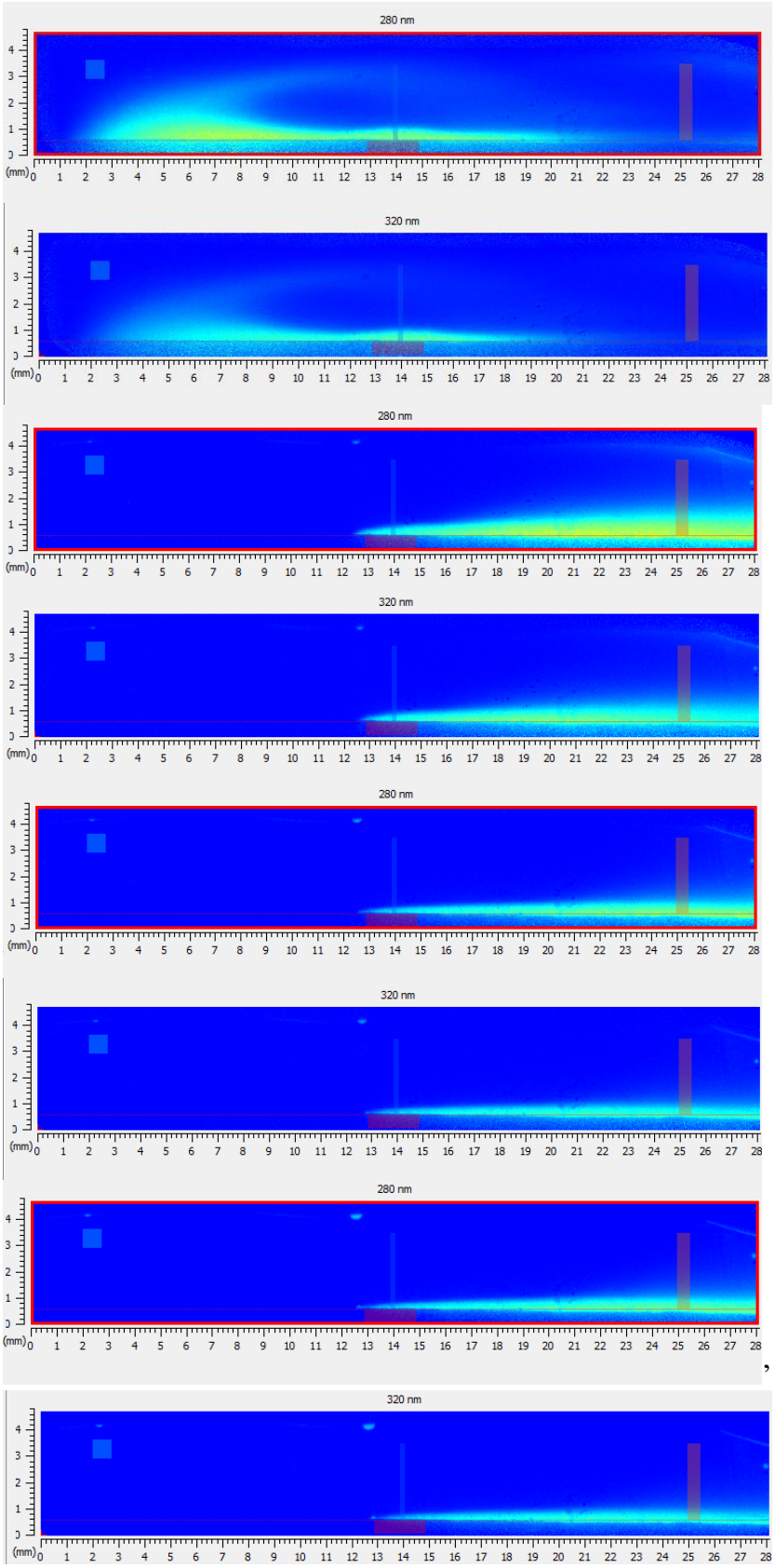

Figure 6: Selected absorbance maps from dissolution experiment on SA in a NaCl solution. Images from t = 2 min, t = 16 min, t = 19 min and t = 30 min

2. Sodium Salicylate

F = 0.5 ml/min, acidic medium pH 1.2

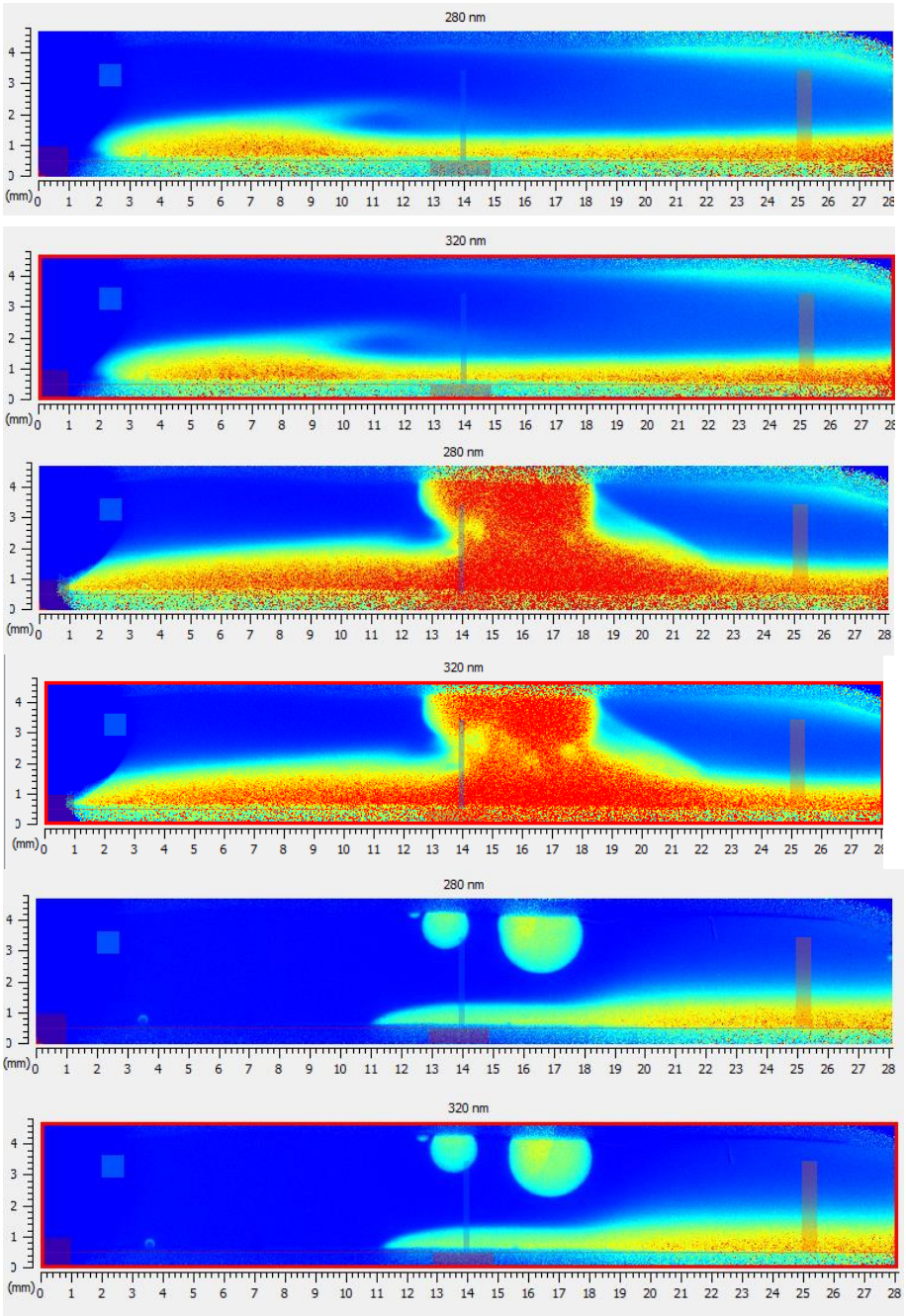

Figure 7: Selected absorbance maps from dissolution experiment on SS in acidic medium pH 1.2 with a flow rate of 0.5 ml/min. Images from t = 2 min, t = 5 min and t= 30 min

F = 1.0 ml/min, acidic medium pH 1.2

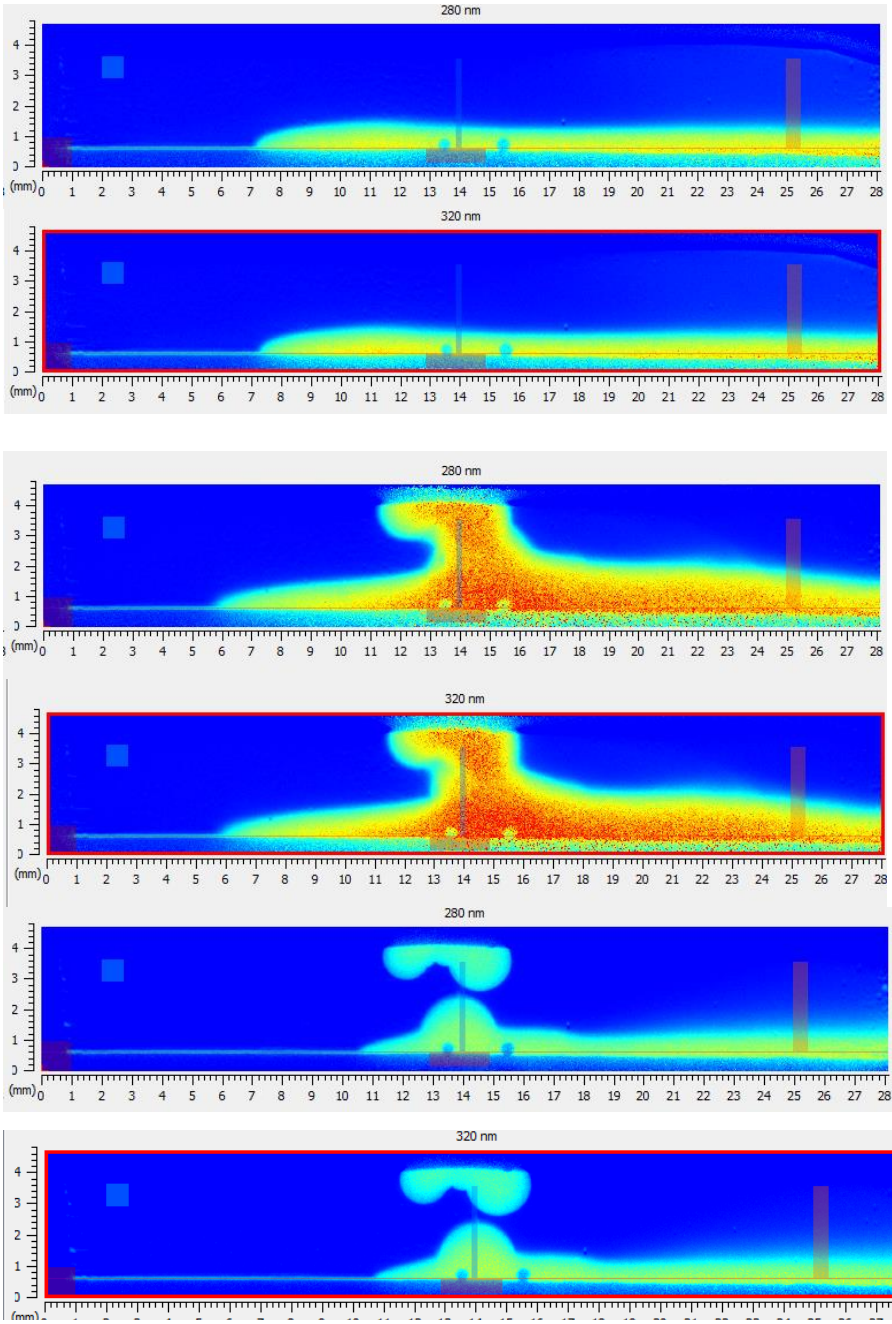

Figure 8: Selected absorbance maps from dissolution experiment on SA in acidic medium pH 1.2 with a flow rate of 1.0 ml/min. Images from t = 2 min, t = 5 min and t= 30 min

F = 0.5 ml/min, phosphate buffer pH 6.5

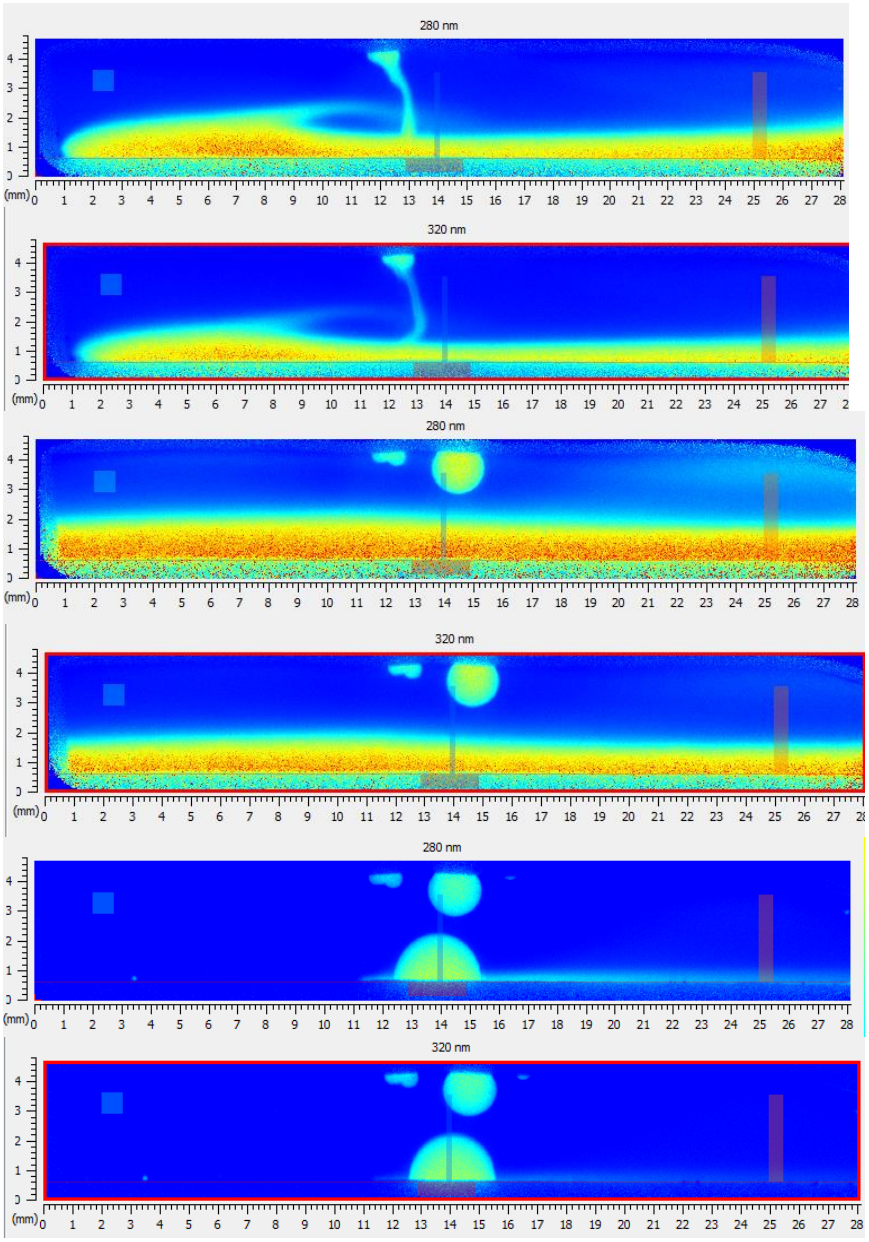

Figure 9: Selected absorbance maps from dissolution experiment on SA in phosphate buffer pH 6.5 with a flow rate of 0.5 ml/min. Images from t = 2 min, t = 5 min and t= 30 min

For the following experiments, F = 3 ml/min from t = 0 min to t = 2 min, F = 0.5 ml/min from t = 2 min to t = 17 min and F = 1 ml/min from t = 17 min to t = 32 min

pH 3 buffer, C = 0.165 M

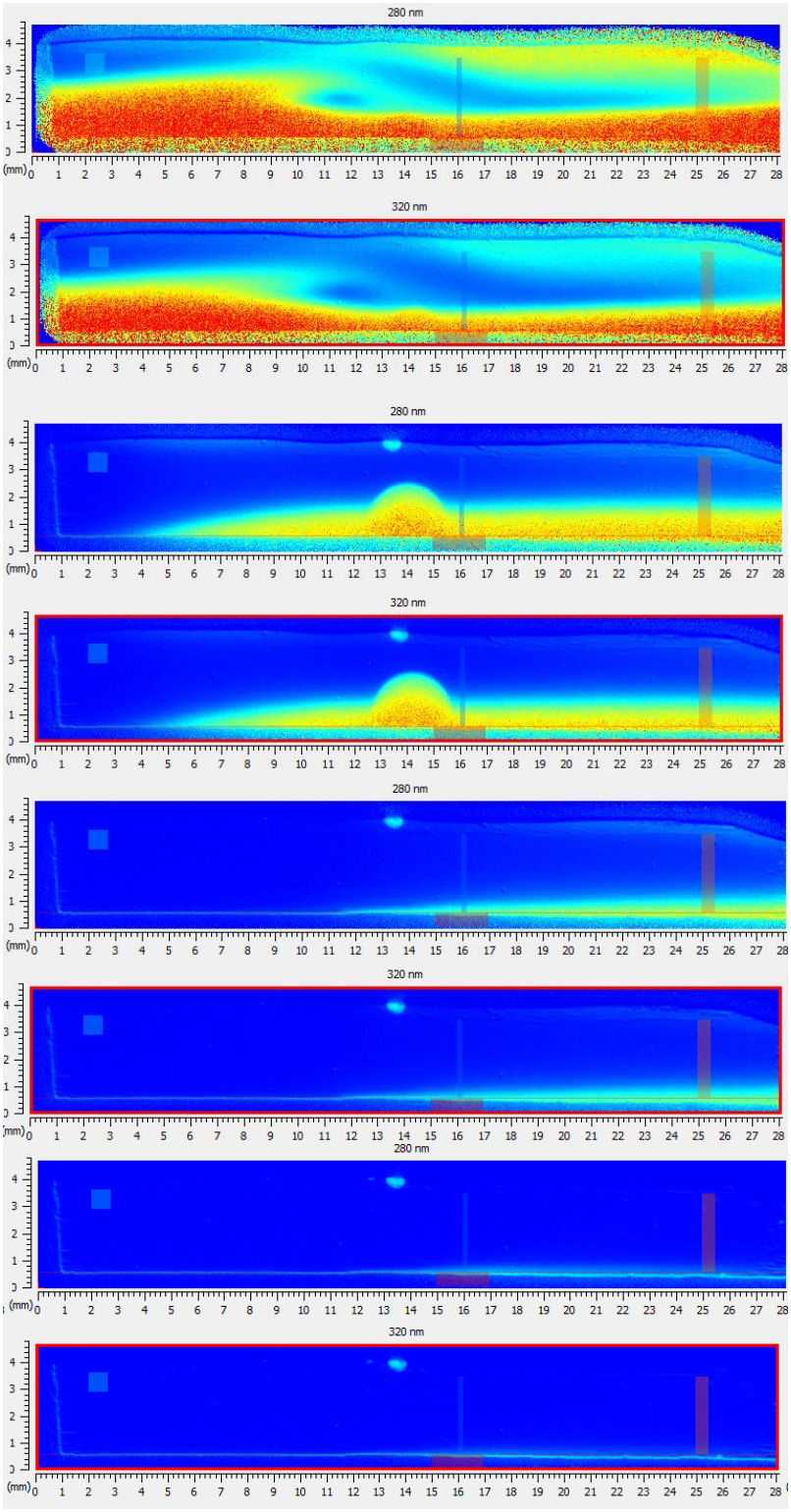

Figure 10: Selected absorbance maps from dissolution experiment on SS in pH 3 buffer. Images from t = 2 min, t = 16 min, t = 19 min and t = 30 min

pH 3 buffer, C = 0.041 M

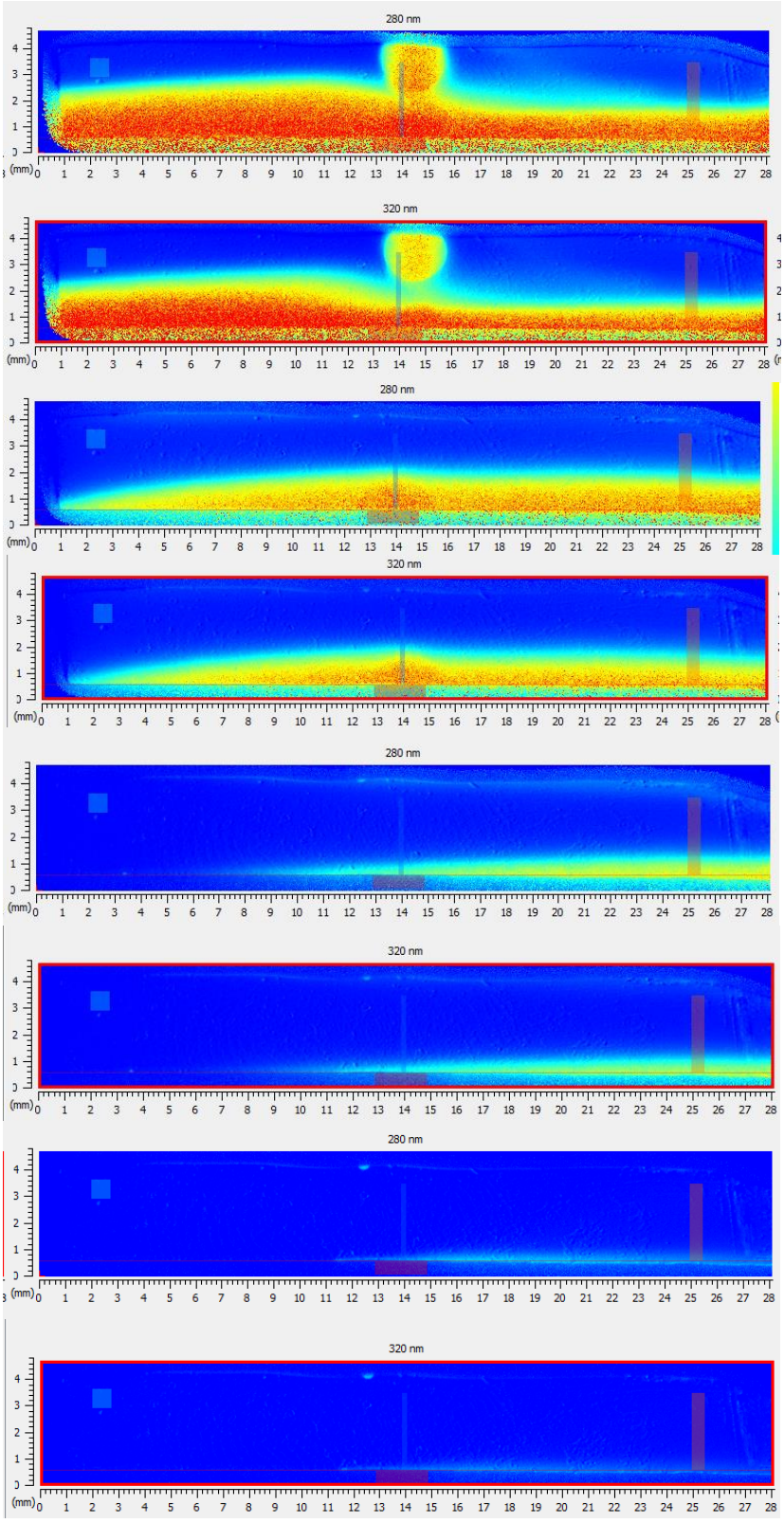

Figure 11: Selected absorbance maps from dissolution experiment on SS in pH 3 buffer. Images from t = 2 min, t = 16 min, t = 19 min and t = 30 min

NaCl Solution

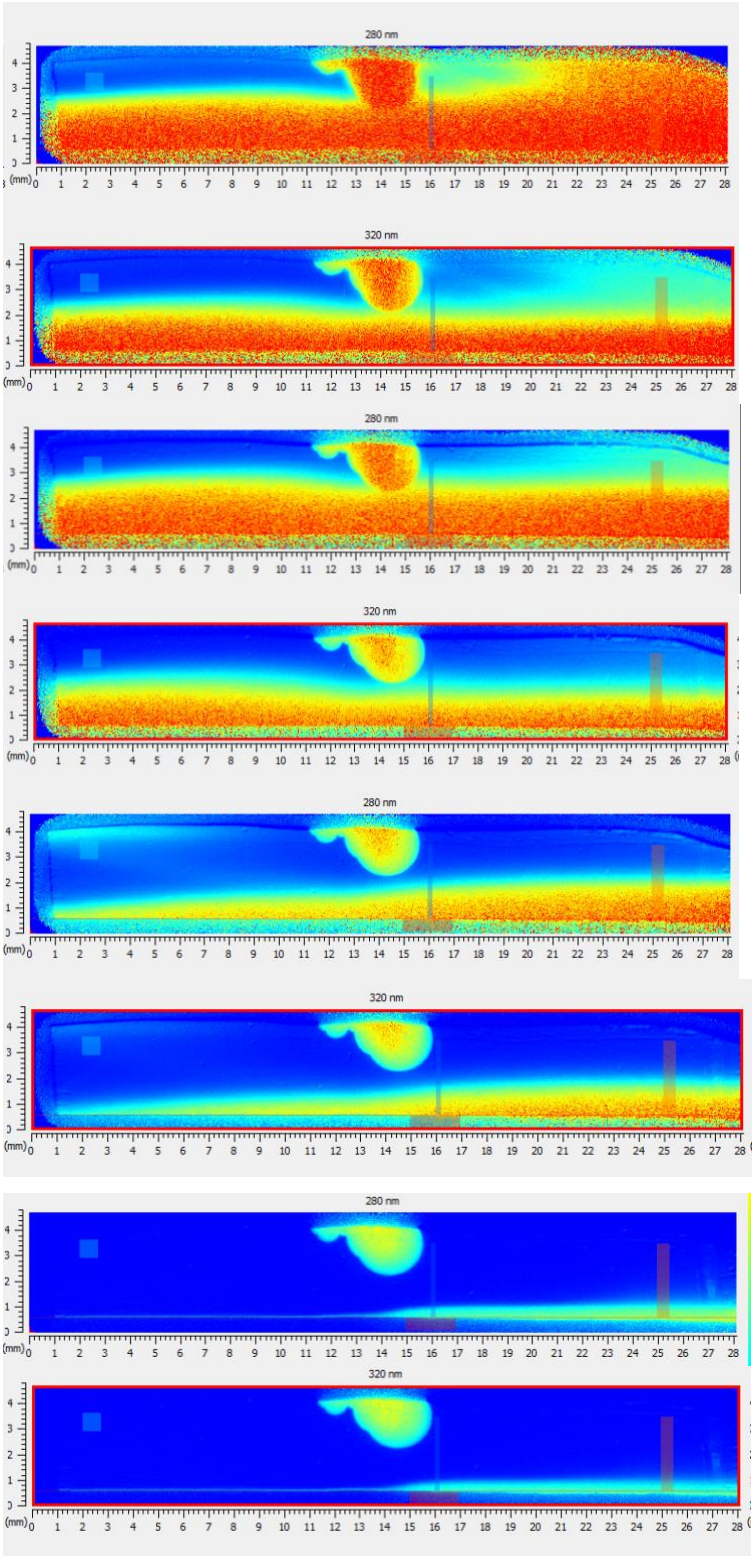

Figure 12: Selected absorbance maps from dissolution experiment on SS in NaCl solution. Images from t = 2 min, t = 16 min, t = 19 min and t = 30 min

3. IDR Calculations

pH 1.2 and pH 6.5 solutions

Table 1: Average IDR values calculated from t = 20 min to t =31 min,

Experiment	pH 1.2, F = 0.5 ml/min	pH 1.2, F = 1.0 ml/min	pH 6.5, F = 0.5 ml/min
IDR SA (280 nm) [µg/min/cm^2]	149	130	351
IDR SA (320 nm) [µg/min/cm^2]	157	137	314
IDR SA (average) [µg/min/cm^2]	153	133	333
IDR SS (280 nm) [µg/min/cm^2]	959	486	109
IDR SS (320 nm) [µg/min/cm^2]	1185	510	191
IDR SS (average) [µg/min/cm^2]	1072	498	100

pH 3 and NaCl solutions

$A_{SS,pH\ 3,\ \lambda} = l * \left(c_{HA^-}\varepsilon_{HA^-,\ \lambda} + c_{H_2A}\varepsilon_{H_2A,\ \lambda}\right) = l * c_{tot} * \varepsilon_{pH\ 3,\ \lambda}$ where $C_{tot} = c_{HA^-} + c_{H_2A}$

$$\varepsilon_{pH\ 3,\ \lambda} = \frac{c_{HA^-}\varepsilon_{HA^-,\ \lambda} + c_{H_2A}\varepsilon_{H_2A,\ \lambda}}{c_{HA^-} + c_{H_2A}}$$

$c_{HA^-} = x_{HA^-} * C_{tot}$ where x_{HA^-} is the fraction of HA^-

$c_{H_2A} = C_{tot} - c_{HA^-} = C_{tot} - x_{HA^-} * C_{tot}$

$$\varepsilon_{pH\ 3} = \frac{(x_{HA^-}*C_{tot})*\varepsilon_{HA^-,\lambda}+(C_{tot}-x_{HA^-}*C_{tot})*\varepsilon_{H_2A,\lambda\lambda}}{(x_{HA^-}*C_{tot})+(C_{tot}-x_{HA^-}*C_{tot})} = \frac{(x_{HA^-}*\varepsilon_{HA^-,\lambda}+(1-x_{HA^-})*\varepsilon_{H_2A,\lambda}}{(x_{HA^-})+(1-x_{HA^-})}$$

x_a = 0.58282 according to

$\frac{c_{HA^-}}{c_{H_2A}} = 10^{3-2.94}$ =1.14815362 (Henderson-Hasselbach Equation)

$$x_a = \frac{\frac{c_{HA^-}}{c_{H_2A}}}{1+\frac{c_{HA^-}}{c_{H_2A}}} = 0.53$$

$\varepsilon_{H_2A,280nm}$ =1.26 (mM)$^{-1}$ cm^{-1}, $\varepsilon_{H_2A,\ 320nm}$=1.17 (mM)$^{-1}$ cm^{-1}, $\varepsilon_{HA^-,280nm}$=1.38 (mM)$^{-1}$cm^{-1} and $\varepsilon_{HA^-,320nm}$ = 0.67 (mM)$^{-1}$ cm^{-1} (Values calculated in Appendix 6)

This gives $\varepsilon_{pH\ 3,280nm}$ = 1.33 (mM)$^{-1}$cm^{-1} and $\varepsilon_{pH\ 2,320nm}$=0.88 (mM)$^{-1}$cm^{-1}

Table 2: Average IDR values calculated from t = 10 min to t=16 min and = 26 min to t=32 min

Experiment	pH 3 0.16 M, F = 0.5 ml/min	pH 3, 0.16 M, F = 1.0 ml/min	pH 3, 0.041 M F = 0.5 ml/min	pH 3, 0.041 M F = 1.0 ml/min	NaCl, F=0.5 ml/min	NaCl, F=1.0 ml/min
IDR SA (280 nm) [µg/min/cm^2]	220 - 450	175	106 - 309	210	191	98
IDR SA (320 nm) [µg/min/cm^2]	194 - 400	167	60 - 240	132	122	52
IDR SA (average) [µg/min/cm^2]	Not calculated	171	Not calculated	171	157	75
IDR SS (280 nm) [µg/min/cm^2]	411 - 867	54	464 - 915	78	875	267
IDR SS (320 nm) [µg/min/cm^2]	424 - 912	52	519 - 1116	65	907	208
IDR SS (average) [µg/min/cm^2]	Not calculated	53	Not calculated	72	891	238

4. Temperature control experiment

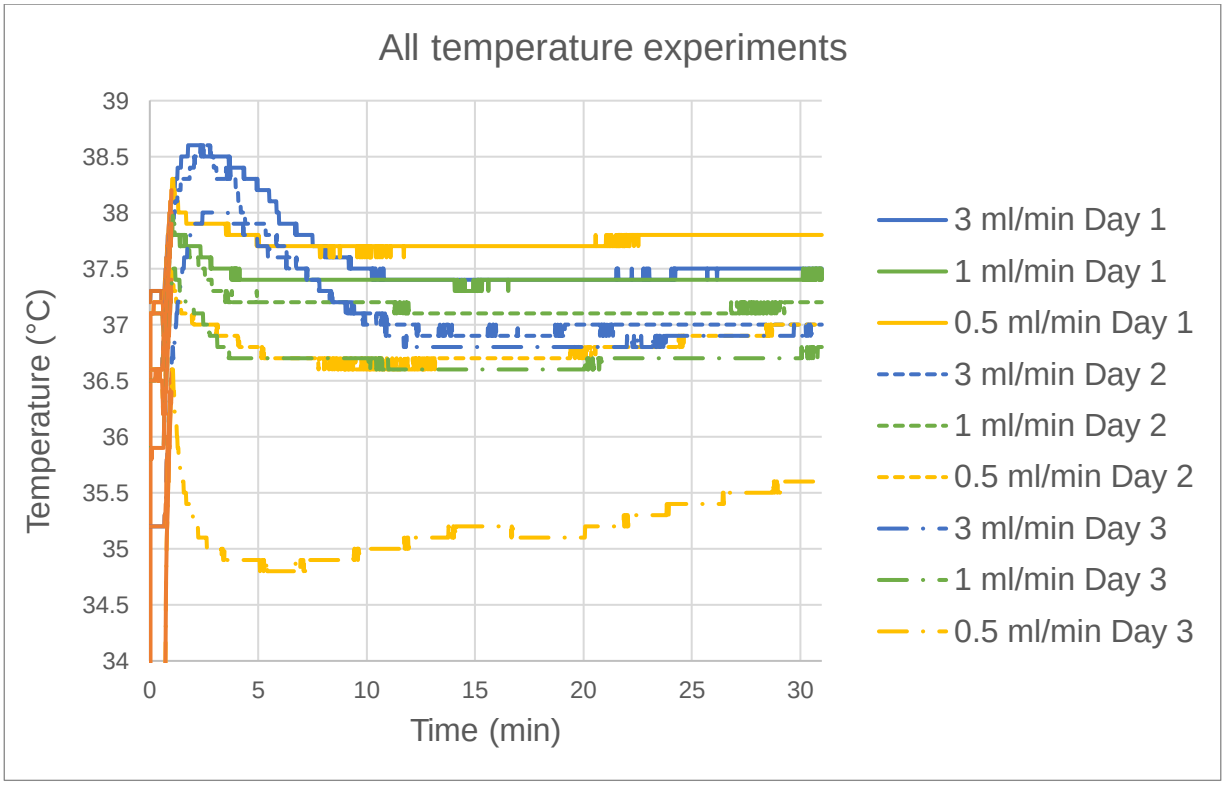

Figure 13: Temperature plotted versus time for all temperature control experiments. The orange part represents the 1 min step used to fill up the flow cell.

5. Flow rate control experiments

Results from flow rate experiments are found in Table 3.

Table 3: Raw data from flow rate measurements

Time point	**Calculated flow rate**
Experiment 1	
t=3 min to t=10 min	2,902646366
t=20 min to t=27 min	2,834908842
t=3 min to t=10 min	0,973924649
t=20 min to t=27 min	0,99305223
t=3 min to t=10 min	0,482460871
t=20 min to t=27 min	0,49314643
Experiment 2	
t=3 min to t=10 min	2,838935701
t=20 min to t=27 min	2,857056567
t=3 min to t=10 min	0,971192137
t=20 min to t=27 min	0,949619678
t=3 min to t=10 min	0,481641118
t=20 min to t=27 min	0,482791649
Experiment 3	
t=3 min to t=10 min	2,859069997
t=20 min to t=27 min	2,85935763
t=3 min to t=10 min	0,977951508
t=20 min to t=27 min	0,954077986
t=3 min to t=10 min	0,479196239
t=20 min to t=27 min	0,482935465

Appendix 5

This Appendix contains raw data from measurements in the Cary spectrophotometer.

1. Calibration curves to calculate MEC of salicylic acid

Table 1: Absorbance measured in the Cary

Conc (mM)	ABS 280nm FaSSIF	ABS 320nm FaSSIF	ABS 280nm HCL	ABS 320nm HCL
3.0	3.1281	1.6643	3.4238	3.5126
1.5	2.6702	0.8834	1.8774	2.3512
0.8	1.4813	0.4644	1.0119	1.2822
0.4	0.7422	0.2267	0.5135	0.6492
0.2	0.4735	0.1446	0.2593	0.3269
0.1	0.1990	0.0621	0.1446	0.1808

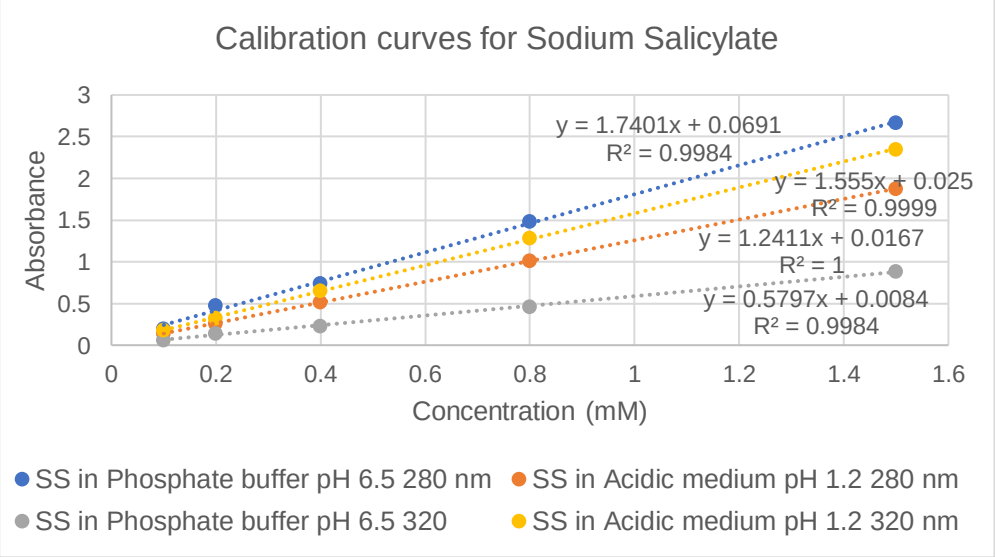

Figure 1: Calibration curves of sodium salicylate in phosphate buffer pH 6.5 and acidic medium pH 1.2. Recorded at 280 nm and 320 nm in the cary spectrophotometer.

The absorbance of the solutions with highest SS concentration, 3 mM, showed a negative deviation from linearity and are therefore exclude from the calibration curves presented in Figure 1.

2. Characterizing the R ratio and calculating pH according to Equation 14

Table 2: Raw data used to calculate pH from absorbance measurements on the Cary.

Solution	pH potentio	Path length	Abs 280nm	Abs 320nm	R	pH
1.5 A	1.41	10	0.43126686	0.50556327	0.853042311	1.78
		2	0.08005927	0.09847099	0.813023917	1.20
		1	0.0556632	0.0580608	0.958705357	2.27
1.5 B	1.40	10	0.682869424	0.822675755	0.830059012	1.54
		2	0.146605202	0.165068382	0.888148297	2.00
		1	0.097451413	0.106116513	0.918343531	2.13
2.0 A	1.96	10	0.4155504	0.4645184	0.894583293	2.03
2.0 B	1.96	10	0.716682135	0.776675164	0.922756602	2.15
2.5 A	2.46	10	0.4275722	0.3919199	1.090968333	2.56
2.5 B	2.46	10	0.75520652	0.67180484	1.124145697	2.61
3.0 A	2.99	10	0.5056611	0.3138843	1.610979268	3.14
		2	0.09286113	0.06031757	1.539536987	3.08
		1	0.0600114	0.0370784	1.618500259	3.14
3.0 B	3.01	10	0.847304981	0.515363734	1.644091203	3.17
		2	0.180549252	0.119595307	1.509668369	3.05
		1	0.082480165	0.057678791	1.429991216	2.97
3.5 A	3.46	10	0.51142	0.26488	1.930761099	3.39
3.5 B	3.46	10	0.852314006	0.433265071	1.967188364	3.42
4.0 A	3.98	10	0.5527365	0.20979	2.634713285	4.07
		2	0.110768	0.0426005	2.600157275	4.02

		1	0,06195	0.025322983	2.44639425	3.84
4.0 B	3.99	10	0.906982311	0.331834176	2.733239603	4.23
		2	0,20173217	0.073156513	2.757542173	4.28
		1	0.092160597	0.034768551	2.650688444	4.09
4.5 A	4.51	10	0.566378	0.190113	2.979165023	5.36
4.5 B	4.50	10	0.9199395	0.298239034	3.08457108	#OGIL TIGTI
5.0 A	4.87	10	0.569936	0.18247	3.12345043	#OGIL TIGTI
5.0 B	4.86	10	0.94722213	0.291532682	3.249111297	#OGIL TIGTI
5.5 A	5.53	10	0.5683227	0.18046	3.149300122	#OGIL TIGTI
5.5 B	5.53	10	0.94321983	0.280942936	3.357335987	#OGIL TIGTI
6.0 A	6.02	10	0.563	0.173	3.25433526	#OGIL TIGTI
		2	0.1095	0.035114	3.118414308	#OGIL TIGTI
		1	0.061244605	0.021754141	2.815307837	4.40
6.0 B	6.03	10	0.946426899	0.286148698	3.307465338	#OGIL TIGTI
		2	0.212460806	0.063476078	3.347100368	#OGIL TIGTI
		1	0.101261862	0.033793856	2.996457789	5.99
6.5 A	6.55	10	0.57989682	0.1842519	3.147304424	#OGIL TIGTI
		2	0.11691117	0.03570918	3.273980808	#OGIL TIGTI
		1	0.0603098	0.0189019	3.190673953	#OGIL TIGTI
6.5 B	6.54	10	0.94958819	0.28953216	3.37559053	#OGIL TIGTI
		2	0.194661423	0.052852276	3.683122776	#OGIL TIGTI
		1	0.091605213	0.027137537	3.375590498	#OGIL TIGTI

Calculated pK'_a

pK'_a was calculated from absorbance and potentiometric pH values presented in Table 2.

Table 2: Calculated values of pK'_a, A_{H_2A} and R^2

Measurment	280nm FaSSIF	320nm FaSSIF	ABS 280nm HCL	ABS 320nm HCL
$\mathbf{pK'_a}$	3.094847	2.797023	2.963511	2.913222
$\mathbf{A_{H_2A}}$	0.414204	0.508321	0.688029	0.830075
$\mathbf{R^2}$	0.968951	0.991995	0.976507	0.996958

Average pKa = 2.94215075

Appendix 6

This Appendix contains raw data from measurements in the SDi2.

1. Calibration curves to calculate MEC of salicylic acid

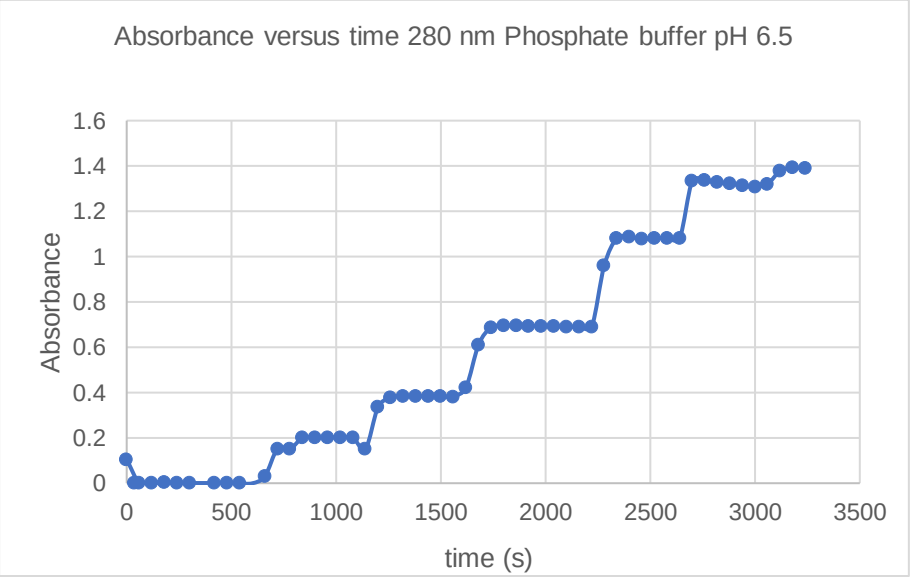

a)

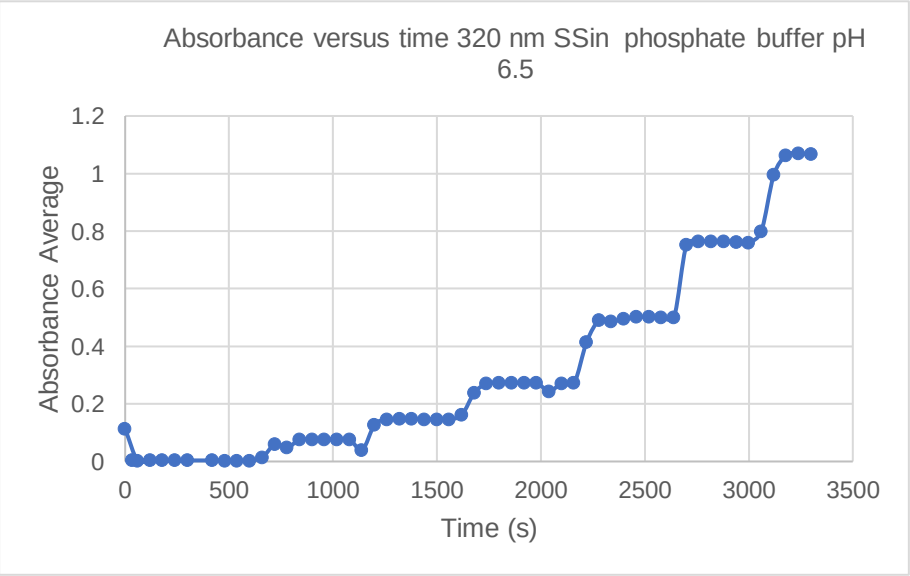

b)

Figure 1: Plot of average absorbance of each time interval (60s) plotted against time for a) 280nm SS in phosphate buffer pH 6.5 and b) 320 nm SS in phosphate buffer pH 6.5

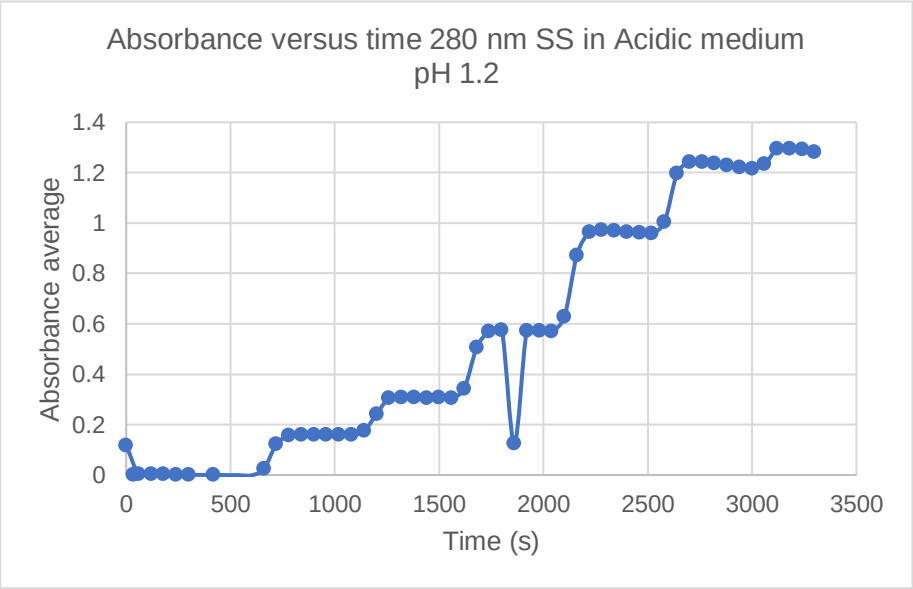

a)

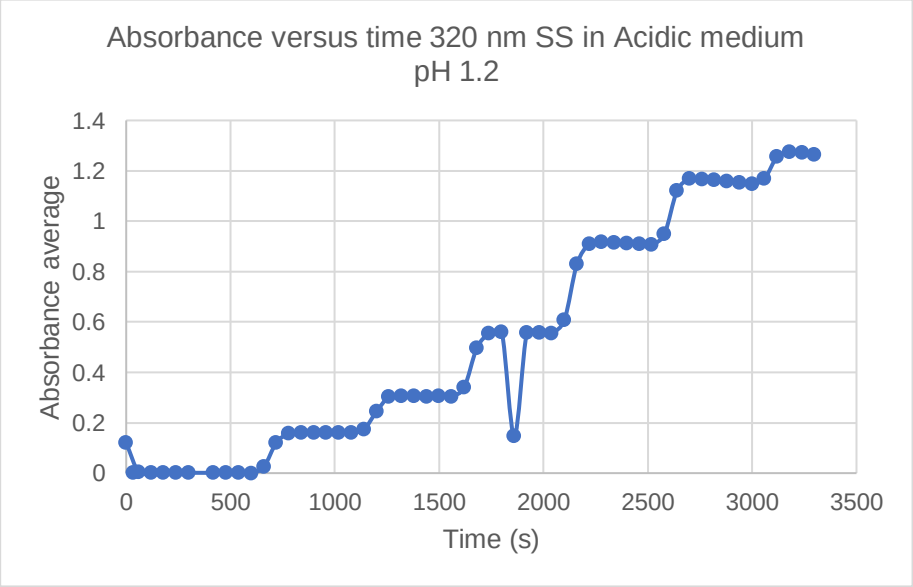

b)

Figure 2: Plot of average absorbance of each time interval (60s) plotted against time for a) 280nm SS in acidic medium pH 1.2 and b) 320 nm SS in acidic medium pH 1.2

Table 1: Absorbance values extracted from Figure 1 and 2.

Conc (mM)	Abs 280nm FaSSIF	Abs 320nm FaSSIF	Abs 280nm HCl	Abs 320nm HCl
0.1	0.2012	0.0769	0.1591	0.1600
1.2	0.3832	0.1471	0.3060	0.3045
0.4	0.69462	0.2740	0.5717	0.5603
0.8	1.0855	0.5025	0.9647	0.9105
1.5	1.3135	0.7636	1.2291	1.1599
3.0	1.3900	1.0694	1.2822	1.2722

2. Characterizing the R ratio and calculating pH according to Equation 13

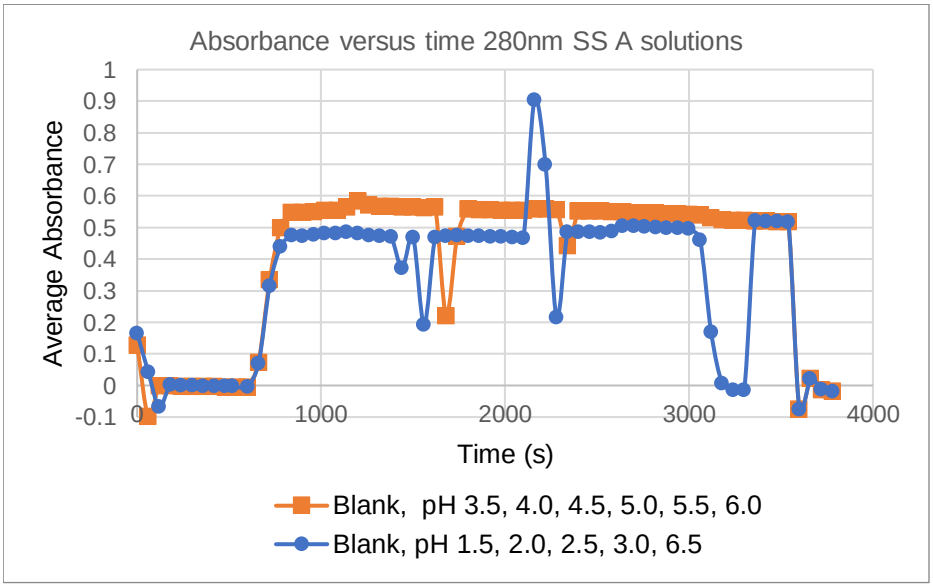

a)

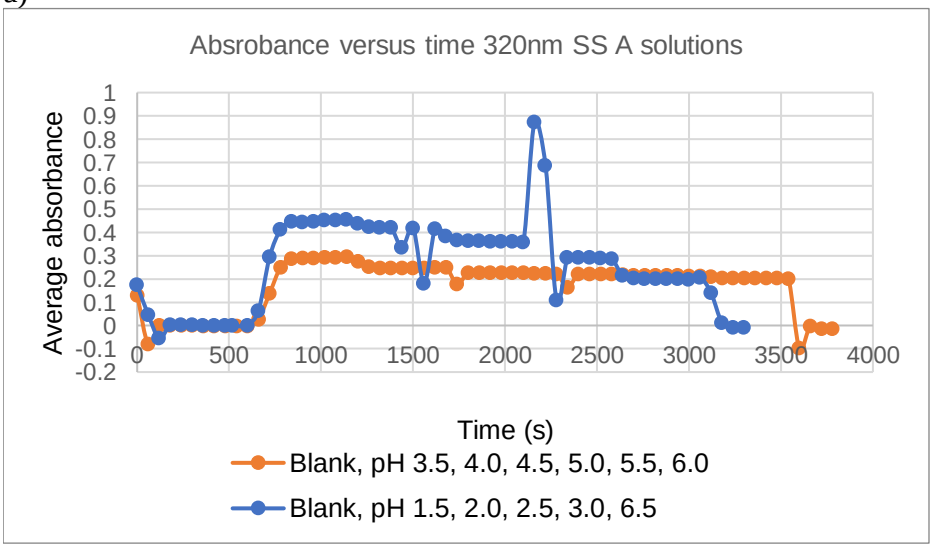

b)

Figure 3: Plot of average absorbance of each time interval (60s) plotted against time for a) A solutions measured at 280 nm and b) A solutions measured at 320 nm

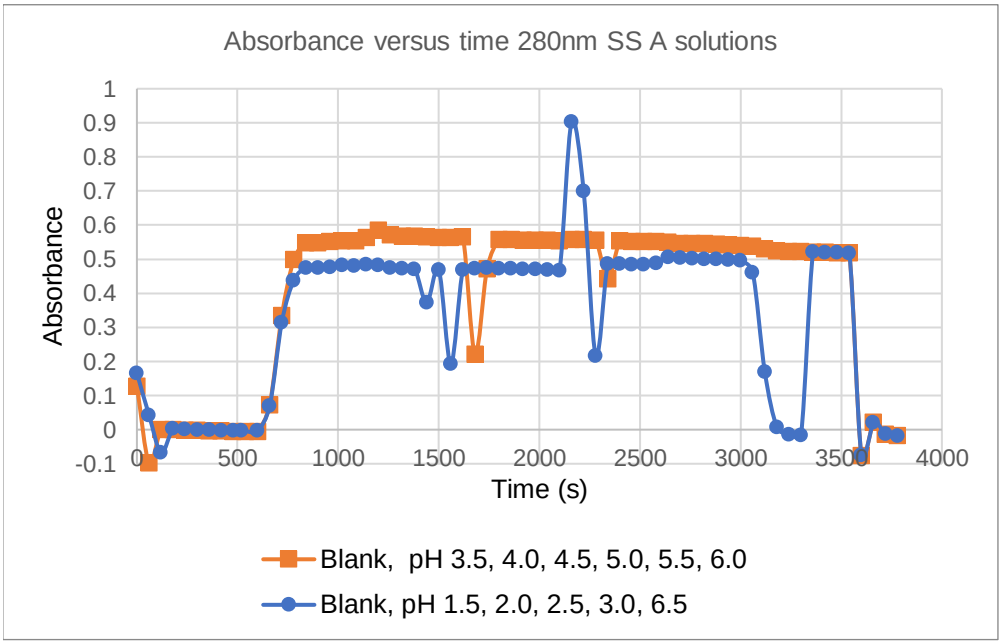

a)

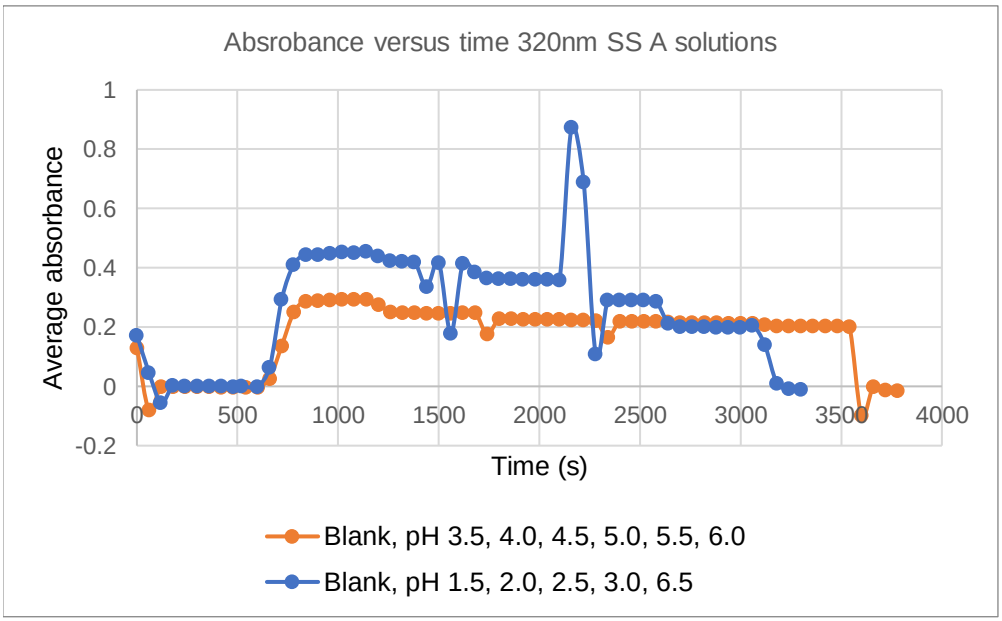

b)

Figure 4: Plot of average absorbance of each time interval (60s) plotted against time for a) B solutions measured at 280 nm and b) B solutions measured at 320 nm.

Table 2: Measured absorbance, calculated R values and pH for all solutions measured in the SDi2

Solution	Abs 280nm	Abs 320 nm	R	pH
1.5 A	0,481106606	0,451257349	1.066146861	#OGILTIGT!
1.5 B	0,76638833	0,71588322	1.07054937	#OGILTIGT!
2.0 A	0,472785817	0,417265477	1.133057593	1.97242802
2.0 B	0,77446833	0,679123881	1.14039331	2.02903041
2.5 A	0,484307294	0,360698275	1.342693679	2.75853198
2.5 B	0,780416807	0,59669489	1.30789926	2.6768872
3.0 A	0,497596046	0,290600055	1.712305409	3.45579237
3.0 B	0,791901156	0,481647789	1.64414988	3.32737325
3.5 A	0,554555807	0,294095541	1.885631469	3.86896679
3.5 B	0,791893404	0,47409989	1.67030919	3.37564874
4.0 A	0,56505967	0,24720456	2.285797924	#OGILTIGT!
4.0 B	0,864966532	0,39577555	2.18549764	#OGILTIGT!
4.5 A	0,558420193	0,225715321	2.474002166	#OGILTIGT!
4.5 B	0,842253128	0,368053835	2.28839655	#OGILTIGT!
5.0 A	0,549466083	0,218152101	2.518729274	#OGILTIGT!
5.0 B	0,837304982	0,358412358	2.33614987	#OGILTIGT!
5.5 A	0,541224927	0,214066826	2.528298929	#OGILTIGT!
5.5 B	0,815603596	0,347459239	2.34733605	#OGILTIGT!
6.0 A	0,519245532	0,203535954	2.551124368	#OGILTIGT!
6.0 B	0,808212193	0,344781239	2.34413043	#OGILTIGT!
6.5 A	0,497596046	0,199484064	2.494415023	#OGILTIGT!
6.5 B	0,791893404	0,334874018	2.36475021	#OGILTIGT!

Table 3: Calculated values of pK'_a, A_{H_2A} and R^2 from measurements in the SDi2

pK'_a	280 NM PHOSHATE BUFFER PH 6.5	320NM PHOSHATE BUFFER PH 6.5	ABS 280NM ACIDIC MEDIUM PH 1.2	ABS 320NM ACIDIC MEDIUM PH 1.2
pK'_a	2.893136	2.968027	2.453944	2.990344
A_{H_2A}	0.468719	0.439907	0.762653	0.707488
R^2	0.564388	0.947062	0.321652	0.966711

3. Calculating microenvironmental pH during dissolution experiments

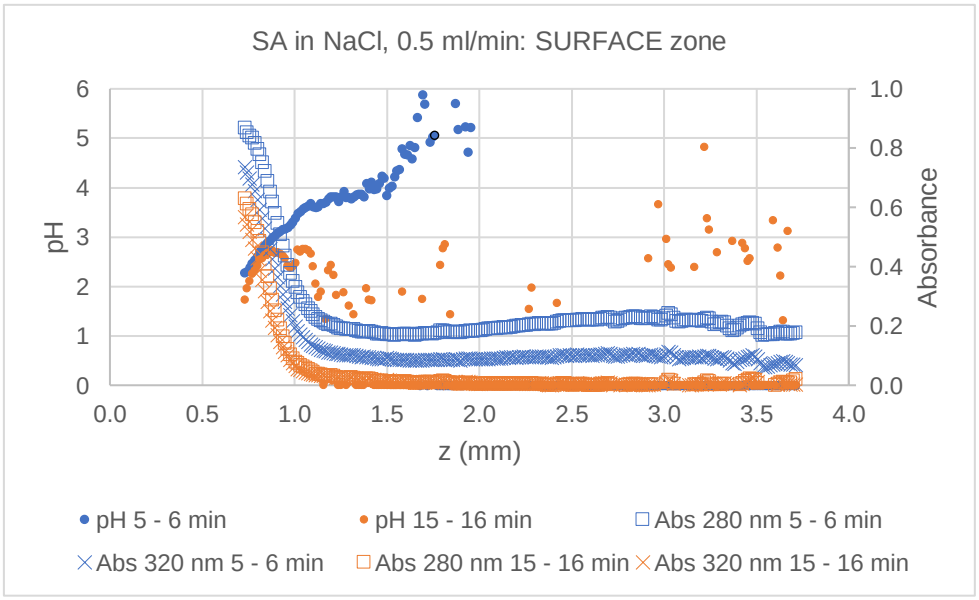

Figure 5: Average measured absorbance and calculated pH for two time intervals of SA dissolving in NaCl plotted against z. Data was collected from the SURFACE zone.

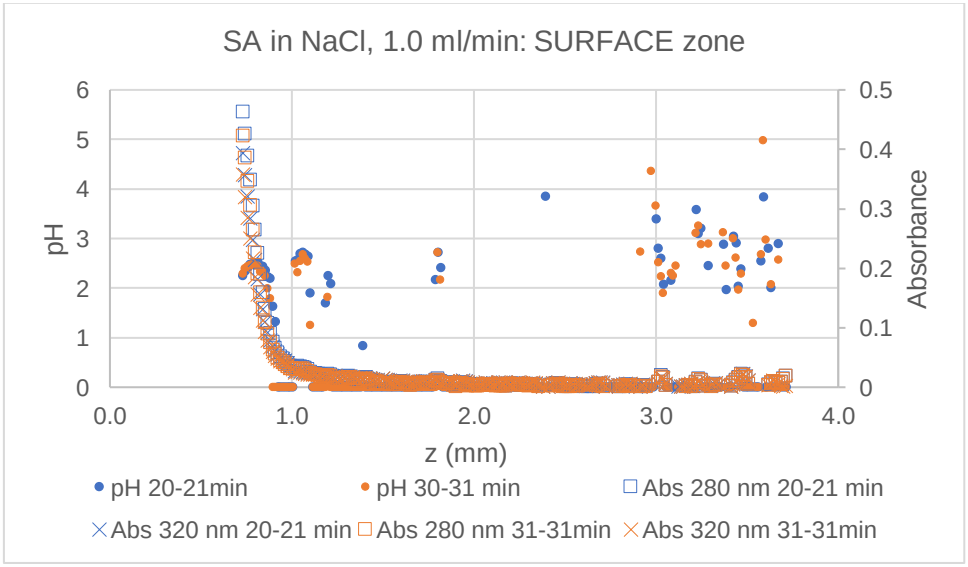

Figure 6: Average measured absorbance and calculated pH for two time intervals of SA dissolving in NaCl plotted against z. Data was collected from the SURFACE zone.

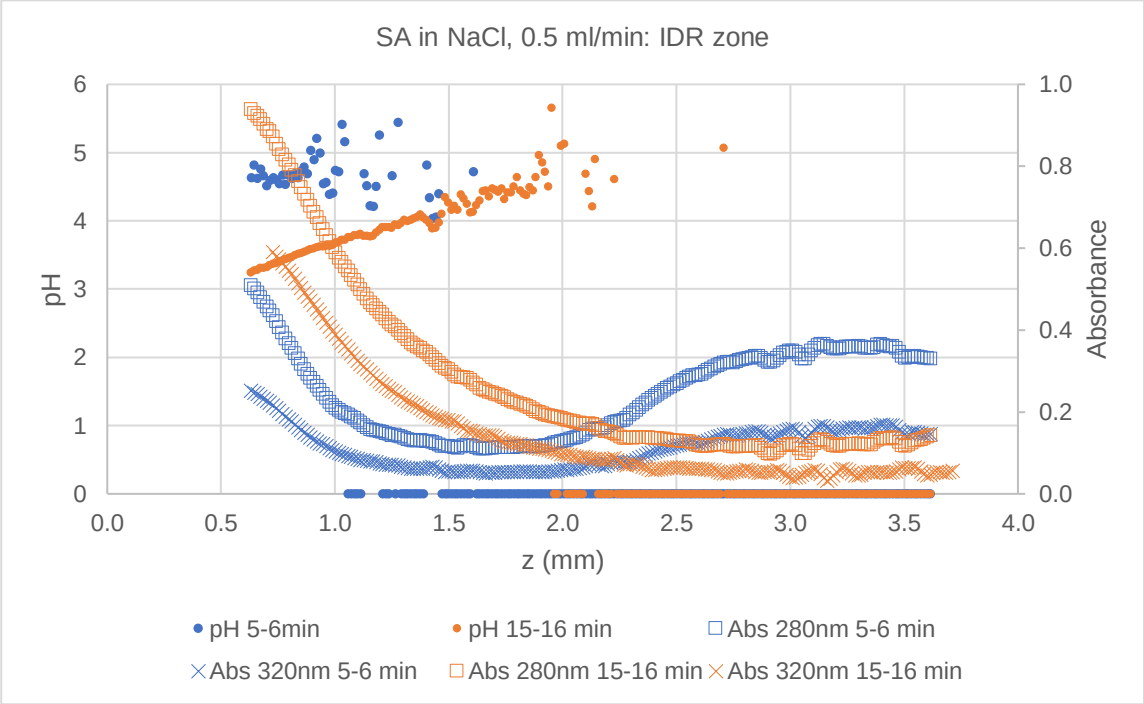

Figure 7: Average measured absorbance and calculated pH for two time intervals of SA dissolving in NaCl plotted against z. Data was collected from the IDR zone.

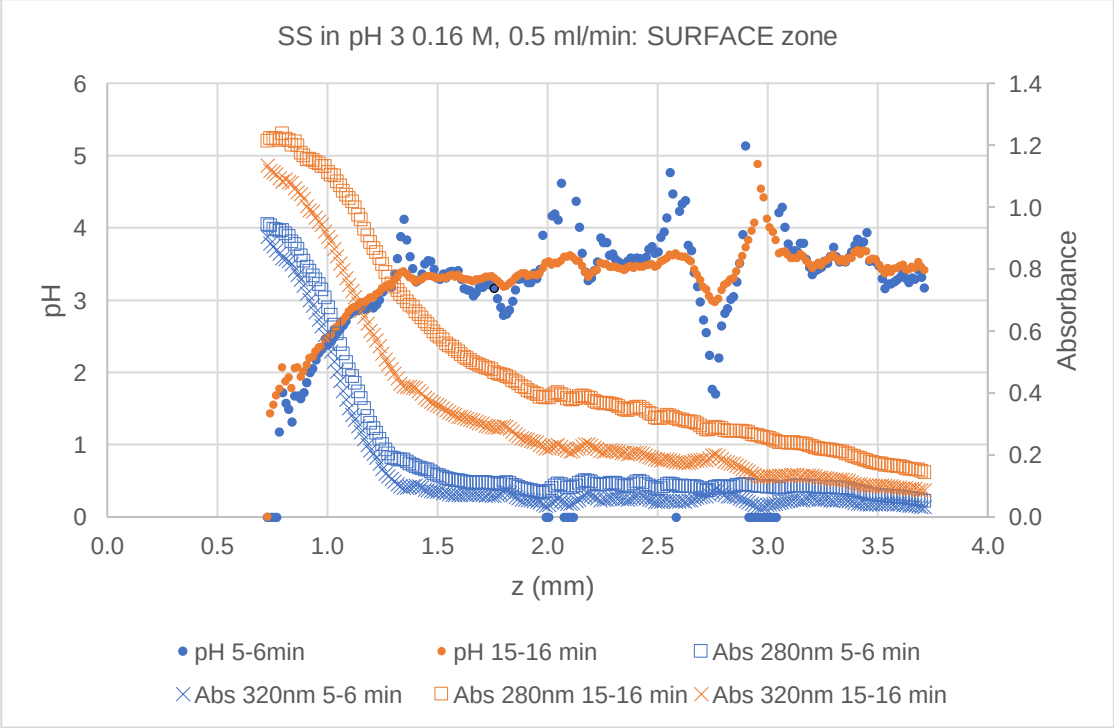

Figure 8: Average measured absorbance and calculated pH for two-time intervals of SA dissolving in pH 3 buffer, C= 0.16 M, plotted against z. Data was collected from the SURFACE zone.

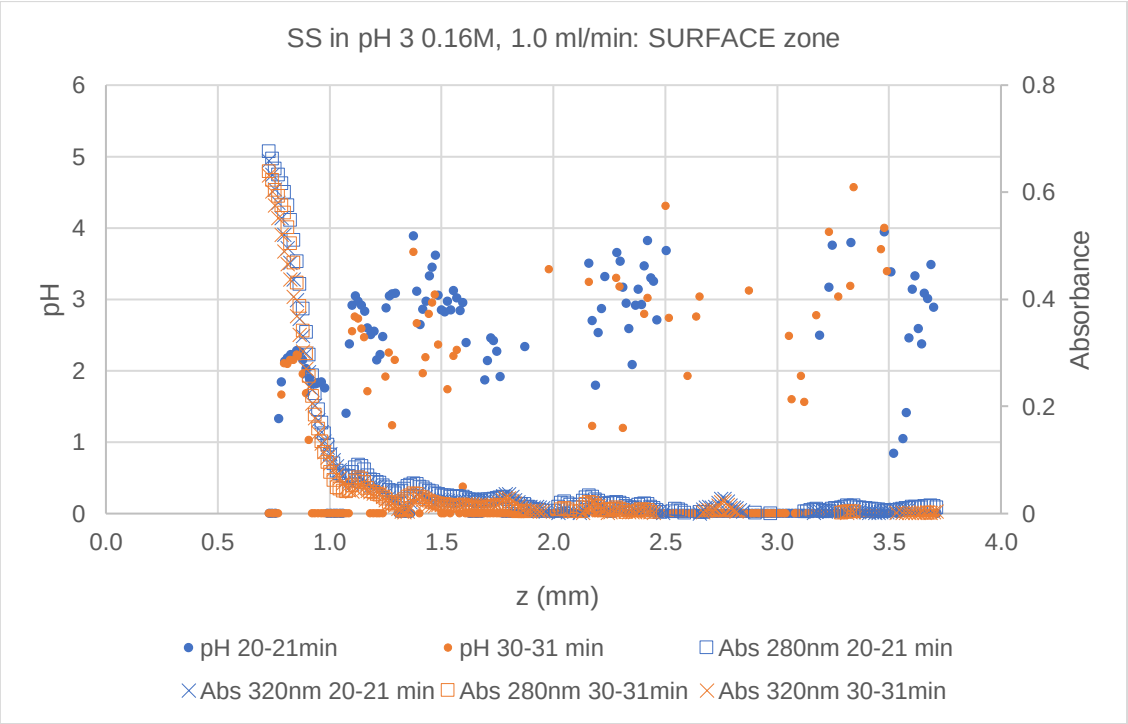

Figure 9: Average measured absorbance and calculated pH for two-time intervals of SA dissolving in pH 3 buffer, C= 0.16 M, plotted against z. Data was collected from the SURFACE zone.

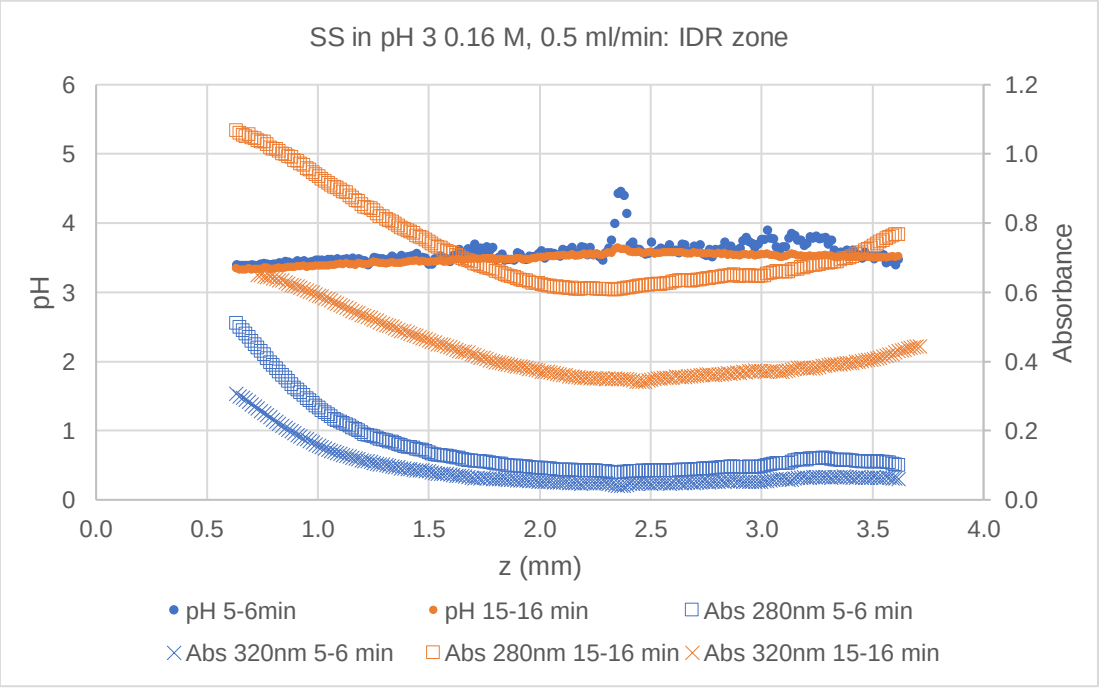

Figure 10: Average measured absorbance and calculated pH for two-time intervals of SA dissolving in pH 3 buffer, C= 0.16 M, plotted against z. Data was collected from the IDR zone.

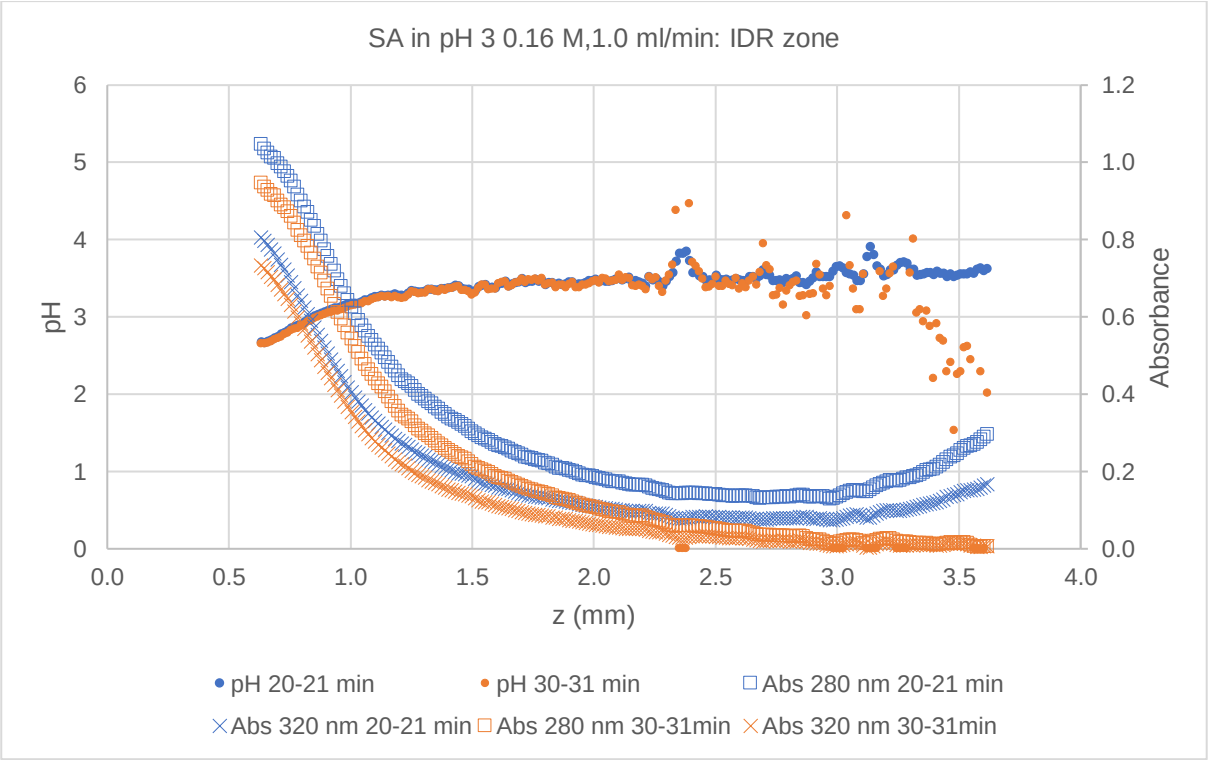

Figure 11: Average measured absorbance and calculated pH for two-time intervals of SA dissolving in pH 3 buffer, C= 0.16 M, plotted against z. Data was collected from the IDR zone.

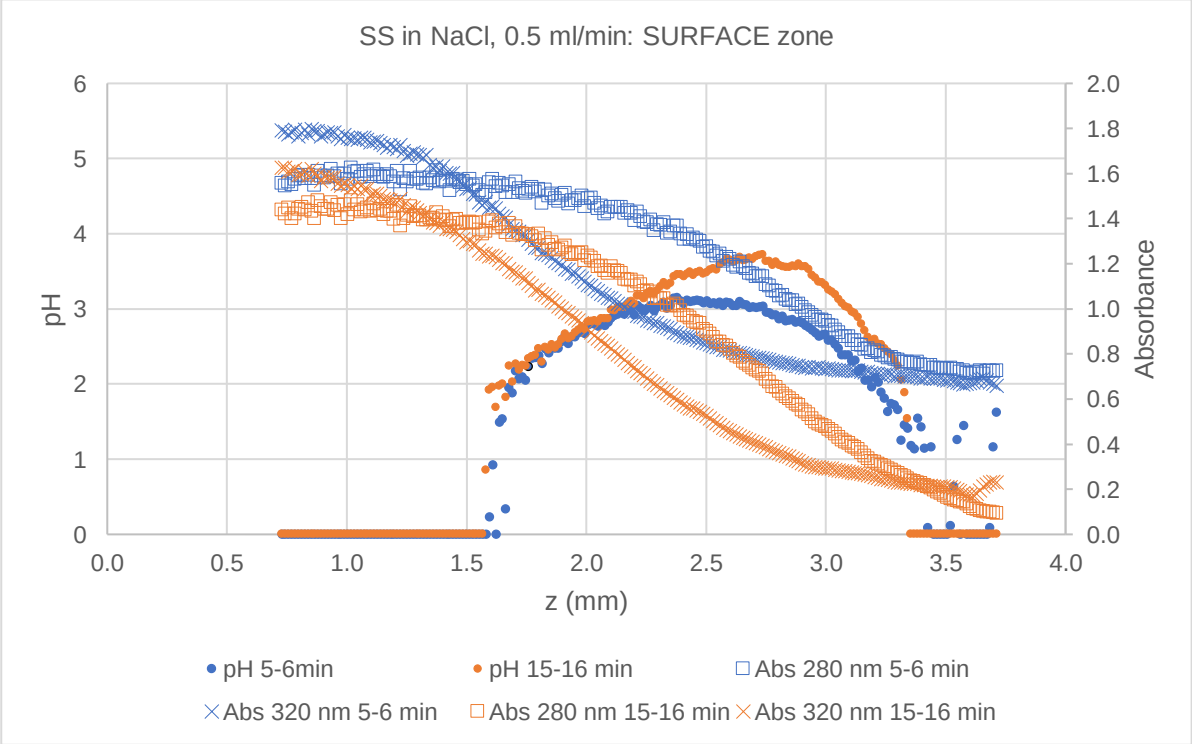

Figure 12: Average measured absorbance and calculated pH for two-time intervals of SS dissolving in NaCl solution plotted against z. Data was collected from the SURFACE zone.

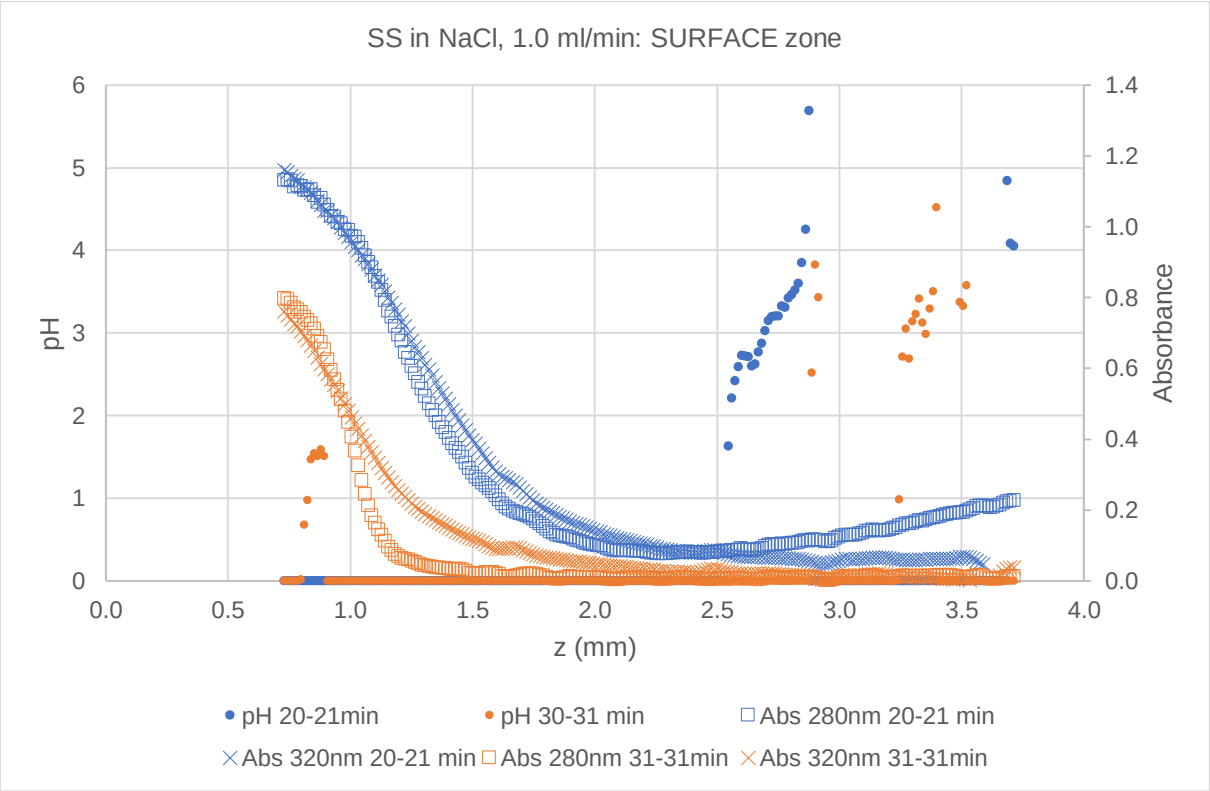

Figure 13: Average measured absorbance and calculated pH for two-time intervals of SS dissolving in NaCl solution plotted against z. Data was collected from the SURFACE zone.

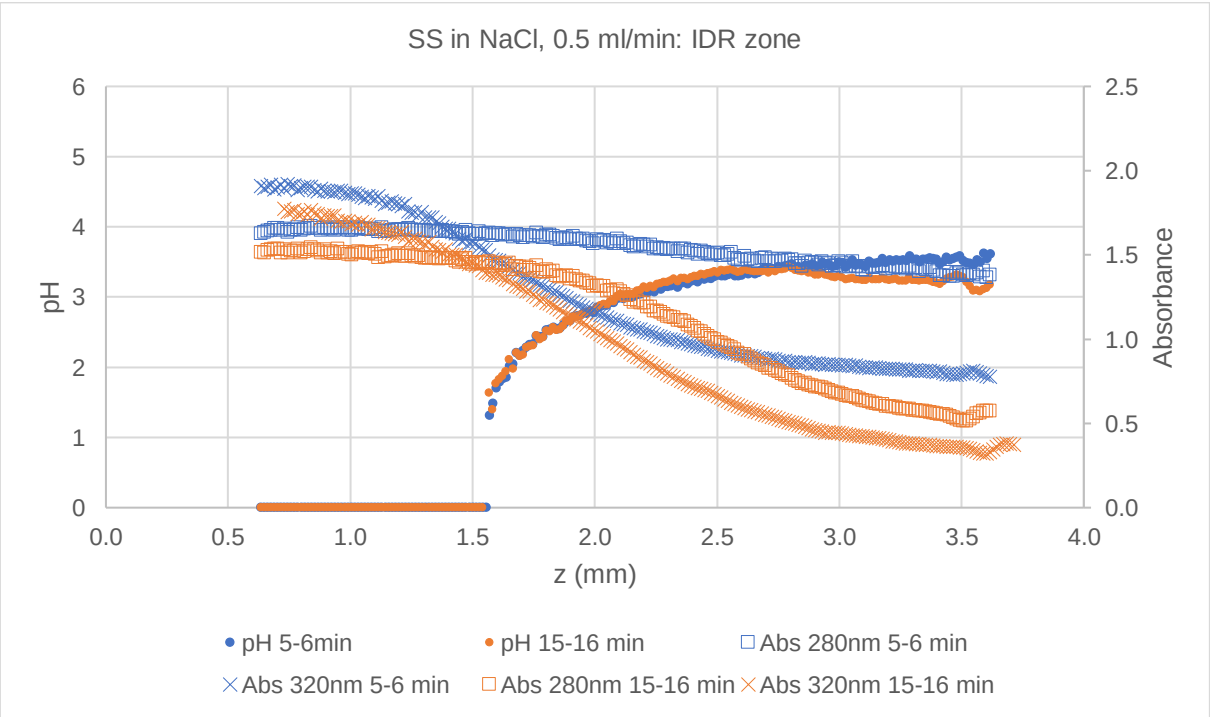

Figure 14: Average measured absorbance and calculated pH for two-time intervals of SS dissolving in NaCl solution plotted against z. Data was collected from the IDR zone.

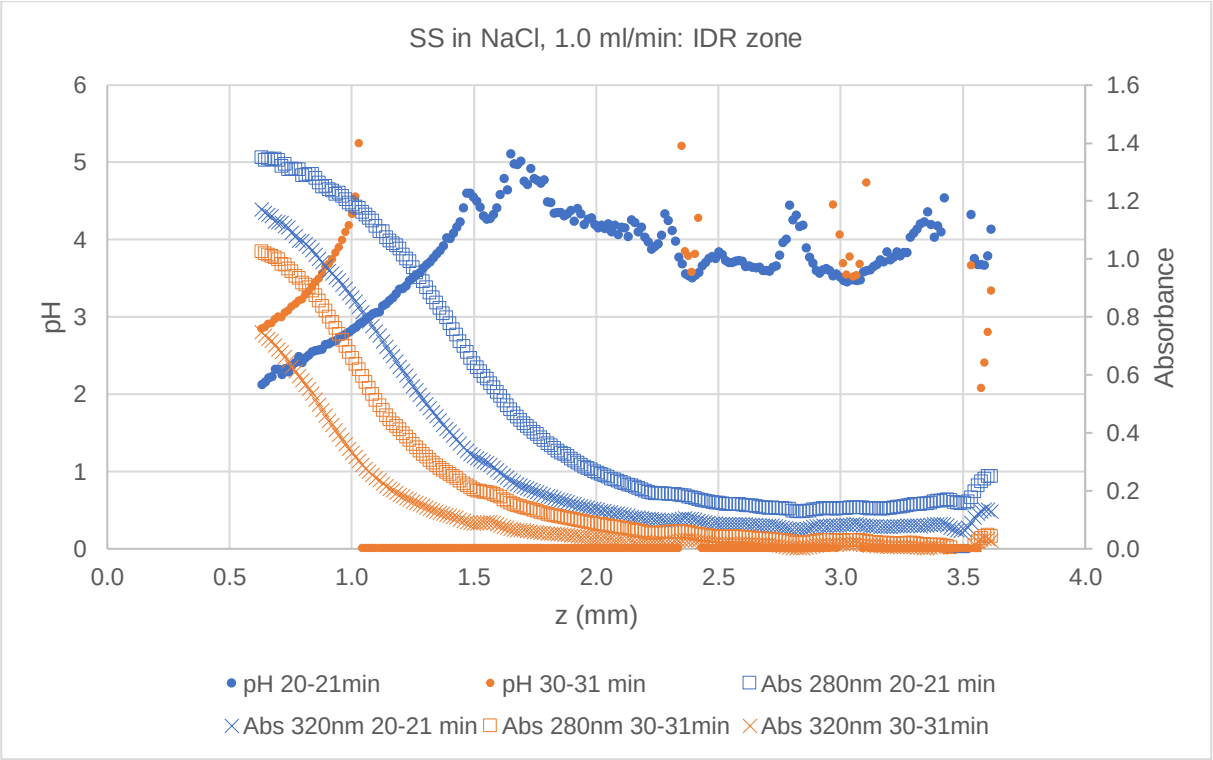

Figure 15: Average measured absorbance and calculated pH for two-time intervals of SS dissolving in NaCl solution plotted against z. Data was collected from the IDR zone.

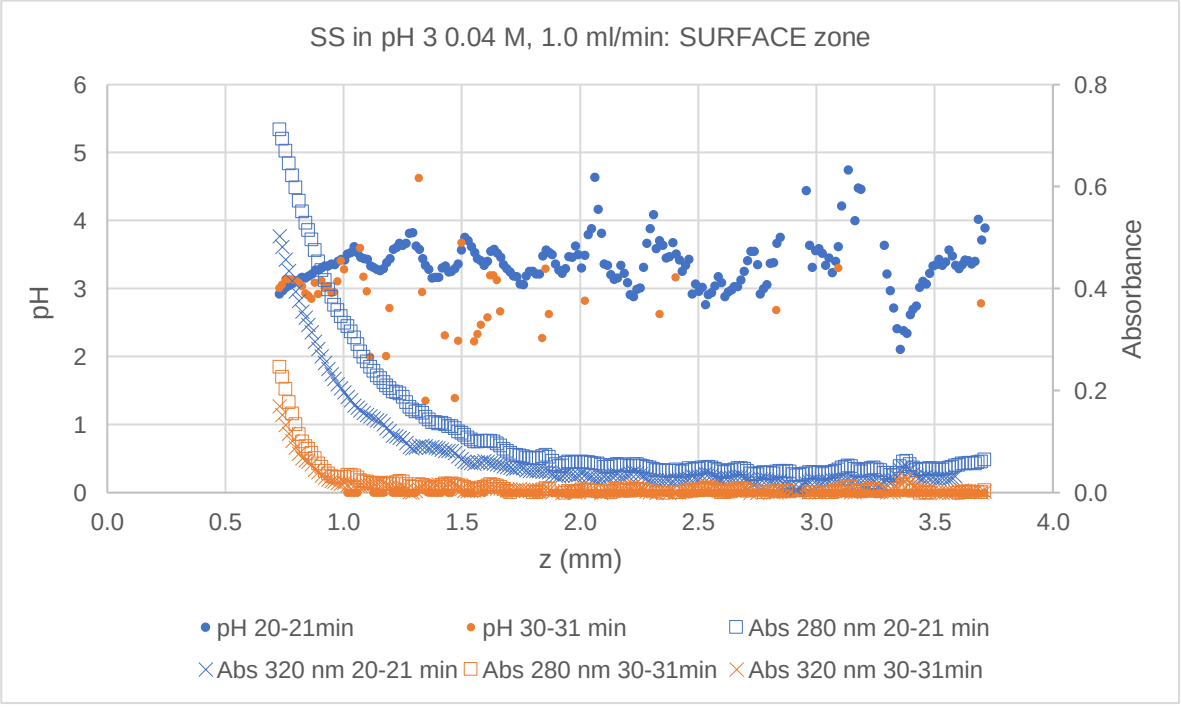

Figure 16: Average measured absorbance and calculated pH for two-time intervals of SS dissolving in pH 3 buffer, C = 0.041 M, plotted against z. Data was collected from the SURFACE zone.

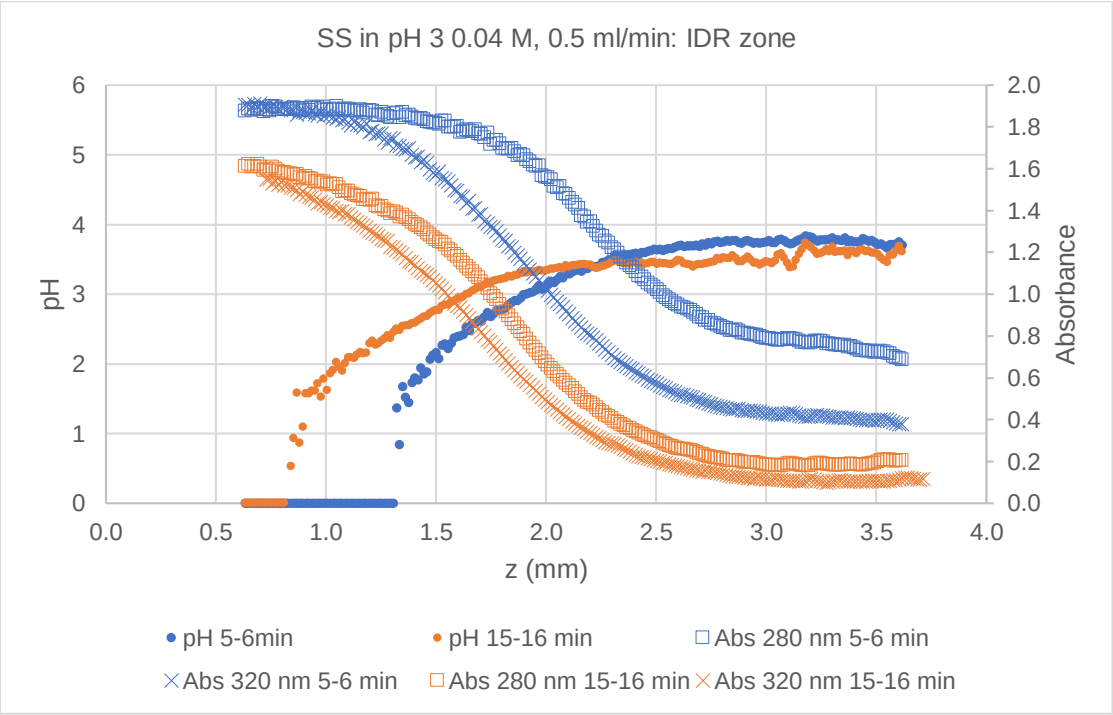

Figure 17: Average measured absorbance and calculated pH for two-time intervals of SS dissolving in pH 3 buffer, C = 0.041 M, plotted against z. Data was collected from the IDR zone.

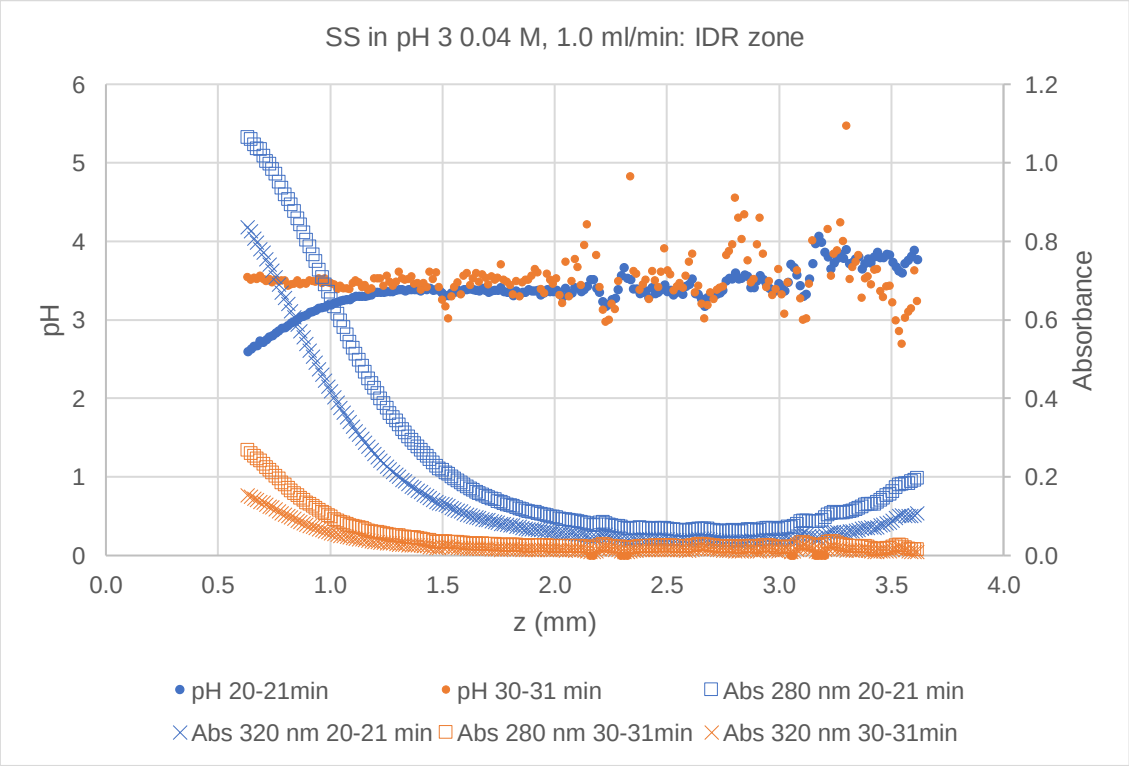

Figure 18: Average measured absorbance and calculated pH for two-time intervals of SS dissolving in pH 3 buffer, C = 0.041 M, plotted against z. Data was collected from the IDR zone.